

Theory of Superconductivity

Tfy-3.4801 (6 cr.) P, I–II.
Aalto University, School of Science and
Technology
Department of Applied Physics
Fall, 2010

N. B. Kopnin
Low Temperature Laboratory, Aalto University
email: kopnin@boojum.hut.fi

August 26, 2010

Contents

1	Introduction to Superconductivity	7
1.1	Superconducting transition	7
1.2	The London model	8
1.2.1	Meissner effect	9
1.3	Phase coherence	10
1.3.1	Magnetic flux quantization	11
1.3.2	Coherence length and the energy gap	12
1.4	Critical currents and magnetic fields	13
1.4.1	Condensation energy	13
1.4.2	Critical currents	14
1.5	Quantized vortices	14
1.5.1	Basic concepts	14
1.5.2	Vortices in the London model	16
1.5.3	Critical fields in type-II superconductors	17
1.5.4	The Little and Parks effect	19
2	The BCS theory	23
2.1	Landau Fermi-liquid	23
2.2	The Cooper problem	27
2.3	The BCS model	31
2.3.1	Wave functions	31
2.3.2	Hamiltonian	33
2.3.3	The Bogoliubov–de Gennes equations	34
2.3.4	The self-consistency equation	36
2.4	Observables	39
2.4.1	Energy spectrum and coherence factors	39
2.4.2	The energy gap	42
2.4.3	Condensation energy	43
2.4.4	Current	44
2.4.5	Negative energies	48
2.5	Impurities. Anderson theorem	48

3	Andreev reflection	53
3.1	Semiclassical approximation	53
3.1.1	Andreev equations	53
3.1.2	Andreev reflection	54
3.2	Andreev states	58
3.2.1	SNS structures	58
3.3	Supercurrent through an SNS structure. Proximity effect	63
3.3.1	Short junctions. Point contacts	63
3.3.2	Long junctions	66
4	Superconductor–Insulator–Normal-metal Interface	73
4.1	Transmission through the barrier	73
4.1.1	Transmission and reflection probabilities	73
4.1.2	Probability conservation	79
4.2	Current through the NIS junction	80
4.2.1	Normal tunnel resistance	83
4.2.2	Landauer formula	84
4.2.3	Tunnel current	85
4.2.4	Excess current	86
4.2.5	NS Andreev current. Current conversion	87
4.3	SIS contact	87
4.3.1	Wave functions and the energy of bound states	87
4.3.2	Supercurrent	88
4.4	Scattering matrix	90
4.4.1	SINIS structures	91
4.4.2	Interference effects in short contacts	93
5	Weak links	95
5.1	Josephson effect	95
5.1.1	D.C and A.C. Josephson effects	95
5.1.2	Superconducting Quantum Interference Devices	98
5.2	Josephson vortices in extended junctions.	98
5.2.1	Low field limit	100
5.2.2	Higher fields. Josephson vortices.	101
5.3	Dynamics of Josephson junctions	103
5.3.1	Resistively shunted Josephson junction	103
5.3.2	The role of capacitance	104
5.3.3	Thermal fluctuations	109
5.3.4	Shapiro steps	111
6	Coulomb blockade in normal double junctions	115
6.1	Orthodox description of the Coulomb blockade	115
6.1.1	Low temperature limit	118
6.1.2	Conductance in the high temperature limit	119

7	Quantum phenomena in Josephson junctions	123
7.1	Quantization	123
7.1.1	Quantum conditions	123
7.1.2	Charge operator	124
7.1.3	The Hamiltonian	126
7.2	Macroscopic quantum tunnelling	127
7.2.1	Effects of dissipation on MQT	129
7.3	Band structure	130
7.3.1	Bloch's theorem	130
7.3.2	Bloch's theorem in Josephson devices	131
7.3.3	Large Coulomb energy: Free-phase limit	132
7.3.4	Low Coulomb energy: Tight binding limit	134
7.4	Coulomb blockade	135
7.4.1	Equation of motion	136
7.4.2	Bloch oscillations and the Coulomb blockade in Josephson junctions	136
7.4.3	Effect of dissipation	138
7.5	Parity effects	140

Chapter 1

Introduction to Superconductivity

1.1 Superconducting transition

Superconductivity manifests itself mainly as an absence of resistivity below some critical temperature. It was discovered in 1911 by H. Kamerlingh Onnes in Leiden, three years after he first liquefied ^4He . He measured the resistivity of mercury. The resistivity behavior as a function of temperature is shown in Fig. 1.1.

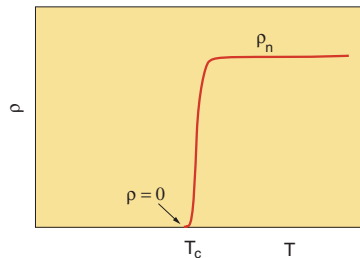


Figure 1.1: Below the transition temperature, the resistivity drops to zero.

The absolute absence of resistivity is a very fundamental phenomenon. In combination with general quantum-mechanical principles, it can lead to quite informative conclusions on the properties of the superconducting state. Here we try to describe the basic picture of superconductivity using minimum amount of input information. We consider the most striking properties of superconductors such as their ideal diamagnetism, macroscopic quantum nature of superconductivity including phase coherence which leads to zero resistivity, to quantization of magnetic flux and to formation of quantized vortices. The maximum values of magnetic fields and currents that can be withstood by superconductors are

Table 1.1: Parameters for metallic superconductors

	T_c , K	H_c , Oe	H_{c2} , Oe	λ_L , Å	ξ_0 , Å	κ	Type
Al	1.18	105		500	16000	0.01	I
Hg	4.15	400		400			I
Nb	9.25	1600	2700	470	390	1.2	II
Pb	7.2	800		390	830	0.47	I
Sn	3.7	305		510	2300	0.15	I
In	3.4	300		400	3000		I
V	5.3	1020		400	~300	~ 0.7	II

Table 1.2: Parameters for some high temperature superconductors

	T_c , K	H_{c2} , T	λ_L , Å	ξ_0 , Å	κ	Type
Nb ₃ Sn	18	25	~2000	115		II
La _{0.925} Sr _{0.072} CuO ₄	34		1500	20	75	II
YBa ₂ Cu ₃ O ₇	92.4	150	2000	15	140	II
Bi ₂ Sr ₂ Ca ₃ CuO ₁₀	111					II
Tl ₂ Sr ₂ Ca ₂ Cu ₃ O ₁₀	123					II
HgBa ₂ Ca ₂ Cu ₃ O ₈	133					II
MgB ₂	36.7	14	1850	50	40	II

also briefly discussed. The rest of the course is devoted to a microscopic theory of superconductivity.

1.2 The London model

We assume that the current flows without dissipation and has the form

$$\mathbf{j}_s = n_s e \mathbf{v}_s$$

whence the velocity of superconducting electrons is $\mathbf{v}_s = \mathbf{j}/n_s e$ where n_s is their density. Now we come to the most important argument [F. London and H. London, 1935]: Being non-dissipative, this current contributes to the kinetic energy of superconducting electrons. The total free energy is a sum of the kinetic energy of superconducting electrons and the magnetic energy

$$\mathcal{F} = \int \left[\frac{n_s m \mathbf{v}_s^2}{2} + \frac{\mathbf{h}^2}{8\pi} \right] dV = \int \left[\frac{m \mathbf{j}_s^2}{2n_s e^2} + \frac{\mathbf{h}^2}{8\pi} \right] dV .$$

Here \mathbf{h} is the “microscopic” magnetic field. Its average over large area in the sample gives the magnetic induction \mathbf{B} . Using the Maxwell equation

$$\mathbf{j}_s = (c/4\pi) \text{curl } \mathbf{h} , \quad (1.1)$$

we transform this to the following form

$$\mathcal{F} = \int \left[\frac{mc^2}{32\pi^2 n_s e^2} (\text{curl } \mathbf{h})^2 + \frac{\mathbf{h}^2}{8\pi} \right] dV = \frac{1}{8\pi} \int dV \left[\mathbf{h}^2 + \lambda_L^2 (\text{curl } \mathbf{h})^2 \right]. \quad (1.2)$$

Here

$$\lambda_L = \left(\frac{mc^2}{4\pi n_s e^2} \right)^{\frac{1}{2}} \quad (1.3)$$

is called the London penetration depth. In equilibrium, the free energy is minimal with respect to distribution of the magnetic field. Variation with respect to \mathbf{h} gives

$$\begin{aligned} \delta\mathcal{F} &= \frac{1}{4\pi} \int dV \left[\mathbf{h} \cdot \delta\mathbf{h} + \lambda_L^2 (\nabla \times \mathbf{h}) \cdot (\nabla \times \delta\mathbf{h}) \right] \\ &= \frac{1}{4\pi} \int dV \left(\mathbf{h} + \lambda_L^2 \nabla \times \nabla \times \mathbf{h} \right) \cdot \delta\mathbf{h} + \frac{1}{4\pi} \int dV \text{div} [\delta\mathbf{h} \times \text{curl } \mathbf{h}]. \end{aligned}$$

Here we use the identity

$$\text{div} [\mathbf{b} \times \mathbf{a}] = \mathbf{a} \cdot [\nabla \times \mathbf{b}] - \mathbf{b} \cdot [\nabla \times \mathbf{a}]$$

and put $\mathbf{a} = \nabla \times \mathbf{h}$, $\mathbf{b} = \delta\mathbf{h}$. Looking for a free energy minimum and omitting the surface term we obtain the London equation:

$$\mathbf{h} + \lambda_L^2 \text{curl curl } \mathbf{h} = 0. \quad (1.4)$$

Since

$$\text{curl curl } \mathbf{h} = \nabla \text{div } \mathbf{h} - \nabla^2 \mathbf{h}$$

and $\text{div } \mathbf{h} = 0$, we find

$$\mathbf{h} - \lambda_L^2 \nabla^2 \mathbf{h} = 0. \quad (1.5)$$

1.2.1 Meissner effect

Equation (1.5) in particular describes the Meissner effect, i.e., an exponential decay of weak magnetic fields and supercurrents in a superconductor. The characteristic length over which the magnetic field decreases is just λ_L . Consider a superconductor which occupies the half-space $x > 0$. A magnetic field h_y is applied parallel to its surface (Fig. 1.2). We obtain from Eq. (1.5)

$$\frac{\partial^2 h_y}{\partial x^2} - \lambda_L^{-2} h_y = 0$$

which gives

$$h_y = h_y(0) \exp(-x/\lambda).$$

The field decays in a superconductor such that there is no field in the bulk. According to Eq. (1.1) the supercurrent also decays and vanishes in the bulk.

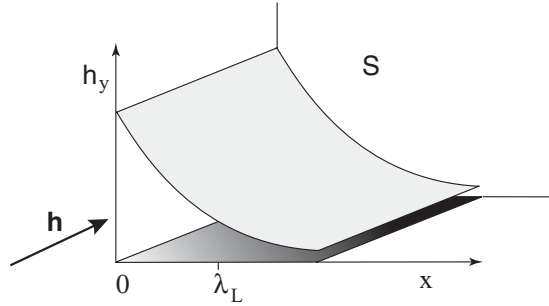


Figure 1.2: The Meissner effect: Magnetic field penetrates into a superconductor only over distances shorter than λ_L .

Therefore,

$$\mathbf{B} = \mathbf{H} + 4\pi\mathbf{M} = 0$$

in a bulk superconductor, where \mathbf{H} is the applied field. The magnetization and susceptibility are

$$\mathbf{M} = -\frac{\mathbf{H}}{4\pi}; \quad \chi = \frac{\partial M}{\partial H} = -\frac{1}{4\pi} \quad (1.6)$$

as for an ideal diamagnetic: Superconductor repels magnetic field lines. The Meissner effect in type I superconductors persists up to the field $H = H_c$ (see Table 1.1, Fig. 1.7, and the section below) above which superconductivity is destroyed. Type II superconductors display the Meissner effect up to much lower fields, after which vortices appear (see Section 1.5).

1.3 Phase coherence

The particle mass flow is determined by the usual quantum-mechanical expression for the momentum per unit volume

$$\mathbf{j}_m = -\frac{i\hbar}{2} [\psi^*\nabla\psi - \psi\nabla\psi^*] = \hbar|\psi|^2\nabla\chi. \quad (1.7)$$

In order to have a finite current in the superconductor it is necessary that ψ is the wave function of all the superconducting electrons with a definite phase χ : the superconducting electrons should all be in a single quantum state. According to the present understanding what happens is that the electrons (Fermi particles) combine into pairs (Cooper pairs, see the next Chapter) which are Bose objects and condense into a Bose condensate. The current appears when the phase χ of the condensate function ψ slowly varies in space. Equation (1.7) suggests that $\mathbf{P} = \hbar\nabla\chi$ is the momentum of a condensate particle (which is a pair in the superconductor). For charged particles, the momentum is $\mathbf{p} = \mathbf{P} - (e^*/c)\mathbf{A}$ where \mathbf{P} is the canonical momentum, \mathbf{A} is the vector potential of the magnetic

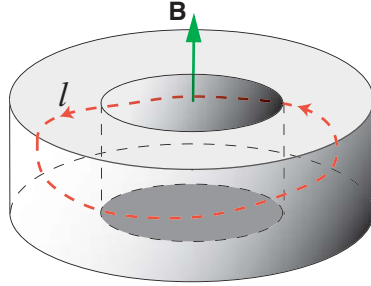


Figure 1.3: Magnetic flux through the hole in a superconductor is quantized.

field, and e^* is the charge of the carrier. In superconductors the charge is carried by pairs of electrons thus $e^* = 2e$ and the Cooper pair mass is $2m$.

Using the definition of the momentum we introduce the velocity of superconducting electrons

$$\mathbf{v}_s = \frac{\hbar}{2m} \left(\nabla\chi - \frac{2e}{\hbar c} \mathbf{A} \right). \quad (1.8)$$

Now the electric current becomes

$$\mathbf{j}_s = n_s e \mathbf{v}_s = -\frac{e^2 n_s}{mc} \left(\mathbf{A} - \frac{\hbar c}{2e} \nabla\chi \right). \quad (1.9)$$

where $|\psi|^2 = n_s/2$ is the density of electron pairs.

It is instructive to compare this equation with Eqs. (1.1) and (1.4). We find from these

$$\text{curl } \mathbf{j} = \frac{c}{4\pi} \text{curl curl } \mathbf{h} = -\frac{c}{4\pi\lambda_L^2} \mathbf{h} = -\frac{c}{4\pi\lambda_L^2} \text{curl } \mathbf{A}$$

Therefore,

$$\mathbf{j} = -\frac{c}{4\pi\lambda_L^2} (\mathbf{A} - \nabla\phi) = -\frac{e^2 n_s}{mc} (\mathbf{A} - \nabla\phi)$$

where $\nabla\phi$ is a gradient of some function. It is seen that this coincides with Eq. (1.9) where $\phi = (\hbar c/2e)\chi$.

1.3.1 Magnetic flux quantization

Let us consider an non-singly-connected superconductor with dimensions larger than λ_L placed in a magnetic field (Fig. 1.3). We choose a contour which goes all the way inside the superconductor around the hole and calculate the contour integral

$$\oint \left(\mathbf{A} - \frac{\hbar c}{2e} \nabla\chi \right) \cdot d\mathbf{l} = \int_S \text{curl } \mathbf{A} \cdot d\mathbf{S} - \frac{\hbar c}{2e} \Delta\chi = \Phi - \frac{\hbar c}{2e} 2\pi n. \quad (1.10)$$

Here Φ is the magnetic flux through the contour. The phase change along the closed contour is $\Delta\chi = 2\pi n$ where n is an integer because the wave function ψ is single valued. Since $\mathbf{j} = 0$ in the bulk, the l.h.s. of Eq. (1.10) vanishes, and we obtain $\Phi = \Phi_0 n$ where

$$\Phi_0 = \frac{\pi\hbar c}{e} \approx 2.07 \times 10^{-7} \text{ Oe} \cdot \text{cm}^2 \quad (1.11)$$

is the quantum of magnetic flux. In SI units, $\Phi_0 = \pi\hbar/e = 2.07 \times 10^{-15} \text{ T} \cdot \text{m}^2$.

1.3.2 Coherence length and the energy gap

Cooper pairs keep their correlation within a certain distance called the coherence length ξ (see the next Chapter). This length introduces an important energy scale. To see this let us argue as follows. Since the correlation of pairs is restricted within ξ the phase gradient $\nabla\chi$ cannot exceed $1/\xi$; thus the superconducting velocity cannot be larger than the critical value

$$v_c = \frac{\hbar}{\alpha m \xi} . \quad (1.12)$$

where $\alpha \sim 1$ is a constant. Thus the energy of a correlated motion of a pair is restricted to $\Delta_0 \sim p_F v_c = \hbar v_F / \alpha \xi$. This gives

$$\xi \sim \frac{\hbar v_F}{\Delta_0} .$$

The quantity Δ_0 is in fact the value of the energy gap $\Delta(0)$ at zero temperature in the single-particle excitation spectrum in the superconducting state. We shall see from the microscopic theory in the next Chapter that the energy of excitations

$$\epsilon = \sqrt{\left(\frac{p^2}{2m} - E_F\right)^2 + \Delta^2}$$

cannot be smaller than a certain value Δ that generally depends on temperature. The coherence length is usually defined as

$$\xi_0 = \frac{\hbar v_F}{2\pi k_B T_c}$$

where $\Delta_0 = 1.76 k_B T_c$ and ξ_0 is the coherence length at zero temperature of a clean (without impurities) material. In alloys with $\ell < \xi_0$,

$$\xi = \sqrt{\xi_0 \ell}$$

where ℓ is the mean free path.

The ratio

$$\kappa = \frac{\lambda_L}{\xi}$$

is called the Ginzburg–Landau parameter. Its magnitude separates all superconductors between type-I ($\kappa < 1/\sqrt{2} \approx 0.7$) and type-II ($\kappa > 1/\sqrt{2}$) superconductors. For alloys with $\ell < \xi_0$

$$\kappa = 0.75 \frac{\lambda_0}{\ell}$$

where λ_0 is the London length in a clean material at zero temperature. The conclusion is that alloys are type-II superconductors. Values of λ_L , ξ_0 , and κ for some materials are listed in Tables 1.1 and 1.2.

1.4 Critical currents and magnetic fields

1.4.1 Condensation energy

The kinetic energy density of condensate (superconducting) electrons cannot exceed

$$F_c = \frac{n_s m v_c^2}{2} = \frac{n_s \hbar^2}{2\alpha^2 m \xi^2}. \quad (1.13)$$

If the velocity v_s increases further, the kinetic energy exceeds the energy gain of the superconducting state with respect to the normal state $F_n - F_s$, and superconductivity disappears. Therefore, $F_c = F_n - F_s$ is just this energy gain which is called the condensation energy.

Assume now that the superconductor is placed in a magnetic field H . It repels the field thus increasing the energy of the external source that creates the field. The energy of the entire system increases and becomes

$$F = F_s + \frac{H^2}{8\pi} = F_n - F_c + \frac{H^2}{8\pi}.$$

In the superconducting state, $F < F_n$. When the energy reaches the energy of a normal state F_n , the superconductivity becomes no longer favorable energetically. Thus the thermodynamic critical magnetic field satisfies

$$F_c = \frac{H_c^2}{8\pi}.$$

Using the expression for λ_L we find from Eq.(1.13)

$$H_c = \frac{\hbar c}{\alpha e \lambda_L \xi} = \frac{\Phi_0}{\alpha \pi \lambda_L \xi}$$

The exact expression for H_c at temperatures close to T_c is

$$H_c = \frac{\Phi_0}{2\sqrt{2}\pi \lambda_L \xi} \quad (1.14)$$

Values of H_c for some materials are given in Table 1.1.

1.4.2 Critical currents

There may be several mechanisms of destruction of superconductivity by a current flowing through it.

Mechanism 1. Large type-I samples: The critical current I_c creates H_c at the sample surface. For a cylinder with a radius R ,

$$2\pi R H_c = \frac{4\pi}{c} I_c .$$

If $R \gg \lambda_L$, the current flows only within the layer of a thickness λ_L near the sample surface. Thus $I_c = 2\pi R \lambda_L j_c$ and

$$j_c = \frac{c H_c}{4\pi \lambda_L} . \quad (1.15)$$

Mechanism 2. If the transverse dimensions of the superconductor a and b are small, $a, b \ll \lambda_L$ the current is distributed uniformly over the cross section of the sample. In this case, the dominating mechanism is the pair-breaking: superconductivity is destroyed by the high velocity of superconducting electrons. The critical current is

$$j_c = n_s e v_c = n_s e \hbar / \alpha m \xi . \quad (1.16)$$

In fact, this current density coincides with the critical current in thick samples. Indeed, inserting H_c and λ_L in Eq. (1.15) we obtain Eq. (1.16). However, the magnetic field created at the surface $H \sim (c/4\pi) j_c a^2 / a \sim (a/\lambda_L) H_c$ is smaller than H_c . The critical current in Eqs. (1.15), (1.16) is very high. For $H_c = 500$ Oe and $\lambda_L = 500 \text{ \AA}$ it can be as high as 10^8 A/cm^2 .

In type-II superconductors, critical magnetic fields and currents are associated with *quantized vortices*.

1.5 Quantized vortices

1.5.1 Basic concepts

Consider a type-II superconductor where the London length is large. The supercurrent and magnetic field do not vanish within the region of the order of λ from the surface: there exists a sizable region of nonzero v_s . If the magnetic field is large enough, v_s can reach high values, $v_s \sim (e/mc) H r$. For fields $H \sim \hbar c / e \xi^2$, the velocity can reach $r \hbar / m \xi^2 \gg v_c$ for $r \gg \xi$. This would lead to destruction of superconductivity if there were no means for compensating a large contribution to v_s due to the magnetic field.

Assume that we have a linear singularity such that the phase χ of the wave function of superconducting electrons ψ changes by $2\pi n$ if one goes around this lines along a closed contour, see Fig. 1.4. Consider again the integral along this contour

$$-\frac{mc}{e} \oint \mathbf{v}_s \cdot d\mathbf{l} = \oint \left(\mathbf{A} - \frac{\hbar c}{2e} \nabla \chi \right) \cdot d\mathbf{l} = \int_S \text{curl } \mathbf{A} \cdot d\mathbf{S} - \frac{\hbar c}{2e} \Delta \chi$$

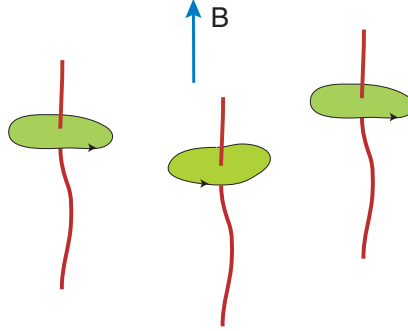


Figure 1.4: Singular lines in a SC with $2\pi n$ phase variations around them.

$$= \Phi - \frac{\hbar c}{2e} 2\pi n = \Phi - \Phi_0 n . \quad (1.17)$$

Here Φ is the magnetic flux through the contour, Φ_0 is the flux quantum. The phase change along the closed contour is $\Delta\chi = 2\pi n$. We observe that the superconducting velocity increase is completely compensated by the phase variation if the magnetic flux is $\Phi = \Phi_0 n$. One can thus expect that in superconductors with large λ_L in high magnetic fields, there will appear linear singularities with a surface density n_L such that the magnetic induction

$$B = (\Phi_0 n) n_L \quad (1.18)$$

is all distributed over vortices. Under these conditions, the superconducting velocity does not increase with distance, and superconductivity is conserved on average.

Each singularity of the phase can exist if the wave function of the superconducting electrons, i.e., the density of superconducting electrons $n_s = 2|\psi|^2$ goes to zero at the singular line. The size of the region where n_s is decreased with respect to its equilibrium value has a size of the order of the coherence length ξ and is called the vortex core. Such singular objects are called quantized vortices: each vortex carries a quantized magnetic flux $\Phi_0 n$. The condition required for existence of vortices is $\lambda > \xi$ or exactly $\kappa > 1/\sqrt{2}$. More favorable energetically are singly quantized vortices which carry one magnetic flux quantum and have a phase circulation 2π around the vortex axis.

Vortices are the objects which play a very special role in superconductors and superfluids. In superconductors, each vortex carries exactly one magnetic-flux quantum. Being magnetically active, vortices determine the magnetic properties of superconductors. In addition, they are mobile if the material is homogeneous. In fact, a superconductor in the vortex state is no longer superconducting in a usual sense. Indeed, there is no complete Meissner effect: some magnetic field penetrates into the superconductor via vortices. In addition, regions with the normal phase appear: since the order parameter turns to zero at the vortex axis and is suppressed around each vortex axis within a vortex core with a radius

of the order of the coherence length, there are regions with a finite low-energy density of states. Moreover, mobile vortices come into motion in the presence of an average (transport) current. This produces dissipation and causes a finite resistivity (the so-called flux flow resistivity): a superconductor is no longer “superconducting”.

To avoid motion of vortices and thus ensure zero resistance of a superconductor, various defects such as granular structure, lattice defects, artificial defects are introduced into the superconducting material. These defects attract vortices, or “pin” them in the superconductor. To overcome the pinning force one has to apply a finite current density, critical depinning current j_c , that produces the Lorentz force

$$\mathbf{F}_L = \frac{\Phi_0}{c} [\mathbf{j}_c \times \hat{\mathbf{z}}]$$

where $\hat{\mathbf{z}}$ is the unit vector in the direction of the magnetic field. Depending on the material, the critical current can be as high as $10^4 \div 10^5$ A/cm². For currents below the depinning current, a type-II superconductor can have zero resistance up to very high magnetic fields H_{c2} which are considerably higher than H_c (see below).

In superfluids, vortices appear in a container with helium rotating at an angular velocity Ω above a critical value which is practically not high and can easily be reached in experiment. Vortices are also created if a superfluid flows in a tube with a sufficiently high velocity. The driving force that pushes vortices is now the Magnus force. Vortices move and experience reaction from the normal component; this couples the superfluid and normal components and produces a “mutual friction” between them. As a result, the superflow is no longer persistent.

1.5.2 Vortices in the London model

Let us take curl of Eq. (1.9). We find

$$\mathbf{h} - \frac{\hbar c}{2e} \text{curl} \nabla \chi = -\frac{mc}{n_s e^2} \text{curl} \mathbf{j}_s = -\lambda_L^2 \text{curl} \text{curl} \mathbf{h} .$$

This looks like Eq. (1.5) except for one extra term. This term is nonzero if there are vortices. In the presence of vortices, the London equation should be modified. For an n -quantum vortex we have

$$\text{curl} \nabla \chi = 2\pi n \hat{\mathbf{z}} \delta^{(2)}(\mathbf{r})$$

where $\hat{\mathbf{z}}$ is the unit vector in the direction of the vortex axis. Therefore, the London equation for a vortex becomes

$$\mathbf{h} + \lambda_L^2 \text{curl} \text{curl} \mathbf{h} = n \Phi_0 \delta^{(2)}(\mathbf{r}) \quad (1.19)$$

where Φ_0 is the vector along the vortex axis with the magnitude of one flux quantum. For a system of vortices

$$\mathbf{h} + \lambda_L^2 \text{curl} \text{curl} \mathbf{h} = n \Phi_0 \sum_k \delta^{(2)}(\mathbf{r} - \mathbf{r}_k) \quad (1.20)$$

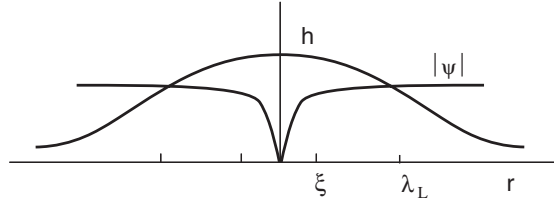


Figure 1.5: Structure of a single vortex. The core region with the radius ξ is surrounded by currents. Together with the magnetic field, they decay at distances of the order of λ_L .

where the sum is over all the vortex positions \mathbf{r}_k .

One can easily find the magnetic field for a single straight vortex (see Problem 1.1). In cylindrical coordinates $\mathbf{h} = (0, 0, h_z(r))$, the magnetic field is

$$h_z(r) = \frac{n\Phi_0}{2\pi\lambda_L^2} \ln\left(\frac{\lambda_L}{r}\right)$$

near the vortex axis $r \ll \lambda_L$. The magnetic field increases logarithmically near the vortex axis. However, in our model, the coordinate r cannot be made shorter than the coherence length since n_s vanishes at the vortex axis, and the London equation does not apply for $r < \xi$. Therefore, at the axis

$$h(0) = \frac{n\Phi_0}{2\pi\lambda_L^2} \ln\left(\frac{\lambda_L}{\xi}\right).$$

We can calculate the current around the vortex near the core.

$$j_\phi = \frac{c}{4\pi} \frac{\partial h_z}{\partial r} = \frac{nc\Phi_0}{8\pi^2\lambda_L^2 r} = \frac{n_s e n \hbar}{2mr}$$

For a single-quantum vortex the superconducting velocity is

$$v_{s,\phi} = \frac{\hbar}{2mr}$$

Therefore, the phase is just the azimuthal angle:

$$\chi = \phi$$

1.5.3 Critical fields in type-II superconductors

The free energy of a single-quantum vortex per unit length is

$$\begin{aligned} \mathcal{F} &= \frac{1}{8\pi} \int [\mathbf{h}(\mathbf{h} + \lambda_L^2 \text{curl curl } \mathbf{h}) + \text{div}[\mathbf{h} \times \text{curl } \mathbf{h}]] d^2r \\ &= \frac{1}{8\pi} \int h_z \Phi_0 \delta^{(2)}(r) d^2r + \frac{1}{8\pi} \int [\mathbf{h} \times \text{curl } \mathbf{h}] d\mathbf{l}. \end{aligned} \quad (1.21)$$

The last integral is taken along a remote contour and vanishes. The first integral gives

$$\mathcal{F}_L = \frac{\Phi_0^2}{16\pi^2\lambda_L^2} \ln \frac{\lambda_L}{\xi} = \frac{\hbar^2\pi n_s}{4m} \ln \frac{\lambda_L}{\xi} . \quad (1.22)$$

For an n -quantum vortex we would obtain

$$\mathcal{F}_L = \frac{n^2\Phi_0^2}{16\pi^2\lambda_L^2} \ln \left(\frac{\lambda_L}{\xi} \right) . \quad (1.23)$$

The energy is proportional to n^2 . Therefore, vortices with $n > 1$ are not favorable energetically. For given induction B , the number of n -quantum vortices is proportional to n^{-1} , while the energy of each vortex is proportional to n^2 . Therefore, the energy of the vortex array grows as n for given induction B . Therefore, the vortex array of single-quantum vortices has lower energy than the array of n -quantum vortices.

Equation (1.22) allows to find the lower critical magnetic field, i.e., the field H above which the first vortex appears. The free energy of a unit volume of a superconductor with a set of single-quantum vortices is $F_L = n_L\mathcal{F}_L = (B/\Phi_0)\mathcal{F}_L$. The proper thermodynamic potential in an external field \mathbf{H} is the Gibbs free energy $G = F - \mathbf{H}\mathbf{B}/4\pi$

$$G = \frac{B\mathcal{F}_L}{\Phi_0} - \frac{BH}{4\pi} = \frac{B\Phi_0}{16\pi^2\lambda_L^2} \ln \left(\frac{\lambda_L}{\xi} \right) - \frac{BH}{4\pi} .$$

If $H < H_{c1}$ where

$$H_{c1} = \frac{\Phi_0}{4\pi\lambda_L^2} \ln \left(\frac{\lambda_L}{\xi} \right) , \quad (1.24)$$

the Gibbs free energy is minimal for $B = 0$. This corresponds to zero field in the bulk: the Meissner effect takes place. The free energy becomes negative if $H > H_{c1}$. Therefore, it decreases with increasing B inside the superconductor. This means that vortices appear for $H > H_{c1}$.

As the magnetic field increases, vortices become more and more dense, see Eq. (1.18), and the normal phase in the cores occupies larger and larger fraction of the sample. The superconductivity is totally destroyed when their cores start to overlap, i.e., when their density $n_L = B/\Phi_0 \sim 1/\pi\xi^2$. The exact condition is

$$H_{c2} = \frac{\Phi_0}{2\pi\xi^2} .$$

Using Eq. (1.14) we note that

$$H_{c1} = H_c \frac{\ln \kappa}{\sqrt{2}\kappa} ; \quad H_{c2} = \sqrt{2}\kappa H_c , \quad (1.25)$$

i.e., for superconductors with a large κ , the critical field H_{c1} is considerably lower than H_{c2} . At the same time, the upper critical field H_{c2} is considerably higher than H_c .

The phase diagram of a type II superconductor is shown in Fig. 1.6.

For more reading on vortices in type II superconductors see Refs. [5, 6, 7, 8].

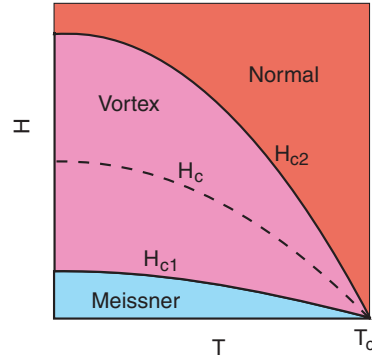


Figure 1.6: Phase diagram of a type II superconductor

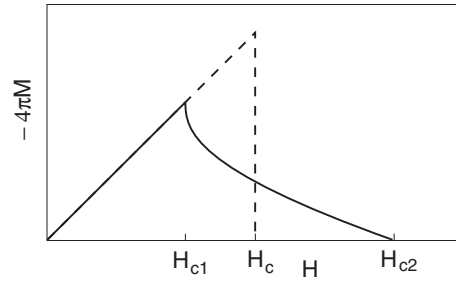


Figure 1.7: Full line: Magnetization of a type II superconductor. The linear part at low fields corresponds to the full Meissner effect Eq. (1.6). Dashed line: Magnetization of a type I superconductor. The Meissner effect persists up to the thermodynamic critical field H_c .

1.5.4 The Little and Parks effect

Let us consider a thin film with thickness d deposited on an insulating cylinder of radius R and length $L \gg R$. It is placed into an external magnetic field H parallel to the cylinder axis, see Fig. 1.8. We assume that $d \ll \lambda_L$ and $d \ll R$. After the superfluid transition a current in an azimuthal direction is generated in the film. The current is distributed homogeneously over the thickness of the film since $d \ll \lambda_L$. The magnetic field inside the cylinder is homogeneous, as well.

Free energy of the system per unit length of the cylinder is

$$\mathcal{F} = \int d^2r \left(\frac{H_{in}^2}{8\pi} + \frac{mj_s^2}{2n_s e^2} \right) = \frac{H_{in}^2 R^2}{8} + \frac{mj_s^2 2\pi R d}{2n_s e^2}$$

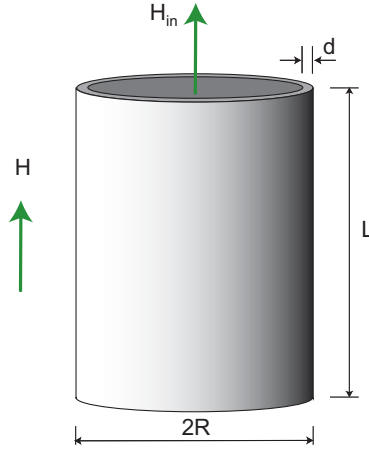


Figure 1.8: Superconducting film of thickness d is deposited on an insulating cylinder of radius R and placed into magnetic field H .

Using the solution of problem 1.6 we have

$$H_{in} \left(1 + \frac{2\lambda^2}{dR} \right) = \frac{n\Phi_0}{\pi R^2} + \frac{2\lambda^2}{dR} H \quad (1.26)$$

and

$$j_s = \frac{c}{4\pi d(1 + 2\lambda^2/dR)} \left(H - \frac{n\Phi_0}{\pi R^2} \right)$$

Therefore, after a little algebra the free energy becomes

$$\mathcal{F} = \frac{R^2}{8(1 + 2\lambda^2/dR)} \left[\left(\frac{n\Phi_0}{\pi R^2} \right)^2 + \frac{2\lambda^2 H^2}{dR} \right]$$

As we know, in an applied magnetic field H , it is the Gibbs free energy (per unit length)

$$G = \mathcal{F} - \int d^2r \frac{HB}{4\pi} = \frac{R^2}{8(1 + 2\lambda^2/dR)} \left[\left(\frac{n\Phi_0}{\pi R^2} \right)^2 + \frac{2\lambda^2 H^2}{dR} \right] - \frac{HH_{in}R^2}{4}$$

which has to be minimized. Using Eq. (1.26) we find

$$G = \frac{R^2}{8(1 + 2\lambda^2/dR)} \left(\frac{n\Phi_0}{\pi R^2} - H \right)^2 - \frac{H^2 R^2}{8}$$

The last term here is the Gibbs free energy of the cylinder interior without the superconductor. It can thus be ignored.

The rest term is the free energy G of the superconductor. It is minimal when the applied magnetic field introduces an integer number of flux quanta

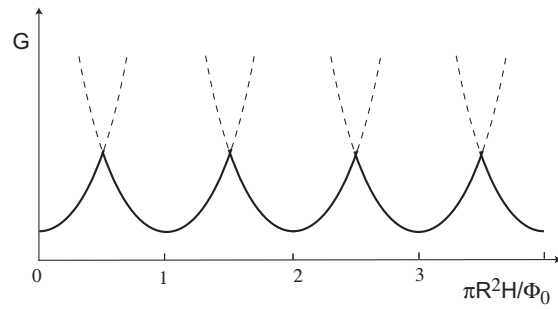


Figure 1.9: Gibbs free energy of a superconducting film deposited on an insulating cylinder and placed into magnetic field H . The plot is a set of parabolas shifted by integer numbers of flux quanta along the horizontal axis. The free energy oscillates as it goes from one parabola to another with increasing magnetic field.

into the cylinder. The free energy as a function of the magnetic field is shown in Fig. 1.9. If the flux quanta can easily pass through the superconducting film to or from the interior of the cylinder, the system will choose the branch with the corresponding number of flux quanta which minimizes the free energy for given H . The free energy thus oscillates as a function of the magnetic field due to entrance of flux quanta into the cylinder. The critical temperature of the superconductor oscillates in a similar manner. This is called the Little and Parks effect.

Problems

Problem 1.1

Calculate the magnetic field and current around a single straight vortex.

Problem 1.2

Calculate the energy of a circular vortex loop with a radius R such that $\xi \ll R \ll \lambda_L$.

Problem 1.3

Find the distribution of the magnetic field and of the current in a superconducting slab of a thickness d placed in an external homogeneous magnetic field H parallel to the slab. The longitudinal dimensions of the slab are much larger than d .

Problem 1.4

Find the distribution of the magnetic field and of the current in a superconducting slab of a thickness d carrying a total current I along the length of the slab. The longitudinal dimensions of the slab are much larger than d .

Problem 1.5

A thin superconducting film with a thickness $d \ll \lambda_L$ is deposited on a dielectric filament (cylinder) of a radius $R \gg d$. The filament is placed into a longitudinal magnetic field at a temperature $T > T_c$ and then cooled down below T_c . The field is then switched off. Find out how the captured magnetic field is quantized.

Problem 1.6

The same setting as in Problem 1.5: A thin superconducting film with a thickness $d \ll \lambda_L$ is deposited on a dielectric filament (cylinder) of a radius $R \gg d$. The filament is placed into a longitudinal magnetic field H at a temperature $T > T_c$ and then cooled down below T_c . Calculate the captured magnetic field inside the dielectric cylinder and the supercurrent in the film.

Chapter 2

The BCS theory

2.1 Landau Fermi-liquid

The ground state of a system of Fermions corresponds to the filled states with energies E below the maximal Fermi energy E_F , determined by the number of Fermions. In an homogeneous system, one can describe particle states by momentum \mathbf{p} such that the spectrum becomes $E_{\mathbf{p}}$. The condition of maximum energy $E_{\mathbf{p}} = E_F$ defines the Fermi surface in the momentum space. In an isotropic system, this is a sphere such that its volume divided by $(2\pi\hbar)^3$

$$n_{\alpha} = \frac{4\pi p_F^3}{3(2\pi\hbar)^3}$$

gives number of particles with the spin projection α per unit (spatial) volume of system. For electrons with spin $\frac{1}{2}$, the total number of particles in the unit volume of the system, i.e., the particle density is twice n_{α}

$$n = \frac{p_F^3}{3\pi^2\hbar^3} \quad (2.1)$$

This ground state corresponds to a ground-state energy E_0 .

Excitations in the Fermi liquid that increase its energy as compared to E_0 are created by moving a particle from a state below the Fermi surface to a state above it. This process can be considered as a superposition of two processes. First is a removal of a particle from the system out of a state below the Fermi surface. The second is adding a particle to a state above the Fermi surface. By taking a particle out of the state with an energy $E_1 < E_F$ we increase the energy of the system and create a hole excitation with a positive energy $\epsilon_1 = E_F - E_1$. By adding a particle into a state with an energy $E_2 > E_F$ we again increase the energy and create a particle excitation with a positive energy $\epsilon_2 = E_2 - E_F$. The energy of the system is thus increased by $\epsilon_1 + \epsilon_2 = E_2 - E_1$.

Shown in Fig. 2.1 are processes of creation of particle and hole excitations in a Fermi liquid. Consider it in more detail. Removing a particle with a

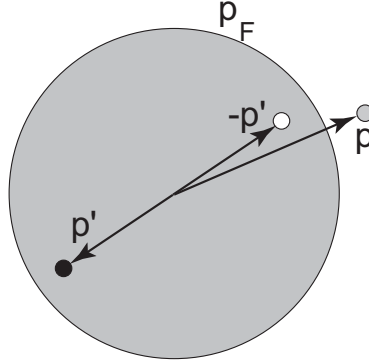


Figure 2.1: Particle (shaded circle) and hole (white circle) excitations in Landau Fermi liquid. The particle excitation is obtained by adding a particle. The hole excitation is obtained by removing a particle (black circle) with an opposite momentum.

momentum \mathbf{p}' and an energy E' from below the Fermi surface, $p' < p_F$ and $E' < E_F$, creates an excitation with a momentum $-\mathbf{p}'$ and an energy $\epsilon_{-\mathbf{p}'} = E_F - E'$. Adding a particle with a momentum \mathbf{p} and energy E above the Fermi surface, $p > p_F$ and $E > E_F$, creates an excitation with momentum \mathbf{p} and energy $\epsilon_{\mathbf{p}} = E - E_F$. For an isotropic system, the excitation spectrum will thus have the form

$$\epsilon_{\mathbf{p}} = \begin{cases} \frac{p^2}{2m} - E_F, & p > p_F \\ E_F - \frac{p^2}{2m}, & p < p_F \end{cases} \quad (2.2)$$

shown in Fig. 2.2.

The particle and hole excitations live in a system of Fermions where a strong correlation exists due to the Pauli principle. How well elementary excitations with a free-particle spectrum Eq. (2.2) are defined here? Consider this condition taking into account the process of quasiparticle-quasiparticle scattering. Assume that a particle with momentum \mathbf{p}_1 above the Fermi surface interacts with an existing particle \mathbf{p}_2 below the Fermi surface after which they both go to the states \mathbf{p}'_1 and \mathbf{p}'_2 above the Fermi surface, see Fig. 2.3. This is the only possibility according to the Pauli exclusion principle. We thus have

$$p_1 > p_F, p_2 < p_F, p'_1 > p_F, p'_2 > p_F \quad (2.3)$$

This process is shown in Fig. 2.3 together with the momentum conservation

$$\mathbf{p}_1 + \mathbf{p}_2 = \mathbf{p}'_1 + \mathbf{p}'_2 \quad (2.4)$$

The probability of such a process is

$$\begin{aligned} P &= 2m \int M \delta(p_1^2 + p_2^2 - p_1'^2 - p_2'^2) \delta^{(n)}(\mathbf{p}_1 + \mathbf{p}_2 - \mathbf{p}'_1 - \mathbf{p}'_2) d^n p_2 d^n p_1' d^n p_2' \\ &= 2m \int M \delta \left[p_1^2 + p_2^2 - p_1'^2 - (\mathbf{p}_1 + \mathbf{p}_2 - \mathbf{p}'_1)^2 \right] d^n p_2 d^n p_1' \end{aligned} \quad (2.5)$$

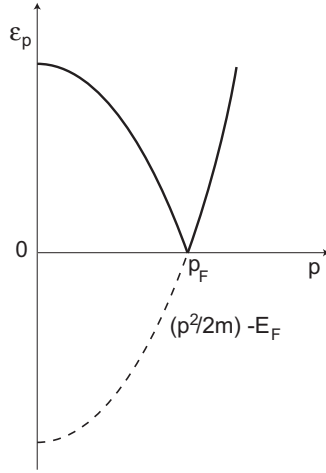


Figure 2.2: Single-particle spectrum $(p^2/2m) - E_F$ (dashed line) is transformed into the Landau excitation spectrum $\epsilon_{\mathbf{p}}$ in a strongly correlated Fermi liquid.

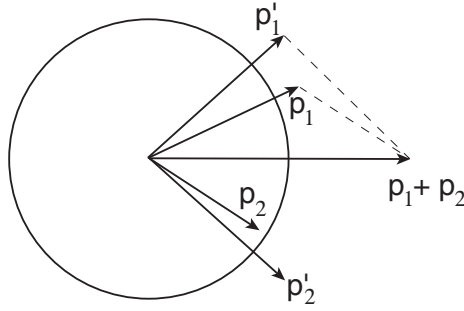


Figure 2.3: Scattering of quasiparticles.

The delta functions in the first line ensure conservations of energy and momenta, M is the corresponding matrix element, n is the dimension of space.

We shall see that the momenta we are interested in are close to the Fermi surface. According to the δ function, this means that \mathbf{p}'_1 almost coincides with \mathbf{p}_1 and \mathbf{p}'_2 is close to \mathbf{p}_2 . Therefore, Eq. (2.4) gives also

$$p_1 + p_2 = p'_1 + p'_2 \quad (2.6)$$

Indeed, from Eq. (2.4) we find

$$p_1^2 + p_2^2 + 2p_1p_2 \cos(\mathbf{p}_1 \hat{\mathbf{p}}_2) = p_1'^2 + p_2'^2 + 2p_1'p_2' \cos(\mathbf{p}'_1 \hat{\mathbf{p}}'_2)$$

Since $p_1p_2 \approx p_1'p_2' \approx p_F^2$ and $\mathbf{p}_1 \hat{\mathbf{p}}_2 = \mathbf{p}'_1 \hat{\mathbf{p}}'_2$ we have $p_1^2 + p_2^2 = p_1'^2 + p_2'^2$ and also

$$p_1^2 + p_2^2 + 2p_1p_2 = p_1'^2 + p_2'^2 + 2p_1'p_2'$$

which leads to Eq. (2.6).

Since $p'_2 > p_F$, we have

$$p'_1 = p_1 + p_2 - p'_2 < p_1 + p_2 - p_F$$

Therefore,

$$0 < p'_1 - p_F < (p_1 - p_F) + (p_2 - p_F) \quad (2.7)$$

On the other hand,

$$p_F - p_2 < p_1 - p'_1 < p_1 - p_F$$

thus

$$0 < p_F - p_2 < p_1 - p_F \quad (2.8)$$

We can now calculate the integral in Eq. (2.5). Consider first the 2D and 3D cases, $n = 2$ or $n = 3$. In these case, the delta function is removed due to integration over the angle between \mathbf{p}'_1 and \mathbf{p}_2 . We then have integrals over the magnitude of momenta. Using Eqs. (2.7) and (2.8) we find

$$\begin{aligned} P &\propto \int dp_2 dp'_1 = \int_0^{p_1 - p_F} d(p_F - p_2) \int_0^{(p_1 - p_F) + (p_2 - p_F)} d(p'_1 - p_F) \\ &= \int_0^{p_1 - p_F} [(p_1 - p_F) - (p_F - p_2)] d(p_F - p_2) = \frac{1}{2} (p_1 - p_F)^2 \end{aligned}$$

The coefficient of proportionality can be established from the dimensions

$$P \sim \frac{v_F^2 (p_1 - p_F)^2}{\hbar E_F} = \frac{\epsilon^2}{\hbar E_F}$$

This means that uncertainty of the quasiparticle energy $\delta\epsilon \sim \hbar P$ is small compared to the energy if $\epsilon \ll E_F$, i.e., near the Fermi surface. In other words, quasiparticles are well defined only near the Fermi surface.

For a one dimensional system, however, there is no angular variable, and the δ function is removed by integration over dp'_1 while the integral over dp_2 gives of the order of p_F . Therefore, there is no small parameter in P . Thus, Landau quasiparticles do not exist. The one-dimensional system of Fermions is known as the Luttinger liquid, which is beyond the present course.

Let us now define the Hamiltonian for particles and holes. For particles, we define a single-electron Hamiltonian

$$\hat{H}_e = \frac{1}{2m} \left(-i\hbar\nabla - \frac{e}{c} \mathbf{A} \right)^2 + U_0(\mathbf{r}) - \mu \quad (2.9)$$

where μ is the chemical potential. In the normal state, $\mu = E_F$. Being applied to a system of totally $\mathcal{N} = \int n dV$ particles, it will produce a Hamiltonian in the form $\mathcal{H} - \mu\mathcal{N}$ where \mathcal{H} is the Hamiltonian of the full system. This is more appropriate for a system where the chemical potential is fixed rather than the number of particles, as is the case, for example, in superconductors connected

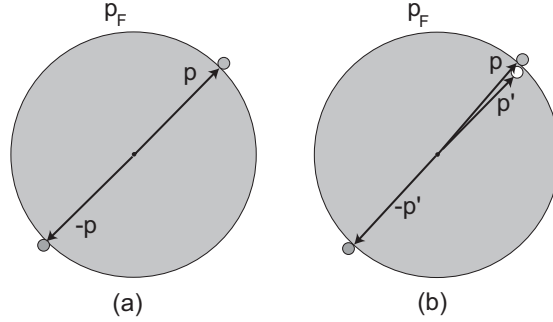


Figure 2.4: (a) A Cooper pair is formed out of a particle excitation with a momentum \mathbf{p} and that with a momentum $-\mathbf{p}$ above the Fermi surface (shaded circles), which is equivalent to (b) a particle excitation with a momentum \mathbf{p} and a removed hole excitation (white circle) with nearly the same momentum \mathbf{p}' .

to an external circuit. The Hamiltonian Eq. (2.9) corresponds to the canonical momentum operator $\hat{\mathbf{P}} = -i\hbar\nabla$ and is assumed to be spin independent.

The wave function of a particle excitation $u_{\epsilon,\mathbf{p}}(\mathbf{r})$ with an energy ϵ and momentum \mathbf{p} satisfies

$$\hat{H}_e u_{\epsilon,\mathbf{p}}(\mathbf{r}) = \epsilon_{\mathbf{p}} u_{\epsilon,\mathbf{p}}(\mathbf{r}) \quad (2.10)$$

Let us now turn to hole excitations. The hole wave function $v_{\epsilon,\mathbf{p}}(\mathbf{r})$ with an energy ϵ and momentum \mathbf{p} satisfies

$$\hat{H}_h v_{\epsilon,\mathbf{p}}(\mathbf{r}) = \epsilon_{\mathbf{p}} v_{\epsilon,\mathbf{p}}(\mathbf{r})$$

A hole excitation is the absence of a particle with the energy $-\epsilon$ and momentum $-\mathbf{p}$. According to the Landau Fermi-liquid description, the hole Hamiltonian is thus

$$\hat{H}_h = -\hat{H}_e^*$$

The Hamiltonian

$$\hat{H}_e^* = \frac{1}{2m} \left(i\hbar\nabla - \frac{e}{c}\mathbf{A} \right)^2 + U_0(\mathbf{r}) - E_F \quad (2.11)$$

corresponds to the canonical momentum operator $-\hat{\mathbf{P}} = i\hbar\nabla$. The hole wave function thus satisfies

$$\hat{H}_e^* v_{\epsilon,\mathbf{p}}(\mathbf{r}) = -\epsilon_{\mathbf{p}} v_{\epsilon,\mathbf{p}}(\mathbf{r}) \quad (2.12)$$

2.2 The Cooper problem

The original Cooper problem is as follows. Consider an object which is made out of a pair of electrons with energies $\epsilon_{\mathbf{p}}$ having momenta \mathbf{p} and $-\mathbf{p}$ slightly beyond the Fermi surface, see Fig. 2.4 (a). Their wave functions are $u_{\mathbf{p}}(\mathbf{r}) =$

$e^{i\mathbf{p}\cdot\mathbf{r}/\hbar}U_{\mathbf{p}}$ and $u_{-\mathbf{p}}(\mathbf{r}) = e^{-i\mathbf{p}\cdot\mathbf{r}/\hbar}U_{-\mathbf{p}}$, respectively. We shall see later that the pair is actually formed out of an electron in a state $u_{\mathbf{p}}(\mathbf{r}) = e^{i\mathbf{p}\cdot\mathbf{r}/\hbar}U_{\mathbf{p}}$ above the Fermi surface and an annihilated hole which was formerly in a state $v_{\mathbf{p}'}(\mathbf{r}) = e^{i\mathbf{p}'\cdot\mathbf{r}/\hbar}V_{\mathbf{p}'}$ with nearly the same momentum $\mathbf{p}' \approx \mathbf{p}$ below the Fermi surface. The annihilated hole is in a sense equivalent to an electron with momentum $-\mathbf{p}'$ and has a wave function $v_{\mathbf{p}'}^*(\mathbf{r}) = u_{-\mathbf{p}'}(\mathbf{r}) = e^{-i\mathbf{p}'\cdot\mathbf{r}/\hbar}V_{\mathbf{p}'}^*$, Fig. 2.4 (b).

The pair wave function is

$$\Psi_{\mathbf{p}}^{\text{pair}}(\mathbf{r}_1, \mathbf{r}_2) = u_{\mathbf{p}}(\mathbf{r}_1)u_{-\mathbf{p}}(\mathbf{r}_2) = e^{i\mathbf{p}\cdot(\mathbf{r}_1-\mathbf{r}_2)/\hbar}U_{\mathbf{p}}V_{\mathbf{p}}^*$$

The linear combination with various \mathbf{p} gives the coordinate wave function

$$\Psi^{\text{pair}}(\mathbf{r}_1, \mathbf{r}_2) = \sum_{\mathbf{p}} e^{i\mathbf{p}\cdot(\mathbf{r}_1-\mathbf{r}_2)/\hbar} a_{\mathbf{p}} \quad (2.13)$$

where $a_{\mathbf{p}} = U_{\mathbf{p}}V_{\mathbf{p}}^*$. The inverse transformation is

$$a_{\mathbf{p}} = V^{-1} \int \Psi(\mathbf{r}) e^{-i\mathbf{p}\cdot\mathbf{r}/\hbar} d^3r$$

where V is the volume of the system.

Assume that the electrons in the pair interact through the potential $W(\mathbf{r}_1, \mathbf{r}_2) = W(\mathbf{r}_1 - \mathbf{r}_2)$. Their Hamiltonian is $\hat{H}_e(1) + \hat{H}_e(2) + W$. The Schrödinger equation has the form

$$\left[\hat{H}_e(\mathbf{r}_1) + \hat{H}_e(\mathbf{r}_2) + W(\mathbf{r}_1, \mathbf{r}_2) \right] \Psi^{\text{pair}}(\mathbf{r}_1, \mathbf{r}_2) = E \Psi^{\text{pair}}(\mathbf{r}_1, \mathbf{r}_2)$$

Multiplying this by $e^{-i\mathbf{p}\cdot(\mathbf{r}_1-\mathbf{r}_2)}$ and calculating the integral over the volume we obtain this equation in the momentum representation,

$$[2\epsilon_{\mathbf{p}} - E_{\mathbf{p}}] a_{\mathbf{p}} = - \sum_{\mathbf{p}_1} W_{\mathbf{p}, \mathbf{p}_1} a_{\mathbf{p}_1}$$

where

$$W_{\mathbf{p}, \mathbf{p}_1} = V^{-1} \int e^{-i(\mathbf{p}-\mathbf{p}_1)\cdot\mathbf{r}/\hbar} W(\mathbf{r}) d^3r$$

Assume that

$$W_{\mathbf{p}, \mathbf{p}_1} = \begin{cases} W/V, & \epsilon_{\mathbf{p}} \text{ and } \epsilon_{\mathbf{p}_1} < E_c \\ 0, & \epsilon_{\mathbf{p}} \text{ or } \epsilon_{\mathbf{p}_1} > E_c \end{cases}$$

where $E_c \ll E_F$. The interaction strength $W \sim W_0 v_0$ where W_0 is the magnitude of the interaction potential while $v_0 = a_0^3$ is the volume where the interaction of a range a_0 is concentrated. We have

$$a_{\mathbf{p}} = \frac{W}{E - 2\epsilon_{\mathbf{p}}} \frac{1}{V} \sum_{\mathbf{p}_1} a_{\mathbf{p}_1} = \frac{W}{E - 2\epsilon_{\mathbf{p}}} \sum'_{\mathbf{p}_1} a_{\mathbf{p}_1} \quad (2.14)$$

Here the sum $\sum_{\mathbf{p}}$ is taken over \mathbf{p} which satisfy $\epsilon_{\mathbf{p}} < E_c$, while the sum \sum' is taken over the states in a unit volume. Let us denote

$$C = \sum'_{\mathbf{p}} a_{\mathbf{p}}$$

Eq. (2.14) yields

$$a_{\mathbf{p}} = \frac{WC}{E - 2\epsilon_{\mathbf{p}}}$$

whence

$$C = WC \sum'_{\mathbf{p}} \frac{1}{E - 2\epsilon_{\mathbf{p}}}$$

This gives

$$\frac{1}{W} = \sum'_{\mathbf{p}} \frac{1}{E - 2\epsilon_{\mathbf{p}}} \equiv \Phi(E) \quad (2.15)$$

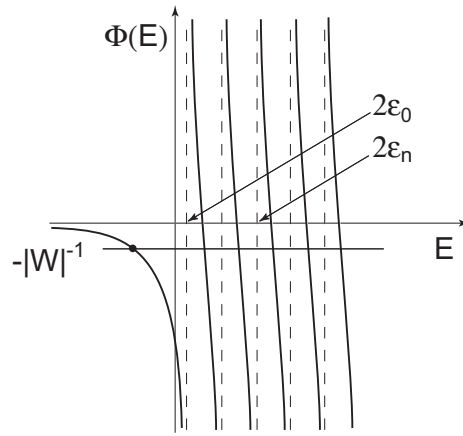


Figure 2.5: The function $\Phi(E)$ for a system with a discrete spectrum ϵ_n .

Equation (2.15) is illustrated in Fig. 2.5. Let us put our system in a large box. The levels $\epsilon_{\mathbf{p}}$ will become a discrete set ϵ_n shown in Fig. 2.5 by vertical dashed lines. The lowest level ϵ_0 is very close to zero and will approach zero as the size of the box increases. The function $\Phi(E)$ varies from $-\infty$ to $+\infty$ as E increases and crosses each $\epsilon_n > 0$. However, for negative $E < 0$, the function $\Phi(E)$ approaches zero as $E \rightarrow -\infty$, and there is a crossing point with a negative level $-1/|W|$ for negative E . This implies that there is a state with $E < 0$ satisfying Eq. (2.15) for a negative $W < 0$.

For an attraction $W < 0$ we have

$$\frac{1}{|W|} = \sum'_{\mathbf{p}} \frac{1}{2\epsilon_{\mathbf{p}} - E}$$

Let $n(\epsilon)$ be the number of states within a unit volume per one spin projection with energies below ϵ . The quantity

$$N(\epsilon) = \frac{dn(\epsilon)}{d\epsilon}$$

is called the density of states (DOS). In the normal state where $\epsilon_{\mathbf{p}} = p^2/2m - E_F$,

$$n(\epsilon) = \frac{(4/3)\pi p^3}{(2\pi\hbar)^3}$$

Therefore,

$$N(\epsilon) = \frac{mp}{2\pi^2\hbar^3}$$

Having this in mind, we substitute the sum with the integral

$$\sum'_{\mathbf{p}} = 2 \int \frac{d^3p}{(2\pi\hbar)^3} = 2 \int \frac{mp}{2\pi^2\hbar^3} d\epsilon_{\mathbf{p}}$$

the factor 2 accounts for the spin.

Now, for negative energy $E = -|E_0|$

$$\frac{1}{|W|} = 2 \int_0^{E_c} \frac{mp}{2\pi^2\hbar^3} \frac{d\epsilon_{\mathbf{p}}}{2\epsilon_{\mathbf{p}} - E_0} = 2N(0) \int_0^{E_c} \frac{d\epsilon}{2\epsilon + |E_0|} = N(0) \ln \left(\frac{|E_0| + 2E_c}{|E_0|} \right) \quad (2.16)$$

Here we replace p with a constant p_F since $E_c \ll E_F$ and thus $|p - p_F| \ll p_F$. We also denote

$$N(0) = \frac{mp_F}{2\pi^2\hbar^3} \quad (2.17)$$

the density of states at the Fermi surface. Eq. (2.16) yields

$$|E_0| = \frac{2E_c}{e^{1/N(0)|W|} - 1} \quad (2.18)$$

The dimensionless factor $\lambda \equiv N(0)W \sim N(0)W_0 a_0^3$ is called the interaction constant. For weak coupling, $N(0)|W| \ll 1$, we find

$$|E_0| = 2E_c e^{-1/N(0)|W|}$$

For a strong coupling, $N(0)|W| \gg 1$,

$$|E_0| = 2N(0)|W|E_c$$

We see that there exists a state of a particle-hole pair (the Cooper pair) with an energy $|E_0|$ below the Fermi surface. It means that the system of normal-state particles and holes is unstable towards formation of pairs provided there is an attraction (however small) between electrons. In conventional superconductors, the attraction is caused by an exchange of phonons. The attraction between electrons can also be caused by magnetic interactions which favors triplet pairing (with a nonzero spin of pair). The Coulomb repulsion is strongly reduced by screening effects at distances of the order of the size of the pair ξ thus it does not destroy pairing. Fig. 2.6 illustrates the effect on the excitation spectrum of coupling between a particle and a hole near the Fermi surface shown in Fig. 2.4.

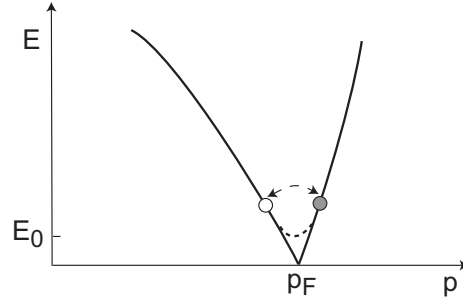


Figure 2.6: The coupling between electron and hole modifies the energy spectrum: The gap equal to $|E_0|$ opens near the Fermi surface.

This Cooper pairing effect provides a basis for understanding of superconductivity. According to this picture, the pairs, being Bose particles, form a Bose condensate in a single state with a wave function that has a single phase for all pairs, which is the basic requirement for existence of a spontaneous supercurrent.

2.3 The BCS model

2.3.1 Wave functions

According to the above picture, excitations in the normal state are particles and holes. Using the Landau description of Fermi liquid systems we assume that the wave functions (annihilation and creation operators) of electrons at a point \mathbf{r} with a spin \uparrow or \downarrow in the superconducting state are linear combinations of these states, i.e., of particles and holes,

$$\Psi^\dagger(\mathbf{r} \uparrow) = \sum_n \left[\gamma_{n\uparrow}^\dagger u_n^*(\mathbf{r}) - \gamma_{n\downarrow} v_n(\mathbf{r}) \right] \quad (2.19)$$

$$\Psi^\dagger(\mathbf{r} \downarrow) = \sum_n \left[\gamma_{n\downarrow}^\dagger u_n^*(\mathbf{r}) + \gamma_{n\uparrow} v_n(\mathbf{r}) \right] \quad (2.20)$$

and

$$\Psi(\mathbf{r} \uparrow) = \sum_n \left[\gamma_{n\uparrow} u_n(\mathbf{r}) - \gamma_{n\downarrow}^\dagger v_n^*(\mathbf{r}) \right] \quad (2.21)$$

$$\Psi(\mathbf{r} \downarrow) = \sum_n \left[\gamma_{n\downarrow} u_n(\mathbf{r}) + \gamma_{n\uparrow}^\dagger v_n^*(\mathbf{r}) \right] \quad (2.22)$$

Here $\gamma_{n\uparrow}^\dagger$ creates a particle in the state n with the spin up while $\gamma_{n\downarrow}$ annihilates hole with the spin down. The wave functions of excitations u and v are also modified as compared to the normal state. Our task is to find the new wave functions.

The electron operators obey the Fermi commutation rules

$$\begin{aligned}\Psi(\mathbf{r}, \alpha)\Psi(\mathbf{r}', \beta) + \Psi(\mathbf{r}', \beta)\Psi(\mathbf{r}, \alpha) &= 0 \\ \Psi^\dagger(\mathbf{r}, \alpha)\Psi^\dagger(\mathbf{r}', \beta) + \Psi^\dagger(\mathbf{r}', \beta)\Psi^\dagger(\mathbf{r}, \alpha) &= 0 \\ \Psi^\dagger(\mathbf{r}, \alpha)\Psi(\mathbf{r}', \beta) + \Psi(\mathbf{r}', \beta)\Psi^\dagger(\mathbf{r}, \alpha) &= \delta_{\alpha\beta}\delta(\mathbf{r} - \mathbf{r}')\end{aligned}\quad (2.23)$$

where α is a spin index. The particle and hole operators also obey the Fermi commutation rules

$$\begin{aligned}\gamma_{n,\alpha}\gamma_{m,\beta} + \gamma_{m,\beta}\gamma_{n,\alpha} &= 0 \\ \gamma_{n,\alpha}^\dagger\gamma_{m,\beta}^\dagger + \gamma_{m,\beta}^\dagger\gamma_{n,\alpha}^\dagger &= 0 \\ \gamma_{n,\alpha}^\dagger\gamma_{m,\beta} + \gamma_{m,\beta}\gamma_{n,\alpha}^\dagger &= \delta_{\alpha\beta}\delta_{mn}\end{aligned}\quad (2.24)$$

To make Eqs. (2.23) and (2.24) compatible the functions u and v should satisfy the completeness condition

$$\sum_n [u_n^*(\mathbf{r})u_n(\mathbf{r}') + v_n^*(\mathbf{r}')v_n(\mathbf{r})] = \delta(\mathbf{r} - \mathbf{r}') \quad (2.25)$$

and, in addition,

$$\sum_n [u_n^*(\mathbf{r})v_n(\mathbf{r}') - u_n^*(\mathbf{r}')v_n(\mathbf{r})] = 0 \quad (2.26)$$

To derive Eq. (2.25) we calculate the last anticommutator in Eqs. (2.23). For example,

$$\begin{aligned}& \Psi^\dagger(\mathbf{r} \uparrow)\Psi(\mathbf{r}' \uparrow) + \Psi(\mathbf{r}' \uparrow)\Psi^\dagger(\mathbf{r} \uparrow) \\ &= \sum_{n,m} [\gamma_{n\uparrow}^\dagger\gamma_{m\uparrow} + \gamma_{m\uparrow}\gamma_{n\uparrow}^\dagger] u_n^*(\mathbf{r})u_m(\mathbf{r}') + \sum_{n,m} [\gamma_{m\downarrow}^\dagger\gamma_{n\downarrow} + \gamma_{n\downarrow}\gamma_{m\downarrow}^\dagger] v_n(\mathbf{r})v_m^*(\mathbf{r}') \\ & \quad - \sum_{n,m} [\gamma_{n\downarrow}\gamma_{m\uparrow} + \gamma_{m\uparrow}\gamma_{n\downarrow}] v_n(\mathbf{r})u_m(\mathbf{r}') - \sum_{n,m} [\gamma_{n\uparrow}^\dagger\gamma_{m\downarrow}^\dagger + \gamma_{m\downarrow}^\dagger\gamma_{n\uparrow}^\dagger] u_n^*(\mathbf{r})v_m^*(\mathbf{r}') \\ &= \sum_n [u_n^*(\mathbf{r})u_n(\mathbf{r}') + v_n(\mathbf{r})v_n^*(\mathbf{r}')] = \delta(\mathbf{r} - \mathbf{r}')\end{aligned}$$

Here we use Eqs. (2.24). To derive Eq. (2.26), let us calculate the second anticommutator in Eq. (2.23)

$$\begin{aligned}0 &= \Psi^\dagger(\mathbf{r} \uparrow)\Psi^\dagger(\mathbf{r}' \downarrow) + \Psi^\dagger(\mathbf{r}' \downarrow)\Psi^\dagger(\mathbf{r} \uparrow) \\ &= \sum_{m,n} [\gamma_{n\uparrow}^\dagger\gamma_{m\downarrow}^\dagger + \gamma_{m\downarrow}^\dagger\gamma_{n\uparrow}^\dagger] u_m^*(\mathbf{r}')u_n^*(\mathbf{r}) - \sum_{m,n} [\gamma_{n\downarrow}\gamma_{m\uparrow} + \gamma_{m\uparrow}\gamma_{n\downarrow}] v_m(\mathbf{r}')v_n(\mathbf{r}) \\ & \quad + \sum_{m,n} [\gamma_{n\uparrow}^\dagger\gamma_{m\uparrow} + \gamma_{m\uparrow}\gamma_{n\uparrow}^\dagger] u_n^*(\mathbf{r})v_m(\mathbf{r}') - \sum_{m,n} [\gamma_{n\downarrow}\gamma_{m\downarrow}^\dagger + \gamma_{m\downarrow}^\dagger\gamma_{n\downarrow}] u_m^*(\mathbf{r}')v_n(\mathbf{r}) \\ &= \sum_n [u_n^*(\mathbf{r})v_n(\mathbf{r}') - u_n^*(\mathbf{r}')v_n(\mathbf{r})]\end{aligned}$$

If the state is specified by a wave vector \mathbf{q} such that $u_{\mathbf{q}}, v_{\mathbf{q}} \propto e^{i\mathbf{q}\cdot\mathbf{r}}$, we have per unit volume

$$\sum_n \rightarrow \int \frac{d^3q}{(2\pi)^3}$$

and the completeness condition becomes

$$\int \frac{d^3q}{(2\pi)^3} [u_{\mathbf{q}}^*(\mathbf{r})u_{\mathbf{q}}(\mathbf{r}') + v_{\mathbf{q}}^*(\mathbf{r}')v_{\mathbf{q}}(\mathbf{r})] = \delta(\mathbf{r} - \mathbf{r}') \quad (2.27)$$

2.3.2 Hamiltonian

The Hamiltonian operator of the system of electrons has the form

$$\mathcal{H} = \mathcal{H}_{kin} + \mathcal{H}_{int}$$

where the “kinetic energy” operator is

$$\mathcal{H}_{kin} = \sum_{\alpha} \int d^3r \Psi^{\dagger}(\mathbf{r}, \alpha) \hat{H}_e \Psi(\mathbf{r}, \alpha) \quad (2.28)$$

and the pairwise point-like interaction is taken in the form $W(\mathbf{r}_1, \mathbf{r}_2) = -W\delta_{\mathbf{r}_1 - \mathbf{r}_2}$. Here $W \sim W_0 a^3$ where W_0 is the magnitude of the interaction while a is its range. The interaction Hamiltonian is

$$\begin{aligned} \mathcal{H}_{int} &= \frac{1}{2} \sum_{\alpha, \beta} \int d^3r_1 d^3r_2 \Psi^{\dagger}(\mathbf{r}_2, \alpha) \Psi^{\dagger}(\mathbf{r}_1, \beta) W(\mathbf{r}_1, \mathbf{r}_2) \Psi(\mathbf{r}_1, \beta) \Psi(\mathbf{r}_2, \alpha) \\ &= -\frac{W}{2} \sum_{\alpha, \beta} \int d^3r \Psi^{\dagger}(\mathbf{r}, \alpha) \Psi^{\dagger}(\mathbf{r}, \beta) \Psi(\mathbf{r}, \beta) \Psi(\mathbf{r}, \alpha) \end{aligned} \quad (2.29)$$

It is attractive provided $W > 0$. The dimension of the pair of operators $\Psi^{\dagger}\Psi$ is the dimension of electron density, i.e. L^{-3} where L is the dimension of length. Therefore, the dimension of the Hamiltonian is $[W]L^{-6}L^3 = [W_0]a^3/L^3$, i.e. it has the dimension of energy. The total Hamiltonian is of the fourth order in $\hat{\Psi}$ operators which makes all calculations extremely complicated.

To simplify the theory, we introduce an effective *mean-field* Hamiltonian which is of the second order in $\hat{\Psi}$:

$$\begin{aligned} \mathcal{H}_{eff} &= \int d^3r \sum_{\alpha} \left[\Psi^{\dagger}(\mathbf{r}, \alpha) \hat{H}_e \Psi(\mathbf{r}, \alpha) + U(\mathbf{r}) \Psi^{\dagger}(\mathbf{r}, \alpha) \Psi(\mathbf{r}, \alpha) \right] \\ &\quad + \int d^3r \left[\Delta(\mathbf{r}) \Psi^{\dagger}(\mathbf{r}, \uparrow) \Psi^{\dagger}(\mathbf{r}, \downarrow) + \Delta^*(\mathbf{r}) \Psi(\mathbf{r}, \downarrow) \Psi(\mathbf{r}, \uparrow) + H_0(\mathbf{r}) \right] \end{aligned} \quad (2.30)$$

It contains yet unknown real effective field $U(\mathbf{r})$ and a complex effective field $\Delta(\mathbf{r})$. The quantity $H_0(\mathbf{r})$ does not depend on the fields Ψ and Ψ^{\dagger} . The idea is that

(1) This Hamiltonian is diagonal in the new operators $\gamma_{n,\alpha}$ and $\gamma_{n,\alpha}^\dagger$,

$$\mathcal{H}_{eff} = E_g + \sum_{n,\alpha} \epsilon_n \gamma_{n,\alpha}^\dagger \gamma_{n,\alpha} , \quad (2.31)$$

where E_g is the energy of the ground state, while ϵ_n is an energy of the excitation in a state n .

(2) The effective fields $U(\mathbf{r})$ and $\Delta(\mathbf{r})$ are chosen such that the effective Hamiltonian is as close to the true Hamiltonian as possible. This means that (i) the statistically averaged $\langle \mathcal{H}_{eff} \rangle$ has a minimum at the same wave functions as the average of the true Hamiltonian $\langle \mathcal{H} \rangle$. Moreover, (ii) these minimal values coincide. By definition, the statistical average is

$$\langle \mathcal{H}_{eff} \rangle = \mathcal{Z}^{-1} \sum_k \langle \psi_k^\dagger | \mathcal{H}_{eff} | \psi_k \rangle \exp(-E_k/T) , \quad (2.32)$$

where ψ_k is the set of eigenfunctions of the Hamiltonian

$$\mathcal{H}_{eff} \psi_k = E_k \psi_k$$

The partition function is

$$\mathcal{Z} = \sum_k \exp(-E_k/T) .$$

Similar equations hold for the true Hamiltonian.

2.3.3 The Bogoliubov–de Gennes equations

To fulfil condition (1) let us calculate the commutators

$$\begin{aligned} [\mathcal{H}_{eff}, \Psi(\mathbf{r}, \uparrow)]_- &= \mathcal{H}_{eff} \Psi(\mathbf{r}, \uparrow) - \Psi(\mathbf{r}, \uparrow) \mathcal{H}_{eff} \\ [\mathcal{H}_{eff}, \Psi(\mathbf{r}, \downarrow)]_- &= \mathcal{H}_{eff} \Psi(\mathbf{r}, \downarrow) - \Psi(\mathbf{r}, \downarrow) \mathcal{H}_{eff} \end{aligned}$$

We find

$$[\mathcal{H}_{eff}, \Psi(\mathbf{r}, \uparrow)]_- = - \left[\hat{H}_e + U(\mathbf{r}) \right] \Psi(\mathbf{r}, \uparrow) - \Delta(\mathbf{r}) \Psi^\dagger(\mathbf{r}, \downarrow) \quad (2.33)$$

$$[\mathcal{H}_{eff}, \Psi(\mathbf{r}, \downarrow)]_- = - \left[\hat{H}_e + U(\mathbf{r}) \right] \Psi(\mathbf{r}, \downarrow) + \Delta(\mathbf{r}) \Psi^\dagger(\mathbf{r}, \uparrow) \quad (2.34)$$

We now express the operators Ψ in both sides of these equations through the operators γ using Eqs. (2.21) and (2.22). The commutators $[\mathcal{H}_{eff}, \gamma_{n,\alpha}]_-$ are then calculated using Eq. (2.31):

$$\begin{aligned} [\mathcal{H}_{eff}, \gamma_{n,\alpha}]_- &= -\epsilon_n \gamma_{n,\alpha} \\ [\mathcal{H}_{eff}, \gamma_{n,\alpha}^\dagger]_- &= \epsilon_n \gamma_{n,\alpha}^\dagger \end{aligned} \quad (2.35)$$

Comparing the terms with γ and γ^\dagger we find that Eqs. (2.35) hold provided the wave functions u and v satisfy the *Bogoliubov-de Gennes equations* (BdGE)

$$\left[\hat{H}_e + U(\mathbf{r}) \right] u(\mathbf{r}) + \Delta(\mathbf{r})v(\mathbf{r}) = \epsilon u(\mathbf{r}) \quad (2.36)$$

$$- \left[\hat{H}_e^* + U(\mathbf{r}) \right] v(\mathbf{r}) + \Delta^*(\mathbf{r})u(\mathbf{r}) = \epsilon v(\mathbf{r}) \quad (2.37)$$

BdGE can be written in the vector form

$$\check{\Omega} \begin{pmatrix} u_n \\ v_n \end{pmatrix} = \epsilon_n \begin{pmatrix} u_n \\ v_n \end{pmatrix} \quad (2.38)$$

where the matrix operator is

$$\check{\Omega} = \begin{pmatrix} \hat{H}_e + U & \Delta \\ \Delta^* & -[\hat{H}_e^* + U] \end{pmatrix}$$

The Hermitian conjugated equation is

$$\left(u_n^*, v_n^* \right) \check{\Omega}^\dagger = \left(u_n^*, v_n^* \right) \epsilon_n$$

where the transposed operator

$$\check{\Omega}^\dagger = \begin{pmatrix} \hat{H}_e^* + U & \Delta \\ \Delta^* & -[\hat{H}_e + U] \end{pmatrix}$$

acts on the left. We now multiply Eq. (2.38) by the conjugated vector (u_m^*, v_m^*) and integrate over space. Transferring the operators \hat{H}_e and \hat{H}_e^* to the left we find

$$(\epsilon_n - \epsilon_m) \int [u_m^*(\mathbf{r})u_n(\mathbf{r}) + v_m^*(\mathbf{r})v_n(\mathbf{r})] d^3r = 0$$

It means that the functions (u, v) are orthogonal

$$\int [u_m^*(\mathbf{r})u_n(\mathbf{r}) + v_m^*(\mathbf{r})v_n(\mathbf{r})] d^3r = \delta_{mn} \quad (2.39)$$

The factor unity in front of δ_{mn} corresponds to the normalization of the wave functions Eq. (2.25), (2.27). For the momentum representation we have

$$\int [u_{\mathbf{q}_1}^*(\mathbf{r})u_{\mathbf{q}_2}(\mathbf{r}) + v_{\mathbf{q}_1}^*(\mathbf{r})v_{\mathbf{q}_2}(\mathbf{r})] d^3r = (2\pi)^3 \delta(\mathbf{q}_1 - \mathbf{q}_2) \quad (2.40)$$

Equations (2.36) and (2.37) possess an important property: If the vector

$$\begin{pmatrix} u_n \\ v_n \end{pmatrix} \text{ belongs to an energy } \epsilon_n \quad (2.41)$$

then the vector

$$\begin{pmatrix} v_n^* \\ -u_n^* \end{pmatrix} \text{ belongs to the energy } -\epsilon_n. \quad (2.42)$$

2.3.4 The self-consistency equation

To fulfil condition (2) we write

$$\begin{aligned} \langle \mathcal{H} \rangle &= \sum_{\alpha} \int d^3r \langle \Psi^{\dagger}(\mathbf{r}, \alpha) \hat{H}_e \Psi(\mathbf{r}, \alpha) \rangle \\ &\quad - \frac{W}{2} \sum_{\alpha, \beta} \int d^3r \langle \Psi^{\dagger}(\mathbf{r}, \alpha) \Psi^{\dagger}(\mathbf{r}, \beta) \Psi(\mathbf{r}, \beta) \Psi(\mathbf{r}, \alpha) \rangle \end{aligned}$$

We now use the Wick's theorem according to which

$$\begin{aligned} \langle \Psi^{\dagger}(\mathbf{r}_1, \alpha) \Psi^{\dagger}(\mathbf{r}_2, \beta) \Psi(\mathbf{r}_3, \gamma) \Psi(\mathbf{r}_4, \delta) \rangle &= \langle \Psi^{\dagger}(\mathbf{r}_1, \alpha) \Psi^{\dagger}(\mathbf{r}_2, \beta) \rangle \langle \Psi(\mathbf{r}_3, \gamma) \Psi(\mathbf{r}_4, \delta) \rangle \\ &\quad + \langle \Psi^{\dagger}(\mathbf{r}_1, \alpha) \Psi(\mathbf{r}_4, \delta) \rangle \langle \Psi^{\dagger}(\mathbf{r}_2, \beta) \Psi(\mathbf{r}_3, \gamma) \rangle \\ &\quad - \langle \Psi^{\dagger}(\mathbf{r}_1, \alpha) \Psi(\mathbf{r}_3, \gamma) \rangle \langle \Psi^{\dagger}(\mathbf{r}_2, \beta) \Psi(\mathbf{r}_4, \delta) \rangle \end{aligned}$$

Therefore

$$\begin{aligned} \sum_{\alpha, \beta} \langle \Psi^{\dagger}(\mathbf{r}, \alpha) \Psi^{\dagger}(\mathbf{r}, \beta) \Psi(\mathbf{r}, \beta) \Psi(\mathbf{r}, \alpha) \rangle &= \langle \Psi^{\dagger}(\mathbf{r}, \uparrow) \Psi^{\dagger}(\mathbf{r}, \downarrow) \rangle \langle \Psi(\mathbf{r}, \downarrow) \Psi(\mathbf{r}, \uparrow) \rangle \\ &\quad + \langle \Psi^{\dagger}(\mathbf{r}, \downarrow) \Psi^{\dagger}(\mathbf{r}, \uparrow) \rangle \langle \Psi(\mathbf{r}, \uparrow) \Psi(\mathbf{r}, \downarrow) \rangle \\ &\quad + \sum_{\alpha, \beta} \langle \Psi^{\dagger}(\mathbf{r}, \alpha) \Psi(\mathbf{r}, \alpha) \rangle \langle \Psi^{\dagger}(\mathbf{r}, \beta) \Psi(\mathbf{r}, \beta) \rangle \\ &\quad - \sum_{\alpha, \beta} \langle \Psi^{\dagger}(\mathbf{r}, \alpha) \Psi(\mathbf{r}, \beta) \rangle \langle \Psi^{\dagger}(\mathbf{r}, \beta) \Psi(\mathbf{r}, \alpha) \rangle \end{aligned}$$

Here we assume that

$$\langle \Psi^{\dagger}(\mathbf{r}, \uparrow) \Psi^{\dagger}(\mathbf{r}, \downarrow) \rangle \neq 0 \text{ and } \langle \Psi(\mathbf{r}, \downarrow) \Psi(\mathbf{r}, \uparrow) \rangle \neq 0$$

due to the Cooper pairing, while

$$\langle \Psi^{\dagger}(\mathbf{r}, \uparrow) \Psi^{\dagger}(\mathbf{r}, \uparrow) \rangle = 0 \text{ and } \langle \Psi(\mathbf{r}, \downarrow) \Psi(\mathbf{r}, \downarrow) \rangle = 0$$

because pairing occurs for particles with opposite spins.

Assume also that

$$\langle \Psi^{\dagger}(\mathbf{r}, \uparrow) \Psi(\mathbf{r}, \downarrow) \rangle = 0 \text{ and } \langle \Psi^{\dagger}(\mathbf{r}, \downarrow) \Psi(\mathbf{r}, \uparrow) \rangle = 0$$

due to the absence of magnetic interaction. Using the anticommutation relations we finally obtain

$$\begin{aligned} \sum_{\alpha, \beta} \langle \Psi^{\dagger}(\mathbf{r}, \alpha) \Psi^{\dagger}(\mathbf{r}, \beta) \Psi(\mathbf{r}, \beta) \Psi(\mathbf{r}, \alpha) \rangle &= 2 \langle \Psi^{\dagger}(\mathbf{r}, \uparrow) \Psi^{\dagger}(\mathbf{r}, \downarrow) \rangle \langle \Psi(\mathbf{r}, \downarrow) \Psi(\mathbf{r}, \uparrow) \rangle \\ &\quad + \sum_{\alpha, \beta} \langle \Psi^{\dagger}(\mathbf{r}, \alpha) \Psi(\mathbf{r}, \alpha) \rangle \langle \Psi^{\dagger}(\mathbf{r}, \beta) \Psi(\mathbf{r}, \beta) \rangle \\ &\quad - \sum_{\alpha} \langle \Psi^{\dagger}(\mathbf{r}, \alpha) \Psi(\mathbf{r}, \alpha) \rangle \langle \Psi^{\dagger}(\mathbf{r}, \alpha) \Psi(\mathbf{r}, \alpha) \rangle \\ &= 2 \langle \Psi^{\dagger}(\mathbf{r}, \uparrow) \Psi^{\dagger}(\mathbf{r}, \downarrow) \rangle \langle \Psi(\mathbf{r}, \downarrow) \Psi(\mathbf{r}, \uparrow) \rangle \\ &\quad + 2 \langle \Psi^{\dagger}(\mathbf{r}, \uparrow) \Psi(\mathbf{r}, \uparrow) \rangle \langle \Psi^{\dagger}(\mathbf{r}, \downarrow) \Psi(\mathbf{r}, \downarrow) \rangle \end{aligned}$$

The variation of the true energy becomes

$$\begin{aligned}
\delta \langle \mathcal{H} \rangle &= \sum_{\alpha} \int d^3r \delta \langle \Psi^{\dagger}(\mathbf{r}, \alpha) \hat{H}_e \Psi(\mathbf{r}, \alpha) \rangle \\
&\quad - W \int d^3r [(\delta \langle \Psi^{\dagger}(\mathbf{r}, \uparrow) \Psi^{\dagger}(\mathbf{r}, \downarrow) \rangle) \langle \Psi(\mathbf{r}, \downarrow) \Psi(\mathbf{r}, \uparrow) \rangle \\
&\quad + \langle \Psi^{\dagger}(\mathbf{r}, \uparrow) \Psi^{\dagger}(\mathbf{r}, \downarrow) \rangle (\delta \langle \Psi(\mathbf{r}, \downarrow) \Psi(\mathbf{r}, \uparrow) \rangle)] \\
&\quad - W \int d^3r [(\delta \langle \Psi^{\dagger}(\mathbf{r}, \uparrow) \Psi(\mathbf{r}, \uparrow) \rangle) \langle \Psi^{\dagger}(\mathbf{r}, \downarrow) \Psi(\mathbf{r}, \downarrow) \rangle \\
&\quad + \langle \Psi^{\dagger}(\mathbf{r}, \uparrow) \Psi(\mathbf{r}, \uparrow) \rangle (\delta \langle \Psi^{\dagger}(\mathbf{r}, \downarrow) \Psi(\mathbf{r}, \downarrow) \rangle)] \quad (2.43)
\end{aligned}$$

Let us now calculate the variation of the effective energy with respect to variations of Ψ :

$$\begin{aligned}
\delta \langle \mathcal{H}_{eff} \rangle &= \sum_{\alpha} \int d^3r \delta \langle \Psi^{\dagger}(\mathbf{r}, \alpha) [\hat{H}_e + U(\mathbf{r})] \Psi(\mathbf{r}, \alpha) \rangle \\
&\quad + \int d^3r [\Delta(\mathbf{r}) \delta \langle \Psi^{\dagger}(\mathbf{r}, \uparrow) \Psi^{\dagger}(\mathbf{r}, \downarrow) \rangle + \Delta^*(\mathbf{r}) \delta \langle \Psi(\mathbf{r}, \downarrow) \Psi(\mathbf{r}, \uparrow) \rangle] \quad (2.44)
\end{aligned}$$

Comparing the corresponding terms in Eqs. (2.43) and (2.44) we find that there should be

$$U(\mathbf{r}) = -W \langle \Psi^{\dagger}(\mathbf{r}, \uparrow) \Psi(\mathbf{r}, \uparrow) \rangle = -W \langle \Psi^{\dagger}(\mathbf{r}, \downarrow) \Psi(\mathbf{r}, \downarrow) \rangle \quad (2.45)$$

and

$$\Delta(\mathbf{r}) = -W \langle \Psi(\mathbf{r}, \downarrow) \Psi(\mathbf{r}, \uparrow) \rangle = W \langle \Psi(\mathbf{r}, \uparrow) \Psi(\mathbf{r}, \downarrow) \rangle \quad (2.46)$$

$$\Delta^*(\mathbf{r}) = -W \langle \Psi^{\dagger}(\mathbf{r}, \uparrow) \Psi^{\dagger}(\mathbf{r}, \downarrow) \rangle = W \langle \Psi^{\dagger}(\mathbf{r}, \downarrow) \Psi^{\dagger}(\mathbf{r}, \uparrow) \rangle \quad (2.47)$$

The pairing field Δ is proportional to a two-particle wave function.

To calculate the averages in Eqs. (2.45) – (2.47) we use

$$\langle \gamma_{n,\alpha}^{\dagger} \gamma_{m,\beta} \rangle = \delta_{nm} \delta_{\alpha\beta} f_n \quad (2.48)$$

$$\langle \gamma_{n,\alpha} \gamma_{m,\beta} \rangle = \langle \gamma_{n,\alpha}^{\dagger} \gamma_{m,\beta}^{\dagger} \rangle = 0 \quad (2.49)$$

where f_n is the distribution function. In equilibrium, it is the Fermi function

$$f_n = \frac{1}{e^{\epsilon_n/T} + 1}$$

Eqs. (2.48) and (2.49) reflect the fact that γ are the single-particle operators in the new basis such that there is no further pairing among them.

Inserting Eqs. (2.19)–(2.22) into Eqs. (2.46), (2.47) we find

$$\Delta(\mathbf{r}) = W \sum_n (1 - f_{n\uparrow} - f_{n\downarrow}) u_n(\mathbf{r}) v_n^*(\mathbf{r}) = W \sum_n (1 - 2f_n) u_n(\mathbf{r}) v_n^*(\mathbf{r}) \quad (2.50)$$

$$\Delta^*(\mathbf{r}) = W \sum_n (1 - f_{n\uparrow} - f_{n\downarrow}) u_n^*(\mathbf{r}) v_n(\mathbf{r}) = W \sum_n (1 - 2f_n) u_n^*(\mathbf{r}) v_n(\mathbf{r}) \quad (2.51)$$

The last equality in each line holds because the distribution is spin independent. We see that the pairing field Δ is a linear combination of pair states made out of particle-like and annihilated hole-like excitations.

The effective potential is

$$U(\mathbf{r}) = -W \sum_n [|u_n(\mathbf{r})|^2 f_n + |v_n(\mathbf{r})|^2 (1 - f_n)] \quad (2.52)$$

Note that the density of particles in the system is

$$n = 2 \langle \Psi^\dagger(\mathbf{r}, \uparrow) \Psi(\mathbf{r}, \uparrow) \rangle = 2 \sum_n [|u_n(\mathbf{r})|^2 f_n + |v_n(\mathbf{r})|^2 (1 - f_n)] \quad (2.53)$$

One can say that it is a combination of particle contribution

$$2 \sum_n |u_n(\mathbf{r})|^2 f_n$$

and a hole contribution

$$2 \sum_n |v_n(\mathbf{r})|^2 (1 - f_n)$$

where the distribution of holes is $1 - f_n$.

The effective field U enters the BdGE together with the chemical potential μ . In a sense, it can be included into μ to make a new chemical potential. In what follows we assume that it is included into μ and omit it from the BdGE.

We can now write the average energy in the state satisfying Eqs. (2.46), (2.47) with the effective field Δ as

$$\langle \mathcal{H} \rangle_\Delta = \int d^3r \left[\sum_\alpha \langle \Psi^\dagger(\mathbf{r}, \alpha) \hat{H}_e \Psi(\mathbf{r}, \alpha) \rangle_\Delta - \frac{|\Delta(\mathbf{r})|^2}{W} \right] \quad (2.54)$$

The average effective Hamiltonian Eq. (2.30) in the state determined by Eqs. (2.46), (2.47) coincides with the true average energy in this state if $H_0(\mathbf{r}) = |\Delta|^2/V$. Therefore, the full expression is

$$\begin{aligned} \mathcal{H}_{eff} &= \int d^3r \left[\sum_\alpha \Psi^\dagger(\mathbf{r}, \alpha) \hat{H}_e \Psi(\mathbf{r}, \alpha) + \frac{|\Delta(\mathbf{r})|^2}{W} \right] \\ &+ \int d^3r [\Delta(\mathbf{r}) \Psi^\dagger(\mathbf{r}, \uparrow) \Psi^\dagger(\mathbf{r}, \downarrow) + \Delta^*(\mathbf{r}) \Psi(\mathbf{r}, \downarrow) \Psi(\mathbf{r}, \uparrow)] \end{aligned} \quad (2.55)$$

With the potential U included into the chemical potential, the BdG equations take the form

$$-\frac{\hbar^2}{2m} \left(\nabla - \frac{ie}{\hbar c} \mathbf{A} \right)^2 u - E_F u + \Delta v = \epsilon u \quad (2.56)$$

$$\frac{\hbar^2}{2m} \left(\nabla + \frac{ie}{\hbar c} \mathbf{A} \right)^2 v + E_F v + \Delta^* u = \epsilon v \quad (2.57)$$

2.4 Observables

2.4.1 Energy spectrum and coherence factors

Consider the case where $\Delta = |\Delta|e^{i\chi}$ is constant in space, and the magnetic field is absent. The BdGE have the form

$$\left[-\frac{\hbar^2}{2m}\nabla^2 - \mu \right] u(\mathbf{r}) + \Delta v(\mathbf{r}) = \epsilon u(\mathbf{r}) \quad (2.58)$$

$$-\left[-\frac{\hbar^2}{2m}\nabla^2 - \mu \right] v(\mathbf{r}) + \Delta^* u(\mathbf{r}) = \epsilon v(\mathbf{r}) \quad (2.59)$$

where $\mu = \hbar^2 k_F^2 / 2m$. We look for a solution in the form

$$u = e^{\frac{i}{2}\chi} U_{\mathbf{q}} e^{i\mathbf{q}\cdot\mathbf{r}}, \quad v = e^{-\frac{i}{2}\chi} V_{\mathbf{q}} e^{i\mathbf{q}\cdot\mathbf{r}} \quad (2.60)$$

where \mathbf{q} is a constant vector. We have

$$\xi_{\mathbf{q}} U_{\mathbf{q}} + |\Delta| V_{\mathbf{q}} = \epsilon_{\mathbf{q}} U_{\mathbf{q}} \quad (2.61)$$

$$-\xi_{\mathbf{q}} V_{\mathbf{q}} + |\Delta| U_{\mathbf{q}} = \epsilon_{\mathbf{q}} V_{\mathbf{q}} \quad (2.62)$$

where

$$\xi_{\mathbf{q}} = \frac{\hbar^2}{2m} [q^2 - k_F^2]$$

The condition of solvability of Eqs. (2.61) and (2.62) gives

$$\epsilon_{\mathbf{q}} = \pm \sqrt{\xi_{\mathbf{q}}^2 + |\Delta|^2} \quad (2.63)$$

According to the Landau picture of Fermi liquid, we consider only energies $\epsilon > 0$. The spectrum is shown in Fig. 2.7.

The wave functions u and v for a given momentum \mathbf{q} are found from Eqs. (2.61), (2.63). We have

$$U_{\mathbf{q}} = \frac{1}{\sqrt{2}} \left(1 + \frac{\xi_{\mathbf{q}}}{\epsilon_{\mathbf{q}}} \right)^{1/2}, \quad V_{\mathbf{q}} = \frac{1}{\sqrt{2}} \left(1 - \frac{\xi_{\mathbf{q}}}{\epsilon_{\mathbf{q}}} \right)^{1/2} \quad (2.64)$$

Normalization is chosen to satisfy Eq. (2.27).

The energy $|\Delta|$ is the lowest single-particle excitation energy in the superconducting state. $2|\Delta|$ corresponds to an energy which is needed to destroy the Cooper pair. Therefore, one can identify $2|\Delta|$ as the pairing energy as determined by the Cooper problem in the previous Section, $|E| = 2|\Delta|$. Using the results of Problem 2.1, one can define the radius of the Cooper pair $\sqrt{\langle R^2 \rangle} \sim \hbar v_F / |\Delta|$. This characteristic scale sets up a very important length scale called the coherence length

$$\xi \sim \hbar v_F / |\Delta|.$$

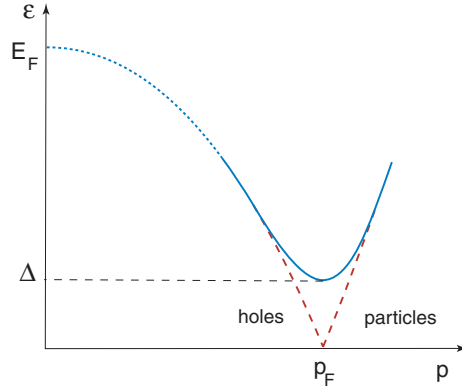


Figure 2.7: The BCS spectrum of excitations in a superconductor. The solid line shows the spectrum of quasiparticles near the Fermi surface where the Landau quasiparticles are well defined. At higher energies closer to E_F the Landau quasiparticles are not well-defined (dotted line). The dashed line at lower energies shows the behavior of the spectrum in the normal state $\epsilon = |\xi_{\mathbf{p}}|$.

For a given energy, there are two possible values of

$$\xi_{\mathbf{q}} = \pm \sqrt{\epsilon^2 - |\Delta|^2} \quad (2.65)$$

that correspond respectively to particles or holes (see Fig. 2.7).

The quantity

$$\frac{d\epsilon}{d(\hbar q)} = v_g$$

is the group velocity of excitations. One has $q^2 = k_F^2 \pm (2m/\hbar^2)\sqrt{\epsilon^2 - |\Delta|^2}$. Therefore,

$$v_g = \frac{\hbar q}{m} \frac{\xi_{\mathbf{q}}}{\sqrt{\xi_{\mathbf{q}}^2 + |\Delta|^2}} = v_F \frac{\xi_{\mathbf{q}}}{\sqrt{\xi_{\mathbf{q}}^2 + |\Delta|^2}} = \pm v_F \frac{\sqrt{\epsilon^2 - |\Delta|^2}}{\epsilon} \quad (2.66)$$

where $v_F = \hbar q/m$ is the velocity at the Fermi surface. We see that the group velocity is positive, i.e., its direction coincides with the direction of \mathbf{q} for excitations outside the Fermi surface $\xi_{\mathbf{q}} > 0$. As we know, these excitations are particle-like. On the other hand, $v_g < 0$ for excitations inside the Fermi surface $\xi_{\mathbf{q}} < 0$, which are known as hole-like excitations.

Another important quantity is the density of states (DOS) $N(\epsilon)$ defined as follows. Let us suppose that there are $n_{\alpha}(q)$ states per spin and per unit volume for particles with momenta up to $\hbar q$. The density of states is the number of states within an energy interval from ϵ to $\epsilon + d\epsilon$, i.e.

$$N(\epsilon) = \frac{dn_{\alpha}(q)}{d\epsilon}$$

As we can see, in a superconductor, there are no excitations with energies $\epsilon < |\Delta|$. The DOS per one spin projection is zero for $\epsilon < |\Delta|$. For $\epsilon > |\Delta|$ we have

$$\begin{aligned} N(\epsilon) &= \frac{1}{2} \left| \frac{d}{d\epsilon} \left(\frac{q^3}{3\pi^2} \right) \right| = \frac{q^2}{2\pi^2} \left| \frac{dq}{d\epsilon} \right|^{-1} \\ &= \frac{mq}{2\pi^2 \hbar^2} \frac{\epsilon}{\sqrt{\epsilon^2 - |\Delta|^2}} \approx N(0) \frac{\epsilon}{\sqrt{\epsilon^2 - |\Delta|^2}} \end{aligned} \quad (2.67)$$

Here

$$N(0) = \frac{mp_F}{2\pi^2 \hbar^3} = \frac{mk_F}{2\pi^2 \hbar^2}$$

is the DOS per one spin projection in the normal state for zero energy excitations, i.e., at the Fermi surface. We have replaced here q with k_F . Indeed, since $\Delta \ll E_F$, the magnitude of q is very close to k_F for $\epsilon \sim \Delta$. This fact is of a crucial importance for practical applications of the BCS theory, as we shall see in what follows.

One finds from Eq. (2.65) that for a given energy ϵ there are two possible values of q^2 :

$$q^2 = k_F^2 + \frac{2m}{\hbar^2} \xi_{\mathbf{q}} = k_F^2 \pm \frac{2m}{\hbar^2} \sqrt{\epsilon^2 - |\Delta|^2} \quad (2.68)$$

Using this we can write Eq. (2.68) in the form

$$q = \pm q_{\pm}$$

where

$$q_{\pm} = k_F \pm \frac{1}{\hbar v_F} \sqrt{\epsilon^2 - |\Delta|^2} \quad (2.69)$$

Therefore, the solution Eq. (2.60) for a given energy consists of four terms

$$\begin{aligned} \begin{pmatrix} u \\ v \end{pmatrix} &= A \begin{pmatrix} e^{\frac{i}{2}\chi} U_0 \\ e^{-\frac{i}{2}\chi} V_0 \end{pmatrix} e^{iq_+x} + B \begin{pmatrix} e^{\frac{i}{2}\chi} V_0 \\ e^{-\frac{i}{2}\chi} U_0 \end{pmatrix} e^{iq_-x} \\ &+ C \begin{pmatrix} e^{\frac{i}{2}\chi} U_0 \\ e^{-\frac{i}{2}\chi} V_0 \end{pmatrix} e^{-iq_+x} + D \begin{pmatrix} e^{\frac{i}{2}\chi} V_0 \\ e^{-\frac{i}{2}\chi} U_0 \end{pmatrix} e^{-iq_-x} \end{aligned} \quad (2.70)$$

Here we have chosen the x axis parallel to \mathbf{q} . The amplitudes A and C describe excitations that have the same directions of the momenta q_+ and of the group velocity v_g , the amplitudes B and D describe excitations that have opposite directions of the momenta q_- and of the group velocity v_g .

The relations between U_0 and V_0 can be found if we insert each term in Eq. (2.70) into Eq. (2.61) or Eq. (2.62). We find

$$U_0 = \frac{1}{\sqrt{2}} \left(1 + \frac{\sqrt{\epsilon^2 - |\Delta|^2}}{\epsilon} \right)^{1/2}, \quad V_0 = \frac{1}{\sqrt{2}} \left(1 - \frac{\sqrt{\epsilon^2 - |\Delta|^2}}{\epsilon} \right)^{1/2} \quad (2.71)$$

The normalization is chosen such that each set of U and V satisfies Eq. (2.27) separately. The amplitudes U and V are sometimes called the coherence factors.

In the normal state $\Delta = 0$ the wave function for a given energy ϵ becomes

$$\begin{pmatrix} u \\ v \end{pmatrix} = A \begin{pmatrix} 1 \\ 0 \end{pmatrix} e^{iq+x} + B \begin{pmatrix} 0 \\ 1 \end{pmatrix} e^{iq-x} \\ + C \begin{pmatrix} 1 \\ 0 \end{pmatrix} e^{-iq+x} + D \begin{pmatrix} 0 \\ 1 \end{pmatrix} e^{-iq-x} \quad (2.72)$$

We thus have particle waves with the group velocity parallel to the momentum

$$u = Ae^{iq+x} + Ce^{-iq+x} \quad (2.73)$$

and, independently, the holes waves with the group velocity antiparallel to the momentum

$$v = Be^{iq-x} + De^{-iq-x} \quad (2.74)$$

2.4.2 The energy gap

For a state Eq. (2.60) specified by a wave vector \mathbf{q} with $U_{\mathbf{q}}$ and $V_{\mathbf{q}}$ from Eq. (2.64) the product uv^* becomes

$$uv^* = e^{ix} U_{\mathbf{q}} V_{\mathbf{q}} = \frac{\Delta}{2\epsilon_{\mathbf{q}}}$$

The self-consistency equation (2.50) yields

$$\Delta = W \sum_{\mathbf{q}} (1 - 2f_{\mathbf{q}}) \frac{\Delta}{2\epsilon_{\mathbf{q}}} \quad (2.75)$$

We replace the sum with the integral

$$\sum_{\mathbf{q}} = \int_{q=0}^{q=\infty} \frac{d^3q}{(2\pi)^3} = \int_{\xi=-E_F}^{\xi=+\infty} \frac{mq}{2\pi^2\hbar^2} d\xi_{\mathbf{q}} \approx N(0) \int_{-\infty}^{+\infty} d\xi_{\mathbf{q}}$$

and notice that, in equilibrium,

$$1 - 2f_{\mathbf{q}} = \tanh\left(\frac{\epsilon_{\mathbf{q}}}{2T}\right)$$

Moreover,

$$\epsilon_{\mathbf{q}} d\epsilon_{\mathbf{q}} = \xi_{\mathbf{q}} d\xi_{\mathbf{q}}$$

When ξ varies from $-\infty$ to $+\infty$, the energy varies from Δ to $+\infty$ taking each value twice. Therefore, the self-consistency equation takes the form

$$\Delta = W \sum_{\mathbf{q}} (1 - 2f_{\mathbf{q}}) \frac{\Delta}{2\epsilon_{\mathbf{q}}} = N(0)W \int_{|\Delta|}^{\infty} \frac{\Delta}{\sqrt{\epsilon^2 - |\Delta|^2}} \tanh\left(\frac{\epsilon}{2T}\right) d\epsilon \quad (2.76)$$

The integral diverges logarithmically at large energies. In fact, the potential of interaction does also depend on energy $W = W_{\epsilon}$ in such a way that it vanishes for high energies exceeding some limiting value $E_c \ll E_F$. We assume that

$$W_{\epsilon} = \begin{cases} W, & \epsilon < E_c \\ 0, & \epsilon > E_c \end{cases}$$

From Eq. (2.76) we obtain the *gap equation*

$$1 = \lambda \int_{|\Delta|}^{E_c} \frac{1}{\sqrt{\epsilon^2 - |\Delta|^2}} \tanh\left(\frac{\epsilon}{2T}\right) d\epsilon \quad (2.77)$$

where the dimensionless parameter $\lambda = N(0)W \sim N(0)W_0 a^3$ is called the interaction constant. For phonon mediated electron coupling, the effective attraction works for energies below the Debye energy Ω_D . Therefore, $E_c = \Omega_D$ in Eq. (2.77). This equation determines the dependence of the gap on temperature.

This equation can be used to determine the critical temperature T_c , at which the gap Δ vanishes. We have

$$1 = \lambda \int_0^{E_c} \tanh\left(\frac{\epsilon}{2T_c}\right) \frac{d\epsilon}{\epsilon} \quad (2.78)$$

This reduces to

$$\frac{1}{\lambda} = \int_0^{E_c/2T_c} \frac{\tanh x}{x} dx \quad (2.79)$$

The integral

$$\int_0^a \frac{\tanh x}{x} dx = \ln(aB)$$

Here $B = 4\gamma/\pi \approx 2.26$ where $\gamma = e^C \approx 1.78$ and $C = 0.577\dots$ is the Euler constant. Therefore,

$$T_c = (2\gamma/\pi)E_c e^{-1/\lambda} \approx 1.13E_c e^{-1/\lambda} \quad (2.80)$$

The interaction constant is usually small, being of the order of $0.1 \div 0.3$ in practical superconductors. Therefore, usually $T_c \ll E_c$.

For zero temperature we obtain from Eq. (2.77)

$$\frac{1}{\lambda} = \int_{|\Delta|}^{E_c} \frac{d\epsilon}{\sqrt{\epsilon^2 - |\Delta|^2}} = \text{Arcosh}\left(\frac{E_c}{|\Delta|}\right) \approx \ln(2E_c/|\Delta|) \quad (2.81)$$

Therefore, at $T = 0$

$$|\Delta| \equiv \Delta(0) = (\pi/\gamma)T_c \approx 1.76T_c$$

2.4.3 Condensation energy

Let us calculate the average energy per unit volume in the superconducting state, Eq. (2.54). Using Eqs. (2.19 - 2.22) and (2.48), (2.49) we have

$$\begin{aligned} \int d^3r \sum_{\alpha} \langle \Psi^{\dagger}(\mathbf{r}, \alpha) \hat{H}_e \Psi(\mathbf{r}, \alpha) \rangle &= \sum_{n,m,\alpha} \left[\langle \gamma_{m\alpha}^{\dagger} \gamma_{n\alpha} \rangle \left(\int u_m^* \hat{H}_e u_n d^3r \right) \right. \\ &\quad \left. + \langle \gamma_{m\alpha} \gamma_{n\alpha}^{\dagger} \rangle \left(\int v_m \hat{H}_e v_n^* d^3r \right) \right] \\ &= 2 \sum_n \left[f_n \left(\int u_n^* \hat{H}_e u_n d^3r \right) + (1 - f_n) \left(\int v_n \hat{H}_e v_n^* d^3r \right) \right] \end{aligned}$$

Using the BdGE and the normalization of u and v we obtain

$$\begin{aligned} & \int d^3r \sum_{\alpha} \langle \Psi^{\dagger}(\mathbf{r}, \alpha) \hat{H}_e \Psi(\mathbf{r}, \alpha) \rangle \\ &= 2 \sum_n [\epsilon_n (f_n |u_n|^2 - (1 - f_n) |v_n|^2) + \Delta v_n u_n^* (1 - 2f_n)] \\ &= 2 \sum_n [\epsilon_n f_n - \epsilon_n |v_n|^2] + \frac{2|\Delta|^2}{W} \end{aligned}$$

Therefore,

$$\langle \mathcal{H} \rangle_{\Delta} = 2 \sum_n \epsilon_n f_n - 2 \sum_n \epsilon_n |v_n|^2 + \frac{|\Delta|^2}{W} \quad (2.82)$$

Let us consider zero temperature. The first term gives the energy of excitations. This energy is zero for $T = 0$, since $f_n = 0$ for any $\epsilon_n > 0$. The rest two terms determine the ground state energy measured from the energy in normal state

$$\begin{aligned} \mathcal{E}_{\Delta} &= -2 \sum_n \epsilon_n |v_n|^2 + \frac{|\Delta|^2}{W} = - \sum_n (\epsilon_n - \xi_n) + \frac{|\Delta|^2}{W} \\ &= -2N(0) \int_0^{E_c} (\sqrt{\xi^2 + |\Delta|^2} - \xi) d\xi + \frac{|\Delta|^2}{W} \end{aligned}$$

We have

$$\begin{aligned} \int_0^{E_c} (\sqrt{\xi^2 + |\Delta|^2} - \xi) d\xi &= \frac{1}{2} \left[\xi \sqrt{\xi^2 + |\Delta|^2} - \xi^2 + |\Delta|^2 \ln(\xi + \sqrt{\xi^2 + |\Delta|^2}) \right]_0^{E_c} \\ &= \frac{|\Delta|^2}{4} + \frac{|\Delta|^2}{2} \ln \left(\frac{2E_c}{|\Delta|} \right) = \frac{|\Delta|^2}{4} + \frac{|\Delta|^2}{2N(0)W} \end{aligned}$$

Here we use that $|\Delta| \ll E_c$ and insert the logarithm from Eq. (2.81). We find

$$\mathcal{E}_{\Delta} = - \frac{N(0)|\Delta(0)|^2}{2} \quad (2.83)$$

The ground state energy of the superconductor is by an amount \mathcal{E}_{Δ} lower than the normal state energy. The energy \mathcal{E}_{Δ} is called the condensation energy.

2.4.4 Current

The quantum mechanical expression for the current density is

$$\begin{aligned} \mathbf{j} &= \frac{e}{2m} \sum_{\alpha} \left\{ \Psi^{\dagger}(\mathbf{r}, \alpha) \left[(-i\hbar\nabla - \frac{e}{c}\mathbf{A}) \Psi(\mathbf{r}, \alpha) \right] \right. \\ &\quad \left. + \left[(i\hbar\nabla - \frac{e}{c}\mathbf{A}) \Psi^{\dagger}(\mathbf{r}, \alpha) \right] \Psi(\mathbf{r}, \alpha) \right\} \quad (2.84) \end{aligned}$$

Using Eqs. (2.19 - 2.22) and (2.48), (2.49) we obtain

$$\begin{aligned} \mathbf{j} &= \frac{e}{m} \sum_n \left[f_n u_n^*(\mathbf{r}) \left(-i\hbar\nabla - \frac{e}{c}\mathbf{A} \right) u_n(\mathbf{r}) \right. \\ &\quad \left. + (1 - f_n) v_n(\mathbf{r}) \left(-i\hbar\nabla - \frac{e}{c}\mathbf{A} \right) v_n^*(\mathbf{r}) + c.c. \right] \end{aligned} \quad (2.85)$$

Identities

One can write Eq. (2.85) in the form

$$\begin{aligned} \mathbf{j} &= -\frac{i\hbar e}{m} \sum_n \left[\left(-\frac{1}{2} + f_{n,\epsilon} \right) u_n^* \left(\nabla - \frac{ie}{\hbar c}\mathbf{A} \right) u_n + \left(\frac{1}{2} - f_{n,\epsilon} \right) v_n \left(\nabla - \frac{ie}{\hbar c}\mathbf{A} \right) - c.c. \right] \\ &\quad - \frac{i\hbar e}{2m} \sum_n \left[u_n^* \left(\nabla - \frac{ie}{\hbar c}\mathbf{A} \right) u_n + v_n \left(\nabla - \frac{ie}{\hbar c}\mathbf{A} \right) v_n^* - c.c. \right] \\ &= \frac{i\hbar e}{2m} \sum_n \left[(1 - 2f_{n,\epsilon}) u_n^* \left(\nabla - \frac{ie}{\hbar c}\mathbf{A} \right) u_n - (1 - 2f_{n,\epsilon}) v_n \left(\nabla - \frac{ie}{\hbar c}\mathbf{A} \right) v_n^* - c.c. \right] \\ &\quad - \frac{i\hbar e}{2m} \sum_n \left[u_n^* \left(\nabla - \frac{ie}{\hbar c}\mathbf{A} \right) u_n + v_n \left(\nabla - \frac{ie}{\hbar c}\mathbf{A} \right) v_n^* - c.c. \right] \end{aligned} \quad (2.86)$$

Therefore,

$$\mathbf{j} = - \sum_n (1 - 2f_n) \mathbf{J}_n + \sum_n \mathbf{P}_n \quad (2.87)$$

where

$$\mathbf{J}_n = -\frac{i\hbar e}{2m} \left[u_n^* \left(\nabla - \frac{ie}{\hbar c}\mathbf{A} \right) u_n - v_n \left(\nabla - \frac{ie}{\hbar c}\mathbf{A} \right) v_n^* - c.c. \right] \quad (2.88)$$

and

$$\mathbf{P}_n = -\frac{i\hbar e}{2m} \left[u_n^* \left(\nabla - \frac{ie}{\hbar c}\mathbf{A} \right) u_n + v_n \left(\nabla - \frac{ie}{\hbar c}\mathbf{A} \right) v_n^* - c.c. \right]. \quad (2.89)$$

For a given state n , the current \mathbf{J}_n is not conserved, see below. On the other hand, \mathbf{P}_n is a conserved quantity (see Problem 2.2.), the quasiparticle flow,

$$\text{div} \mathbf{P}_n = 0 \quad (2.90)$$

Now, we multiply Eq. (2.56) by u^* and subtract the complex conjugated equation. Next, we multiply Eq. (2.57) by v^* and subtract the complex conjugated equation. Finally, subtracting the two resulting equations we find

$$\text{div} \mathbf{J}_n = -\frac{2ie}{\hbar} (\Delta u_n^* v_n - \Delta^* u_n v_n^*). \quad (2.91)$$

Applying Eqs. (2.87) and (2.90) we can calculate the divergence of the total current

$$\text{div} \mathbf{j} = \frac{2ie}{\hbar} \left[\Delta \sum_n u_n^* v_n (1 - 2f_n) - \Delta^* \sum_n u_n v_n^* (1 - 2f_n) \right] = 0 \quad (2.92)$$

due to the self-consistency equation. The sum here is taken over all states. The total current is conserved as it should be.

Currents in clean superconductors

If the vector potential varies slowly, one can use a gauge where it is included into \mathbf{k} . Assume that the order parameter has a superconducting momentum

$$\Delta = |\Delta|e^{i\mathbf{k}\cdot\mathbf{r}}$$

The wave functions have the form

$$u(\mathbf{r}) = e^{i(\mathbf{q}+\mathbf{k}/2)\cdot\mathbf{r}}U_{\mathbf{q}}, \quad v(\mathbf{r}) = e^{i(\mathbf{q}-\mathbf{k}/2)\cdot\mathbf{r}}V_{\mathbf{q}} \quad (2.93)$$

The energy spectrum is (see Problem 2.2)

$$\epsilon_{\mathbf{q}} = \hbar\mathbf{q} \cdot \mathbf{v}_s + \sqrt{\xi_{\mathbf{q}}^2 + |\Delta|^2} \quad (2.94)$$

or

$$\epsilon_{\mathbf{q}} = \hbar\mathbf{q} \cdot \mathbf{v}_s + \epsilon_{\mathbf{q}}^{(0)} \quad (2.95)$$

where

$$\epsilon_{\mathbf{q}}^{(0)} = \sqrt{\xi_{\mathbf{q}}^2 + |\Delta|^2}$$

and

$$\mathbf{v}_s = \frac{\hbar\mathbf{k}}{2m}$$

is the superconducting velocity. The factors $U_{\mathbf{q}}$ and $V_{\mathbf{q}}$ are given by

$$U_{\mathbf{q}} = \frac{1}{\sqrt{2}} \left(1 + \frac{\xi_{\mathbf{q}}}{\epsilon_{\mathbf{q}}^{(0)}}\right)^{1/2}, \quad V_{\mathbf{q}} = \frac{1}{\sqrt{2}} \left(1 - \frac{\xi_{\mathbf{q}}}{\epsilon_{\mathbf{q}}^{(0)}}\right)^{1/2} \quad (2.96)$$

similar to Eq. (2.64).

Note that the gap vanishes for excitations with \mathbf{q} antiparallel to \mathbf{v}_s if $v_s \geq v_c$ where

$$v_c = |\Delta|/p_F$$

is called the critical velocity.

Using Eqs. (2.64) and (2.93) we obtain from Eq. (2.85)

$$\begin{aligned} \mathbf{j} &= \frac{2\hbar e}{m} \sum_{\mathbf{q}} \left[\left(\mathbf{q} + \frac{\mathbf{k}}{2}\right) f_{\mathbf{q}} U_{\mathbf{q}}^2 - \left(\mathbf{q} - \frac{\mathbf{k}}{2}\right) (1 - f_{\mathbf{q}}) V_{\mathbf{q}}^2 \right] \\ &= \frac{\hbar e}{m} \mathbf{k} \sum_{\mathbf{q}} [f_{\mathbf{q}} U_{\mathbf{q}}^2 + (1 - f_{\mathbf{q}}) V_{\mathbf{q}}^2] + \frac{2\hbar e}{m} \sum_{\mathbf{q}} \mathbf{q} [f_{\mathbf{q}} U_{\mathbf{q}}^2 - (1 - f_{\mathbf{q}}) V_{\mathbf{q}}^2] \end{aligned}$$

The distribution function here is

$$f_{\mathbf{q}} \equiv f(\epsilon_{\mathbf{q}}) = \frac{1}{e^{\epsilon_{\mathbf{q}}/T} + 1}$$

where $\epsilon_{\mathbf{q}}$ is determined by Eq. (2.94). We can write

$$\begin{aligned}
\mathbf{j} &= \frac{\hbar e}{m} \mathbf{k} \sum_{\mathbf{q}} \left[f(\epsilon_{\mathbf{q}}^{(0)}) U_{\mathbf{q}}^2 + (1 - f(\epsilon_{\mathbf{q}}^{(0)})) V_{\mathbf{q}}^2 \right] \\
&+ \frac{2\hbar e}{m} \sum_{\mathbf{q}} \mathbf{q} \left[f(\epsilon_{\mathbf{q}}^{(0)}) U_{\mathbf{q}}^2 - (1 - f(\epsilon_{\mathbf{q}}^{(0)})) V_{\mathbf{q}}^2 \right] \\
&+ \frac{\hbar e}{m} \mathbf{k} \sum_{\mathbf{q}} \left[f(\epsilon_{\mathbf{q}}) - f(\epsilon_{\mathbf{q}}^{(0)}) \right] [U_{\mathbf{q}}^2 - V_{\mathbf{q}}^2] \\
&+ \frac{2\hbar e}{m} \sum_{\mathbf{q}} \mathbf{q} \left[f(\epsilon_{\mathbf{q}}) - f(\epsilon_{\mathbf{q}}^{(0)}) \right] [U_{\mathbf{q}}^2 + V_{\mathbf{q}}^2]
\end{aligned} \tag{2.97}$$

The first term in Eq. (2.97) gives

$$\mathbf{j}_0 = \frac{\hbar e n}{2m} \mathbf{k} = n e \mathbf{v}_s$$

where particle density n is given by Eq. (2.53). The current \mathbf{j}_0 corresponds to the flow of *all* particles with the velocity \mathbf{v}_s . The second term in Eq. (2.97) vanishes after summation over directions of \mathbf{q} . The third term also vanishes since $U_{\mathbf{q}}^2 - V_{\mathbf{q}}^2$ is an odd function of $\xi_{\mathbf{q}}$. The current becomes $\mathbf{j} = \mathbf{j}_0 - \mathbf{j}_{norm}$ where

$$\mathbf{j}_{norm} = \frac{2\hbar e}{m} \sum_{\mathbf{q}} \mathbf{q} \left[f(\epsilon_{\mathbf{q}}^{(0)}) - f(\epsilon_{\mathbf{q}}) \right]$$

is determined by the fourth term. This is the current produced by excitations which form the normal component of the superconductor. We have

$$f(\epsilon_{\mathbf{q}}^{(0)}) - f(\epsilon_{\mathbf{q}}) = \frac{1}{e^{\sqrt{\epsilon_{\mathbf{q}}^2 + |\Delta|^2}/T} + 1} - \frac{1}{e^{(\sqrt{\epsilon_{\mathbf{q}}^2 + |\Delta|^2} + \hbar \mathbf{q} \cdot \mathbf{v}_s)/T} + 1}$$

The normal current is thus directed along \mathbf{v}_s . We will obtain

$$\mathbf{j}_{norm} = e n_{norm} \mathbf{v}_s$$

where n_{norm} is the density of the normal component, which generally depends on v_s . The total current is

$$\mathbf{j} = e(n - n_{norm}) \mathbf{v}_s = e n_s \mathbf{v}_s$$

where $n_s = n - n_{norm}$ is the density of superconducting electrons. It also generally depends on v_s .

For small v_s we have a linear dependence

$$\mathbf{j}_{norm} = -\frac{2\hbar^2 e}{m} \sum_{\mathbf{q}} \mathbf{q} (\mathbf{q} \cdot \mathbf{v}_s) \frac{df(\epsilon_{\mathbf{q}}^{(0)})}{d\epsilon_{\mathbf{q}}^{(0)}} = -\frac{2\hbar^2 e}{3m} \mathbf{v}_s \sum_{\mathbf{q}} \mathbf{q}^2 \frac{df(\epsilon_{\mathbf{q}}^{(0)})}{d\epsilon_{\mathbf{q}}^{(0)}}$$

Therefore,

$$\begin{aligned} n_{norm} &= -\frac{2p_F^2}{3m} \sum_{\mathbf{q}} \frac{df(\epsilon_{\mathbf{q}}^{(0)})}{d\epsilon_{\mathbf{q}}^{(0)}} = -\frac{2p_F^2}{3m} N(0) \int_{-\infty}^{\infty} \frac{df(\epsilon_{\mathbf{q}}^{(0)})}{d\epsilon_{\mathbf{q}}^{(0)}} d\xi_{\mathbf{q}} \\ &= -n \int_{-\infty}^{\infty} \frac{df(\epsilon_{\mathbf{q}}^{(0)})}{d\epsilon_{\mathbf{q}}^{(0)}} d\xi_{\mathbf{q}} = -2n \int_{|\Delta|}^{\infty} \frac{\epsilon}{\sqrt{\epsilon^2 - |\Delta|^2}} \frac{df(\epsilon)}{d\epsilon} d\epsilon \quad (2.98) \end{aligned}$$

For $\Delta = 0$ we have $n_{norm} = n$. The normal density \mathcal{N}_{norm} is exponentially small for $T \ll |\Delta|$.

2.4.5 Negative energies

Owing to the property of the BdG equations expressed by Eqs. (2.41) and (2.42), one can introduce into consideration negative energies of excitations. This also complies with the negative sign of Eq. (2.63). With the negative energies, the self-consistency equation (2.50) takes the form

$$\begin{aligned} \Delta &= V \sum_n (1 - 2f_n) u_n(\epsilon_n) v_n^*(\epsilon_n) \\ &= \frac{V}{2} \sum_{n, \epsilon > 0} [[1 - 2f(\epsilon_n)] u_n(\epsilon_n) v_n^*(\epsilon_n) - [1 - 2f(\epsilon_n)] v_n^*(-\epsilon_n) u_n(-\epsilon_n)] \\ &= \frac{V}{2} \sum_{n, \epsilon > 0} [1 - 2f(\epsilon_n)] u_n(\epsilon_n) v_n^*(\epsilon_n) - \frac{V}{2} \sum_{n, \epsilon < 0} [1 - 2f(-\epsilon_n)] u_n(\epsilon_n) v_n^*(\epsilon_n) \end{aligned}$$

In the second term we made a change $\epsilon \rightarrow -\epsilon$. In equilibrium,

$$1 - 2f(\epsilon) = \tanh \frac{\epsilon}{2T}$$

is an odd function of ϵ . We have

$$\Delta = \frac{V}{2} \sum_{n, \text{all } \epsilon} [1 - 2f(\epsilon)] \frac{\Delta}{2\epsilon_n}$$

or

$$\Delta = V \sum_{n, \epsilon > 0} \frac{\Delta}{2\epsilon} \tanh \frac{\epsilon}{2T} \quad (2.99)$$

which coincides with Eq. (2.76).

2.5 Impurities. Anderson theorem

So far we considered a pure material that has no impurities. Generally, impurities affect all the properties of superconductors. However, for a superconductor *with nonmagnetic impurities* in a *zero magnetic field* that *does not carry current*, the critical temperature and the energy gap are the same as in the clean host material. This is the contents of the Anderson theorem [9].

To see this we consider the BdG equations

$$\begin{aligned} \left[-\frac{\hbar^2}{2m}\nabla^2 - \mu + U(\mathbf{r}) \right] u(\mathbf{r}) + \Delta v(\mathbf{r}) &= \epsilon u(\mathbf{r}) \\ - \left[-\frac{\hbar^2}{2m}\nabla^2 - \mu + U(\mathbf{r}) \right] v(\mathbf{r}) + \Delta^* u(\mathbf{r}) &= \epsilon v(\mathbf{r}) \end{aligned}$$

Here U includes the impurity potential. The gap Δ does not depend on coordinates since there is no magnetic field and current. Consider the single-electron functions of the normal metal $w_n(\mathbf{r})$ that satisfy

$$\left[-\frac{\hbar^2}{2m}\nabla^2 - \mu + U(\mathbf{r}) \right] w_n(\mathbf{r}) = \xi_n w_n(\mathbf{r})$$

Since $\Delta = \text{const}$ we have obviously

$$\begin{aligned} u_n(\mathbf{r}) &= w_n(\mathbf{r})U_n \\ v_n(\mathbf{r}) &= w_n(\mathbf{r})V_n \end{aligned}$$

where U_n and V_n satisfy

$$\begin{aligned} (\xi_n - \epsilon_n)U_n + \Delta V_n &= 0 \\ -(\xi_n + \epsilon_n)V_n + \Delta^* U_n &= 0 \end{aligned}$$

This gives the usual energy spectrum

$$\epsilon_n = \sqrt{\xi_n^2 + |\Delta|^2}$$

and the coherence factors

$$|U_n|^2 = \frac{1}{2} \left(1 + \frac{\xi_n}{\epsilon_n} \right), \quad |V_n|^2 = \frac{1}{2} \left(1 - \frac{\xi_n}{\epsilon_n} \right)$$

The self-consistency equation becomes

$$\Delta = W \sum_n |w_n(\mathbf{r})|^2 (1 - 2f_n) \frac{\Delta}{2\epsilon_n}$$

We also use the definition of the density of states

$$N_\xi(\mathbf{r}) = \sum_n |w_n(\mathbf{r})|^2 \delta(\xi_n - \xi)$$

The self-consistency equation takes the form

$$\Delta(\mathbf{r}) = W \int N_\xi(\mathbf{r}) d\xi (1 - 2f[\epsilon(\xi)]) \frac{\Delta}{2\epsilon(\xi)}$$

The wave functions of the normal metal $w_n(\mathbf{r})$ oscillate as functions of \mathbf{r} over atomic distances. The squared $|w_n(\mathbf{r})|^2$ averages into a spatially uniform

function if one looks at it at distances of the order of the coherence length essential for superconductivity. Moreover, $\xi \ll E_F$. Therefore, after averaging we finally find

$$\Delta = W\bar{N}_0 \int d\xi (1 - 2f(\epsilon)) \frac{\Delta}{2\epsilon}$$

where \bar{N}_0 is the average density of states in the normal metal at the Fermi energy which coincides with that in the clean host material. It is clear that the gap and thus the critical temperature are the same as in the clean material.

The superconducting and normal density, however, are strongly modified by the impurities because they are defined for a current-carrying state.

Problems

Problem 2.1.

Calculate the mean square radius of the Cooper pair.

Problem 2.2.

Derive equations (2.90) where \mathbf{P} is defined by Eq. (2.89).

Problem 2.3.

Derive equations (2.91) where \mathbf{J} is defined by Eq. (2.88).

Problem 2.4.

Find the energy spectrum and the coherence factors for the order parameter $\Delta = |\Delta|e^{i\mathbf{k}\cdot\mathbf{r}}$.

Problem 2.5.

Derive the gap equation that determines the dependence of $|\Delta|$ on v_s for the order parameter in the form $\Delta = |\Delta|e^{i\mathbf{k}\cdot\mathbf{r}}$.

Problem 2.6

Find the temperature dependence of the gap for $T \rightarrow T_c$.

Problem 2.7

Find the temperature dependence of the normal density for $T \rightarrow 0$.

Problem 2.8

Find the temperature dependence of the superconducting density for $T \rightarrow T_c$.

Chapter 3

Andreev reflection

3.1 Semiclassical approximation

3.1.1 Andreev equations

We assume that there are no barriers or other potentials that vary over distances of the order of the electronic wave length k_F^{-1} . The energy gap should also be smooth over the distances of the order of the electronic wave length. It may, however, vary at distances shorter than the coherence length ξ . In this case the quasiparticle momentum of the order of $\hbar k_F$ is a good quantum number such that we can look for a solution in the form

$$\begin{pmatrix} u \\ v \end{pmatrix} = e^{i\mathbf{k}\cdot\mathbf{r}} \begin{pmatrix} U(x) \\ V(x) \end{pmatrix} \quad (3.1)$$

where $|\mathbf{k}| = k_F$ while $U(x)$ and $V(x)$ vary slowly over distances of the order of k_F^{-1} . Inserting this into the BdG equations Eqs. (2.56) and (2.57)

$$-\frac{\hbar^2}{2m} \left(\nabla - \frac{ie}{\hbar c} \mathbf{A} \right)^2 u - \frac{\hbar^2 k_F^2}{2m} u + \Delta v = \epsilon u \quad (3.2)$$

$$\frac{\hbar^2}{2m} \left(\nabla + \frac{ie}{\hbar c} \mathbf{A} \right)^2 v + \frac{\hbar^2 k_F^2}{2m} v + \Delta^* u = \epsilon v \quad (3.3)$$

and neglecting the second derivatives of U and V , we find

$$-i\hbar\mathbf{v}_F \cdot \left(\nabla - \frac{ie}{\hbar c} \mathbf{A} \right) U + \Delta V = \epsilon U \quad (3.4)$$

$$i\hbar\mathbf{v}_F \cdot \left(\nabla + \frac{ie}{\hbar c} \mathbf{A} \right) V + \Delta^* U = \epsilon V \quad (3.5)$$

The transformation we use is known as the WKB or semiclassical approximation. It is essentially based on the fact that the electronic wave length is the shortest length scale in superconductors. The new equations are called Andreev equations. Each of them is a first-order equation, which may considerably reduce the complexity of the problem.

3.1.2 Andreev reflection

Consider a particle incident from the normal region on the superconducting half-space $x > 0$ (see Fig. 3.1) with a momentum parallel to the x axis. Assume that the gap varies over distances longer than the electron wave length k_F^{-1} and that both the normal metal and the superconductor have the same Fermi velocity, and there are no insulating barriers between them. We assume that the magnetic field is absent. In this case Δ and all other potentials depend only on one coordinate x and the Andreev equations take the form

$$-i\hbar v_x \frac{dU}{dx} + \Delta V = \epsilon U \quad (3.6)$$

$$i\hbar v_x \frac{dV}{dx} + \Delta^* U = \epsilon V \quad (3.7)$$

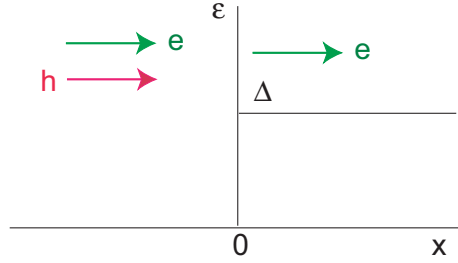


Figure 3.1: The NS structure.

Consider first the case of high energies $\epsilon > |\Delta|$. The particle will penetrate into the superconductor and partially will be reflected back into the normal metal. However, since the gap varies slowly, the reflection process where the momentum is changed such that $\mathbf{k} \rightarrow -\mathbf{k}$ is prohibited. We thus can use the semiclassical approximation.

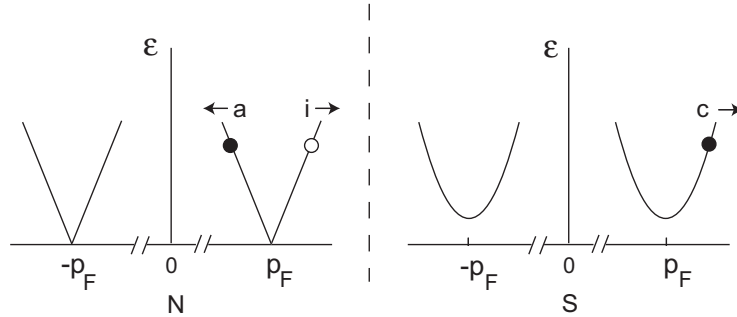


Figure 3.2: The Andreev reflection.

In the normal region (on the left) the order parameter decreases to zero at distances shorter than ξ , so that one can consider $\Delta = 0$ for $x < 0$. Therefore the functions $U(x)$ and $V(x)$ are independent for $x < 0$. We look for the wave function in the form

$$\begin{pmatrix} U(x) \\ V(x) \end{pmatrix}_L = e^{i\lambda_N x} \begin{pmatrix} 1 \\ 0 \end{pmatrix} + a e^{-i\lambda_N x} \begin{pmatrix} 0 \\ 1 \end{pmatrix} \quad (3.8)$$

We find from Eqs. (3.6), (3.7)

$$\lambda_N = \frac{\epsilon}{\hbar v_x} \quad (3.9)$$

The wave function thus contains an incident particle [state (i) in Fig. 3.2] and a reflected hole [state (a)]. We choose the coefficient unity in front of the incident wave to ensure the unit density of particles in the incident wave.

The wave function on the right (in the S region) has the form

$$\begin{pmatrix} U(x) \\ V(x) \end{pmatrix}_R = c e^{i\lambda_S x} \begin{pmatrix} U_0 \\ V_0 \end{pmatrix} \quad (3.10)$$

Eqs. (3.4), (3.5) give

$$\lambda_S = \frac{\sqrt{\epsilon^2 - |\Delta|^2}}{\hbar v_x} \quad (3.11)$$

It describes a transmitted particle. The coherence factors U_0 and V_0 are determined by Eq. (2.71). They satisfy

$$U_0^2 - V_0^2 = \frac{\sqrt{\epsilon^2 - |\Delta|^2}}{\epsilon}, \quad U_0 V_0 = \frac{|\Delta|}{2\epsilon}$$

The boundary conditions for first-order differential equations require continuity of the functions at the interface whence

$$a = V_0/U_0, \quad c = 1/U_0 \quad (3.12)$$

The coefficient a describes a process when a particle is reflected as a hole from a spatially non-uniform gap; this process is called the Andreev reflection [10].

Using Eq. (3.12), the balance of the probabilities in the semi-classical approximation gives

$$|a|^2 + (U_0^2 - V_0^2)|c|^2 = 1$$

or

$$v_g(N)|a|^2 + v_g(S)|c|^2 = v_g(N) \quad (3.13)$$

where, as in Eq. (2.66),

$$v_g(S) = v_F(U_0^2 - V_0^2) = v_F \frac{\sqrt{\epsilon^2 - |\Delta|^2}}{\epsilon}$$

is the group velocity in the superconducting state, and $v_g(N) = v_F$ is the group velocity in the normal state. Eq. (3.13) complies with the conservation of the quasiparticle flow \mathbf{P} determined by Eq. (2.89).

For the sub-gap energy $\epsilon < |\Delta|$, there are no states below the gap in the S region, thus the wave should decay for $x > 0$. The wave function on the right is

$$\begin{pmatrix} U(x) \\ V(x) \end{pmatrix}_R = ce^{i\tilde{\lambda}_S x} \begin{pmatrix} \tilde{U}_0 \\ \tilde{V}_0 \end{pmatrix} \quad (3.14)$$

where

$$\tilde{\lambda}_S = i \frac{\sqrt{|\Delta|^2 - \epsilon^2}}{\hbar v_x} \quad (3.15)$$

and

$$\tilde{U}_0 = \frac{1}{\sqrt{2}} \left(1 + i \frac{\sqrt{|\Delta|^2 - \epsilon^2}}{\epsilon} \right), \quad \tilde{V}_0 = \frac{1}{\sqrt{2}} \left(1 - i \frac{\sqrt{|\Delta|^2 - \epsilon^2}}{\epsilon} \right)$$

The coefficients are

$$a = \tilde{V}_0 / \tilde{U}_0, \quad c = 1 / \tilde{U}_0$$

However, now

$$|a|^2 = 1 \quad (3.16)$$

The Andreev reflection is complete since there are no transmitted particles.

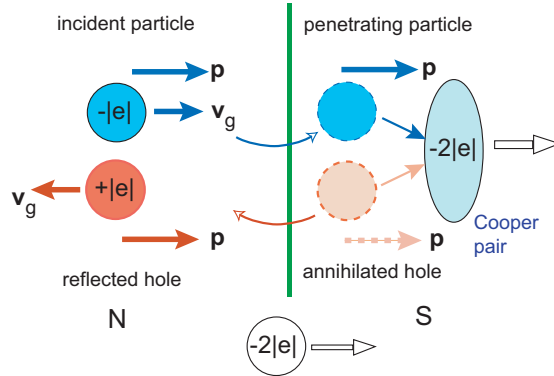


Figure 3.3: Illustration of the nature of Andreev reflection for $\epsilon < |\Delta|$ at an ideal SN interface: An incident electron forms a Cooper pair in the superconductor together with an annihilated hole. This hole is expelled into the normal metal and moves back as a reflected object.

The Andreev reflection has an interesting and surprising property. Consider a three-dimensional motion. Eq. (3.8) for the normal region gives

$$\begin{pmatrix} u \\ v \end{pmatrix} = e^{i(k_x + \epsilon/\hbar v_x)x + ik_y y + ik_z z} \begin{pmatrix} 1 \\ 0 \end{pmatrix} + a e^{i(k_x - \epsilon/\hbar v_x)x + ik_y y + ik_z z} \begin{pmatrix} 0 \\ 1 \end{pmatrix}$$

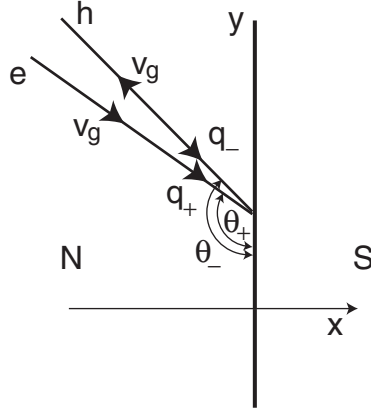


Figure 3.4: The trajectories of an incident particle and the Andreev reflected hole.

The magnitude squared of the particle momentum is

$$p^2 = p_x^2 + p_y^2 + p_z^2 = \hbar^2[(k_x \pm \epsilon/\hbar v_x)^2 + k_y^2 + k_z^2] = \hbar^2 \left[k_F^2 \pm \frac{2k_x \epsilon}{\hbar v_x} \right] = \hbar^2 k_F^2 \pm 2m\epsilon$$

The total momentum of the incident particle is thus $p = \hbar k_F + \epsilon/v_F$ such that $p > p_F$. Its energy corresponds to the rising (right) part of the spectrum branch [point (i)] in Fig. 3.2,

$$\epsilon(p) = v_F(p - p_F)$$

The reflected hole has the momentum $p = p_F - \epsilon/v_F$ such that $p < p_F$. Its energy thus corresponds to the decreasing (left) part of the spectrum branch [point (a)] in Fig. 3.2,

$$\epsilon(p) = v_F(p_F - p)$$

One can calculate the components of the group velocity

$$v_{gx} = \frac{\partial \epsilon}{\partial p_x} = \pm \frac{p_x}{m} \approx \pm v_x$$

$$v_{gy} = \frac{\partial \epsilon}{\partial p_y} = \pm \frac{p_y}{m} \approx \pm v_y$$

We see that particle and hole have opposite signs of the group velocity but with almost the same magnitude. Therefore, Andreev reflected hole moves *along the same trajectory as the incident particle but in the opposite direction!*

In fact, directions of the incident and reflected trajectories are slightly different (see Problem 3.1). Indeed, the change in the momentum during the Andreev reflection is

$$\Delta p_x = (\hbar k_x - \epsilon/v_x) - (\hbar k_x + \epsilon/v_x) = -2\epsilon/v_x$$

This change is much smaller than the momentum itself. This is because the energy of interaction $\sim \Delta$ is much smaller than E_F . At the same time, the momentum projections p_y and p_z are conserved. As a result, the trajectory of the reflected hole deviates, but only slightly, from the trajectory of the incident particle (see Fig. 3.4).

3.2 Andreev states

3.2.1 SNS structures

Consider an SNS structure consisting of a normal slab in the plane (y, z) having a thickness d in between two superconducting half-spaces $x < -d/2$ and $x > d/2$ (see Fig. 3.5). The electrons in both superconductors and in the normal metal have the same Fermi velocity, and there are no insulating barriers between them. As before, we assume that electrons do not scatter on impurities or on other objects like phonons. We also assume that there is no electron–electron scattering. This means that the size d is shorter than the electron mean free path. For short d the mean free path should be larger than the superconducting coherence length ξ or ξ_N (see below).

We use the semi-classical approximation and look for the wave function in the form

$$\begin{pmatrix} u \\ v \end{pmatrix} = e^{i\mathbf{k}\cdot\mathbf{r}} \begin{pmatrix} U(x) \\ V(x) \end{pmatrix}$$

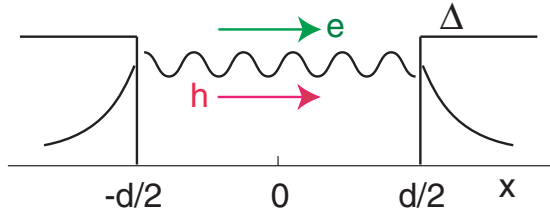


Figure 3.5: The Andreev bound states in the SNS structure.

Consider energy $\epsilon < |\Delta|$. A particle that moves in the normal region to the right will be Andreev reflected from the NS interface into a hole. The hole will then move to the left and is Andreev reflected into the particle, and so on. It is thus localized in the N region having a discrete energy spectrum.

Assume that the gap in the right superconductor has the phase $\phi/2$ while the phase in the left superconductor is $-\phi/2$ so that the phase difference is ϕ . The wave function in the N region is

$$\begin{pmatrix} U(x) \\ V(x) \end{pmatrix}_N = A \left[e^{i\lambda_N x} \begin{pmatrix} 1 \\ 0 \end{pmatrix} + a e^{-i\lambda_N x} \begin{pmatrix} 0 \\ 1 \end{pmatrix} \right] \quad (3.17)$$

where

$$\lambda_N = \frac{\epsilon}{\hbar v_x}$$

If the momentum projection on the x axis is positive, $k_x > 0$, the wave function in the right superconductor $x > d/2$ is

$$\begin{pmatrix} U(x) \\ V(x) \end{pmatrix}_R = d_1 e^{-\tilde{\lambda}_S x} \begin{pmatrix} \tilde{U} e^{i\phi/4} \\ \tilde{V} e^{-i\phi/4} \end{pmatrix} \quad (3.18)$$

where

$$\tilde{\lambda}_S = \frac{\sqrt{|\Delta|^2 - \epsilon^2}}{\hbar |v_x|}$$

The wave function in the left superconductor $x < -d/2$ is

$$\begin{pmatrix} U(x) \\ V(x) \end{pmatrix}_L = d'_1 e^{\tilde{\lambda}_S x} \begin{pmatrix} \tilde{V} e^{-i\phi/4} \\ \tilde{U} e^{i\phi/4} \end{pmatrix} \quad (3.19)$$

Applying continuity at the right interface $x = d/2$ we find

$$\begin{aligned} A e^{i\lambda_N d/2} &= d_1 e^{-\tilde{\lambda}_S d/2} \tilde{U} e^{i\phi/4} \\ A e^{-i\lambda_N d/2} &= d_1 e^{-\tilde{\lambda}_S d/2} \tilde{V} e^{-i\phi/4} \end{aligned}$$

whence

$$a e^{-i\lambda_N d} = \frac{\tilde{V}}{\tilde{U}} e^{-i\phi/2}$$

Continuity at the left interface gives

$$a e^{i\lambda_N d} = \frac{\tilde{U}}{\tilde{V}} e^{i\phi/2}$$

Excluding a we find

$$e^{2i(\lambda_N d - \phi/2)} = \frac{\epsilon + i\sqrt{|\Delta|^2 - \epsilon^2}}{\epsilon - i\sqrt{|\Delta|^2 - \epsilon^2}}$$

We denote

$$\sin \alpha = \frac{\epsilon}{|\Delta|}$$

The range of α is determined in such a way that

$$\cos \alpha = |\Delta|^{-1} \sqrt{|\Delta|^2 - \epsilon^2}$$

is positive to ensure the decay of wave functions in the N regions, i.e.,

$$-\pi/2 < \alpha < \pi/2$$

We obtain

$$e^{2i(\lambda_N d - \phi/2)} = e^{-2i\alpha + i\pi}$$

or

$$\epsilon = \hbar\omega_x \left[\frac{\phi}{2} - \arcsin \frac{\epsilon}{|\Delta|} + \pi \left(l + \frac{1}{2} \right) \right] \quad (3.20)$$

where l is an integer and

$$\omega_x = \frac{v_x}{d} = t_x^{-1}$$

is the inverse time needed for a particle to fly from one end of the normal region to the other.

Consider now particles that have a negative projection $k_x < 0$ on the x axis. The wave function in the right superconductor $x > d/2$ becomes

$$\begin{pmatrix} U(x) \\ V(x) \end{pmatrix}_R = d_2 e^{-\tilde{\lambda}_S x} \begin{pmatrix} \tilde{V} e^{i\phi/4} \\ \tilde{U} e^{-i\phi/4} \end{pmatrix} \quad (3.21)$$

The wave function in the left superconductor $x < -d/2$ is

$$\begin{pmatrix} U(x) \\ V(x) \end{pmatrix}_L = d_2' e^{\tilde{\lambda}_S x} \begin{pmatrix} \tilde{U} e^{-i\phi/4} \\ \tilde{V} e^{i\phi/4} \end{pmatrix} \quad (3.22)$$

Applying continuity at the right interface $x = d/2$ we find

$$a e^{-i\lambda_N d} = \frac{\tilde{U}}{\tilde{V}} e^{-i\phi/2}$$

Continuity at the left interface gives

$$a e^{i\lambda_N d} = \frac{\tilde{V}}{\tilde{U}} e^{i\phi/2}$$

As a result,

$$e^{2i(\lambda_N d - \phi/2)} = \frac{\epsilon - i\sqrt{|\Delta|^2 - \epsilon^2}}{\epsilon + i\sqrt{|\Delta|^2 - \epsilon^2}}$$

or

$$e^{2i(\lambda_N d - \phi/2)} = e^{2i\alpha - i\pi}$$

Since $\lambda_N = \epsilon/\hbar v_x = -\epsilon/\hbar|v_x|$ we find

$$\epsilon = -\hbar|\omega_x| \left[\frac{\phi}{2} + \arcsin \frac{\epsilon}{|\Delta|} + \pi \left(l - \frac{1}{2} \right) \right] \quad (3.23)$$

Combining this with Eq. (3.20) we finally obtain

$$\epsilon = \pm \hbar|\omega_x| \left[\frac{\phi}{2} \mp \arcsin \frac{\epsilon}{|\Delta|} + \pi \left(l \pm \frac{1}{2} \right) \right] \quad (3.24)$$

The upper sign refers to $k_x > 0$, the lower sign refers to $k_x < 0$.

Normalization of the wave function $|A|^2$ is determined from

$$\int (|u|^2 + |v|^2) dx = 1$$

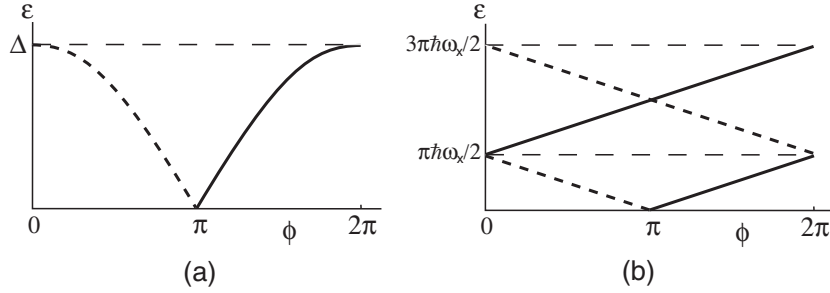


Figure 3.6: The Andreev bound states in (a) short, $\omega_x \gg |\Delta|$, and (b) long, $\omega_x \ll |\Delta|$, SNS structures. The solid lines refer to $v_x > 0$, while the dotted lines are for $v_x < 0$.

In the normal region $|u|^2 + |v|^2 = 2|A|^2$. In the right region

$$|u|^2 + |v|^2 = |d_1|^2 e^{-2\lambda_s x} \left(|\tilde{U}|^2 + |\tilde{V}|^2 \right) = 2|d_1|^2 e^{-2\lambda_s x} |\tilde{U}|^2$$

since $|\tilde{U}|^2 = |\tilde{V}|^2$. Employing the continuity of the wave functions $|A|^2 = |d_1|^2 e^{-\lambda_s d} |\tilde{U}|^2$ we find that in the right region

$$|u|^2 + |v|^2 = 2|A|^2 e^{-2\lambda_s(x-d/2)}$$

In the left region we similarly obtain

$$|u|^2 + |v|^2 = 2|A|^2 e^{-2\lambda_s(x+d/2)}$$

Calculating the integrals from $-\infty$ to $-d/2$ then from $-d/2$ to $d/2$ and from $d/2$ to ∞ we find

$$|A|^2 = \frac{1}{2(d + \lambda_s^{-1})} = \frac{1}{2} \frac{\sqrt{|\Delta|^2 - \epsilon^2}}{\hbar|v_x| + d\sqrt{|\Delta|^2 - \epsilon^2}} \quad (3.25)$$

Consider the limit of a small width of normal region

$$d \ll \hbar|v_x|/|\Delta|$$

such that $d \gg \xi \cos \theta$ where

$$\xi \sim \hbar v_F/|\Delta|$$

is the coherence length, and θ is the angle between the momentum \mathbf{k} and the x axis. We have $\omega_x \gg |\Delta|$. Eq. (3.24) gives

$$\frac{\phi}{2} \mp \arcsin \frac{\epsilon}{|\Delta|} + \pi \left(l \pm \frac{1}{2} \right) = 0$$

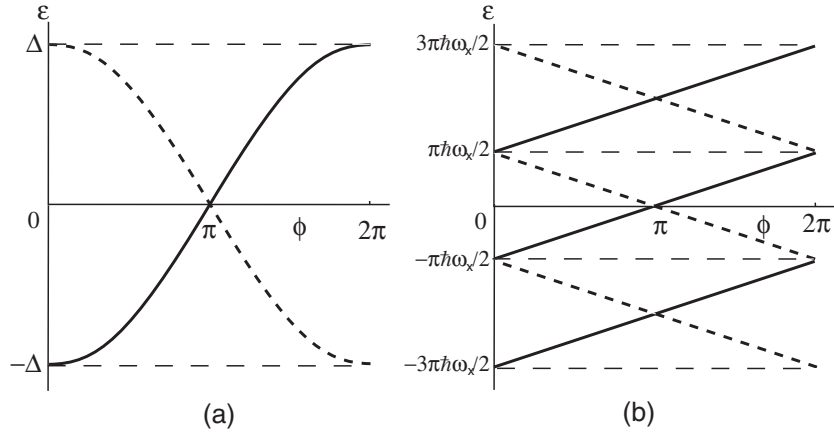


Figure 3.7: The Andreev bound states in (a) short, $\omega_x \gg |\Delta|$, and (b) long, $\omega_x \ll |\Delta|$, SNS structures for extended energy range $-|\Delta| < \epsilon < |\Delta|$. The solid lines refer to $v_x > 0$, while the dotted lines are for $v_x < 0$.

Recall that $\alpha = \arcsin[\epsilon/|\Delta|]$. For $v_x > 0$ we have to choose $l = -1$ to have $-\pi/2 < \alpha < \pi/2$. For $v_x < 0$, the choice is $l = 0$. Therefore, the spectrum becomes [see Fig. 3.6 (a)]

$$\epsilon = \mp |\Delta| \cos \frac{\phi}{2} \quad (3.26)$$

For a long N region, $d \gg \xi_0$, when

$$d \gg \hbar|v_x|/|\Delta|, \quad \omega_x \ll |\Delta|$$

we can neglect $\arcsin(\epsilon/|\Delta|)$ so that [see Fig. 3.6 (b)]

$$\epsilon = \pm \hbar|\omega_x| \left(\frac{\phi}{2} - \frac{\pi}{2} \right) + \pi \hbar|\omega_x|l \quad (3.27)$$

where $l = 0, 1, \dots$

It is useful here to consider negative energies of excitations. Using Eqs. (2.41) and (2.42) we notice that if a state with $\epsilon > 0$ belongs to $k_x > 0$ then the state with $-\epsilon < 0$ belongs to $-k_x < 0$. Therefore, the spectrum Eq. (2.41) now allows both signs of ϵ for any phase difference in the range $0 < \phi < 2\pi$.

For short junctions, the spectrum becomes

$$\epsilon = \mp |\Delta| \cos(\phi/2) \quad (3.28)$$

for $0 < \phi < 2\pi$ with the upper sign for $v_x > 0$ and lower sign for $v_x < 0$. Similarly, for long junctions,

$$\epsilon = \pm \hbar|\omega_x| \left(\frac{\phi}{2} - \frac{\pi}{2} \right) + \pi \hbar|\omega_x|l \quad (3.29)$$

where $l = 0, \pm 1, \pm 2, \dots$ for the entire region $0 < \phi < 2\pi$. These spectra are shown in Fig. 3.7

3.3 Supercurrent through an SNS structure. Proximity effect

The current is given by Eq. (2.85)

$$\mathbf{j} = -\frac{i\hbar e}{m} \sum_n [f_n (u_n^*(\mathbf{r}) \nabla u_n(\mathbf{r})) + (1 - f_n) (v_n(\mathbf{r}) \nabla v_n^*(\mathbf{r})) - c.c] \quad (3.30)$$

where n labels various quantum states. It is more convenient to calculate it in the N region. Applying the semi-classical approximation, we calculate the derivatives only of the rapidly varying functions $e^{i\mathbf{k}\cdot\mathbf{r}}$. Using Eqs. (3.17) and (3.25) and multiplying the current density by the area of the contact S we obtain for the total current carried by the states with $\epsilon < |\Delta|$

$$I_x = -\frac{e}{\hbar} \sum_n (1 - 2f_n) \frac{\hbar v_x \sqrt{|\Delta|^2 - \epsilon_n^2}}{\hbar |v_x| + d \sqrt{|\Delta|^2 - \epsilon_n^2}}$$

Here ϵ_n is the bound state energy determined by Eq. (3.24). The quantum number n describes various states, i.e., the states that belong to various k_y , k_z and $k_x(\epsilon)$ within the area S .

To calculate the supercurrent we assume that there is no voltage across the junction and the distribution functions correspond to equilibrium.

For the bound states, at a given phase difference ϕ there is only a finite number of states satisfying the conditions either $\epsilon = \epsilon_>(k_x)$ or $\epsilon = \epsilon_<(k_x)$ for different signs of k_x . Therefore,

$$I_x = -\frac{e}{\hbar} \left[\sum_{n, k_x > 0} (1 - 2f(\epsilon_>)) \frac{\hbar v_x \sqrt{|\Delta|^2 - \epsilon_>^2}}{\hbar v_x + d \sqrt{|\Delta|^2 - \epsilon_>^2}} - \sum_{n, k_x < 0} (1 - 2f(\epsilon_<)) \frac{\hbar |v_x| \sqrt{|\Delta|^2 - \epsilon_<^2}}{\hbar |v_x| + d \sqrt{|\Delta|^2 - \epsilon_<^2}} \right] \quad (3.31)$$

3.3.1 Short junctions. Point contacts

One can check that for short contacts $d \ll \xi$, the states in the continuum $\epsilon > |\Delta|$ (see Problem 3.3) do not contribute to the current: the contributions of particles flying from the left and of those flying from the right cancel in equilibrium. Therefore, Eq. (3.31) gives the full expression for the current.

The simplest case is the limit of short junctions $d \ll \xi_0$ when one can neglect the term with d in the energy spectrum. The latter is given by Eq. (3.26). Since for a given ϕ there exists only one state for either $v_x > 0$ or $v_x < 0$ according to $\epsilon_{>,<} = \mp \epsilon_\phi$ where

$$\epsilon_\phi = |\Delta| \cos \frac{\phi}{2}$$

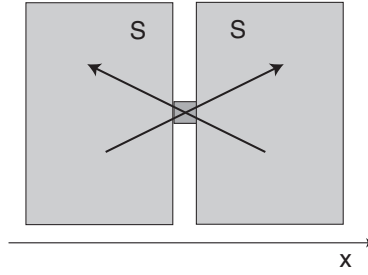


Figure 3.8: The point contact SNS structure.

we find

$$I = \frac{eN_{>}|\Delta|\sin(\phi/2)}{\hbar} \tanh \frac{|\Delta|\cos(\phi/2)}{2T} \quad (3.32)$$

$N_{>}$ is the total number of states per unit volume with $v_x > 0$ and all possible k_y and k_z flying through the contact of an area S . Eq. (3.32) can be written as

$$I = -\frac{2eN_{>}}{\hbar} \frac{\partial \epsilon_\phi}{\partial \phi} \tanh \frac{\epsilon_\phi}{2T} \quad (3.33)$$

We will see that this is a very general form for a current through superconducting junctions.

Eq. (3.32) can be applied only when the phase in the superconducting regions is constant in space, i.e., that it does not vary at distances of the order of $\lambda_S^{-1} \sim \xi$, i.e., when the current is smaller than the critical current in the superconductor. For a wide contact where $N_{>}$ in the normal part is of the same order as in superconductors, it is only true when the phase difference is small, $\phi \ll 1$.

In a general case Eq. (3.32) holds if the number of transverse modes in the normal part $N_{>}$ is much smaller than that in the superconducting regions, which ensures a small value of the current. One of the examples is the so called point contact, i.e., a structure where two superconductors are connected through a narrow (with a cross section of an area $S \sim a^2$ where the transverse dimension is $a \ll \xi$) and short $d \ll \xi$ normal piece called constriction (see Fig. 3.8). In fact, since the wave function has no possibility to vary within the constriction, the results do not change if the constriction is also superconducting.

To calculate the current through the point contact it is more convenient to start with Eq. (3.31). The energy spectrum of a point contact is given by Eq. (3.26); the normalization of the wave function is

$$|A|^2 = \frac{\sqrt{|\Delta|^2 - \epsilon^2}}{2\hbar v_F} \quad (3.34)$$

(see Problem 3.4). The current through the point contact is found from Eq.

(3.31)

$$\begin{aligned}
 I &= -\frac{e}{\hbar} \left[\sum_{k_x > 0} (1 - 2f(\epsilon_{>})) \sqrt{|\Delta|^2 - \epsilon_{>}^2} - \sum_{k_x < 0} (1 - 2f(\epsilon_{<})) \sqrt{|\Delta|^2 - \epsilon_{<}^2} \right] \frac{|v_x|}{v_F} \\
 &= \frac{e|\Delta| \sin(\phi/2)}{\hbar} \tanh \frac{|\Delta| \cos(\phi/2)}{2T} \sum_{v_x > 0} \frac{v_x}{v_F} \quad (3.35)
 \end{aligned}$$

Counting of the states can be performed as follows. First we write

$$\sum_n \Rightarrow \int \frac{4\pi S p_F^2 dp}{(2\pi\hbar)^3} \frac{d\Omega_{\mathbf{p}}}{4\pi}$$

We put $p = p_F + \hbar\lambda_N = p_F + \epsilon/v_F$ and write for a discrete spectrum

$$\frac{dp}{2\pi\hbar} = d\epsilon [\delta(\epsilon - \epsilon_{>}) + \delta(\epsilon - \epsilon_{<})] \quad (3.36)$$

Indeed, in our case the integral $\int_{-\infty}^{\infty} dp/2\pi\hbar = 2$ since there is exactly one state per unit volume for a given phase difference ϕ for $p < p_F$ and one for $p > p_F$. We note here that while p in Eq. (3.36) can be both $p < p_F$ and $p > p_F$, the energy only assumes positive values. As a result,

$$\sum_n \Rightarrow 2\pi\hbar N(0)v_F S \int_{\epsilon > 0} d\epsilon \frac{d\Omega_{\mathbf{p}}}{4\pi} [\delta(\epsilon - \epsilon_{>}) + \delta(\epsilon - \epsilon_{<})]$$

Therefore

$$\begin{aligned}
 \sum_{v_x > 0} \frac{v_x}{v_F} &= 2\pi\hbar N(0)v_F S \int_{\epsilon > 0} d\epsilon \int_{v_x > 0} \frac{d\Omega_{\mathbf{v}}}{4\pi} \frac{v_x}{v_F} [\delta(\epsilon - \epsilon_{>}) + \delta(\epsilon - \epsilon_{<})] \\
 &= 2\pi\hbar N(0)v_F S \int_{v_x > 0} \frac{d\Omega_{\mathbf{v}}}{4\pi} \frac{v_x}{v_F} = \frac{\pi\hbar N(0)v_F S}{2}
 \end{aligned}$$

Finally,

$$\begin{aligned}
 I &= \frac{N(0)v_F S \pi e |\Delta| \sin(\phi/2)}{2} \tanh \frac{|\Delta| \cos(\phi/2)}{2T} \\
 &= \frac{\pi |\Delta| \sin(\phi/2)}{e R_{\text{Sh}}} \tanh \frac{|\Delta| \cos(\phi/2)}{2T} \quad (3.37)
 \end{aligned}$$

where

$$\frac{1}{R_{\text{Sh}}} = \frac{e^2 N(0)v_F S}{2} = \frac{e^2}{\pi\hbar} \frac{\pi k_F^2 S}{(2\pi)^2}$$

is the so called Sharvin conductance (inverse resistance) of the contact in the normal state. One can write it as

$$\frac{1}{R_{\text{Sh}}} = \frac{N_{>}}{R_0} \quad (3.38)$$

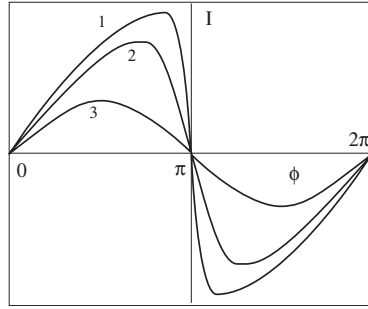


Figure 3.9: The supercurrent through the point contact. Curve (1) corresponds to a low temperature $T \ll T_c$, curve (3) is for a temperature close to T_c .

Here

$$N_{>} = \frac{\pi k_F^2 S}{(2\pi)^2}$$

is the effective number of states (for both spin projections) penetrating through the contact. Each state that contributes to the current is called the conducting channel or conducting transverse mode. The quantity

$$R_0 = \frac{\pi \hbar}{e^2} \approx 12.9 \text{ k}\Omega$$

is the (two-spin) quantum of resistance (see the next Chapter).

The dependence Eq. (3.37) is shown in Fig. 3.9 for various temperatures. It has a maximum which is called the critical current: A point contact cannot sustain nondissipative currents larger than I_c . For low temperatures, the critical current

$$I_c = \frac{\pi |\Delta|}{e R_{\text{Sh}}}$$

is reached near $\phi = \pi$. For temperatures close to T_c the critical current

$$I_c = \frac{\pi |\Delta|^2}{4 T e R_{\text{Sh}}}$$

is reached at $\phi = \pi/2$.

3.3.2 Long junctions

In long junctions, the states with energies larger than $|\Delta|$ do also contribute to the supercurrent. However, in some cases their contribution is negligible. Here we consider the current at low temperatures, when the main contribution comes from the bound states.

3.3. SUPERCURRENT THROUGH AN SNS STRUCTURE. PROXIMITY EFFECT 67

For long junctions $d \gg \xi_0$ we neglect the term $\hbar v_x$ in the denominator in Eq. (3.31) and find

$$\begin{aligned}
 I_x &= -\frac{e}{d} \left[\sum_{n, k_x > 0} |v_x| (1 - 2f(\epsilon_{>})) - \sum_{n, k_x < 0} |v_x| (1 - 2f(\epsilon_{<})) \right] \\
 &= -\frac{e}{d} \sum_{k_x > 0} |v_x| \left(\sum_{l=0}^{l_0} \tanh \left[\frac{\hbar|\omega_x|(\phi - \pi)/2 + \hbar|\omega_x|\pi l}{2T} \right] \right. \\
 &\quad \left. - \sum_{l=1}^{l_0} \tanh \left[\frac{-\hbar|\omega_x|(\phi - \pi)/2 + \hbar|\omega_x|\pi l}{2T} \right] \right) \\
 &= -\frac{e}{d} \sum_{k_x > 0} |v_x| \sum_{l=-l_0}^{l_0} \tanh \left[\frac{\hbar|\omega_x|(\phi - \pi)/2 + \hbar|\omega_x|\pi l}{2T} \right]
 \end{aligned}$$

Here l_0 corresponds to $\epsilon = |\Delta|$, i.e., $l_0 = |\Delta|/\pi\hbar|\omega_x| \gg 1$.

Consider the limit of low temperatures $T \ll |\Delta|$ and very long junction, $|\omega_x| \ll T$ i.e., $d \gg \hbar v_F/T$. In the sum over l one can replace the upper limit by infinity. In this case all what happens at energies $\epsilon > |\Delta|$ has no effect, thus the delocalized states can be ignored. The sum becomes

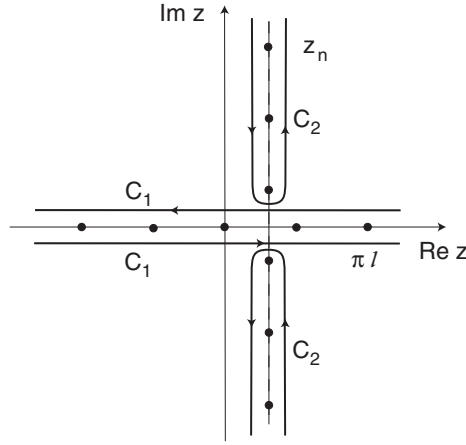
$$\Sigma = \sum_{l=-\infty}^{\infty} \tanh \left[\frac{\hbar|\omega_x|(\phi - \pi)/2 + \hbar|\omega_x|\pi l}{2T} \right]$$

If one considers the variable $\hbar|\omega_x|\pi l$ as continuous and replaces the summation with integration, the sum turns to zero being a sum of an odd function. Therefore, we need to take into account the discrete nature of summation. To do this, we write

$$\begin{aligned}
 &\sum_{l=-\infty}^{\infty} \tanh \left[\frac{\hbar|\omega_x|(\phi - \pi)/2 + \hbar|\omega_x|\pi l}{2T} \right] \\
 &= \frac{1}{2\pi i} \int_{C_1} \tanh \left[\frac{\hbar|\omega_x|(\phi - \pi)/2 + \hbar|\omega_x|z}{2T} \right] \cot z \, dz
 \end{aligned}$$

where the contour C_1 in the complex plane is shown in Fig. 3.10. It goes around all poles of $\cot z$ at $z = \pi l$. By shifting the contour into the upper and lower half-planes we obtain

$$\begin{aligned}
 \Sigma &= -\frac{1}{2\pi i} \int_{C_2} \tanh \left[\frac{\hbar|\omega_x|(\phi - \pi)/2 + \hbar|\omega_x|z}{2T} \right] \cot z \, dz \\
 &= -\frac{T}{\pi i \hbar|\omega_x|} \int_{C_2} \tanh \left[\frac{\hbar|\omega_x|(\phi - \pi)/2}{2T} + \tilde{z} \right] \cot \left[\frac{2T\tilde{z}}{\hbar|\omega_x|} \right] d\tilde{z} \\
 &= -\frac{2T}{\hbar|\omega_x|} \sum_{n=-\infty}^{\infty} \cot \left[\frac{2T\tilde{z}_n}{\hbar|\omega_x|} \right] = -\frac{2T}{\hbar|\omega_x|} \sum_{n=-\infty}^{\infty} \frac{\tanh \alpha_n \sin \beta - i \cos \beta}{\tanh \alpha_n \cos \beta + i \sin \beta}
 \end{aligned}$$

Figure 3.10: The contours of integration in the complex plane z .

$$= -\frac{2T}{\hbar|\omega_x|} \left[\sum_{n=0}^{\infty} \frac{\tanh \alpha_n \sin \beta - i \cos \beta}{\tanh \alpha_n \cos \beta + i \sin \beta} + c.c. \right]$$

where

$$\tilde{z}_n = i\pi \left(n + \frac{1}{2} \right) - \frac{\hbar|\omega_x|(\phi - \pi)/2}{2T}$$

are the poles of the \tanh function, and

$$\alpha_n = \omega_n/|\omega_x|, \quad \beta = (\phi - \pi)/2$$

where

$$\hbar\omega_n = 2\pi T \left(n + \frac{1}{2} \right)$$

are the so called Matsubara frequencies.

In the limit of very long junction, $|\omega_x| \ll T$ i.e., $d \gg \hbar v_F/T$ the factor $\alpha_n \gg 1$ so that

$$\tanh \alpha_n \approx 1 - 2e^{-2\alpha_n}$$

Therefore, only the term with $n = 0$ is important in the sum and

$$\frac{\tanh \alpha_0 \sin \beta - i \cos \beta}{\tanh \alpha_0 \cos \beta + i \sin \beta} = -i - 2ie^{-2\alpha_0 - 2i\beta}$$

Therefore,

$$\Sigma = -\frac{8T}{\hbar|\omega_x|} e^{-2\alpha_0} \sin \phi = -\frac{8Td}{\hbar|v_x|} e^{-2\pi Td/\hbar|v_x|} \sin \phi$$

The current becomes

$$I_x = \frac{8Te \sin \phi}{\hbar} \sum_{v_x > 0} e^{-2\pi Td/\hbar v_x} \quad (3.39)$$

3.3. SUPERCURRENT THROUGH AN SNS STRUCTURE. PROXIMITY EFFECT 69

To sum over the states with $v_x > 0$ we write

$$\sum_{v_x > 0} \Rightarrow S \int \frac{2\pi p_\perp dp_\perp dp_x}{(2\pi\hbar)^3} = \frac{2\pi p_F^2 S}{(2\pi\hbar)^3} \int_0^{\pi/2} \sin\theta \cos\theta d\theta \int dp_x = \frac{N(0)v_F S}{2} \int_0^1 x dx \int dp_x$$

where $p_\perp = p_F \sin\theta$ is the projection of the momentum on the (y, z) plane while θ is the angle between the momentum and the x axis, and $x = \cos\theta$. We have similarly to Eqs. (3.36), (??)

$$dp_x = 2\pi\hbar [\delta(\epsilon - \epsilon_>) + \delta(\epsilon - \epsilon_<)] d\epsilon$$

Therefore

$$\begin{aligned} I_x &= \frac{4N(0)v_F S T e \sin\phi}{\hbar} \int_0^1 x dx \int dp_x e^{-2\pi T d / \hbar v_x} \\ &= 8\pi N(0)v_F S T e \sin\phi \int_0^1 x dx e^{-2\pi T d / \hbar v_F x} \end{aligned}$$

We put $x = 1/y$ and find

$$\int_0^1 x dx e^{-2\pi T d / \hbar v_x} = \int_1^\infty \frac{dy}{y^3} e^{-(2\pi T d / \hbar v_F) y} \approx \int_1^\infty e^{-(2\pi T d / \hbar v_F) y} dy = \frac{\hbar v_F}{2\pi T d} e^{-2\pi T d / \hbar v_F}$$

since $\hbar v_F / 2\pi T d \ll 1$. Finally,

$$I_x = \frac{4\hbar N(0)v_F^2 S e}{d} e^{-d/\xi_N} \sin\phi = \frac{1}{2eR_{\text{Sh}}} \frac{8\hbar v_F}{d} e^{-d/\xi_N} \sin\phi \quad (3.40)$$

where

$$\xi_N = \frac{\hbar v_F}{2\pi T}$$

is the ‘‘normal-state’’ coherence length. Eq. (3.40) can be written as

$$I = I_c \sin\phi$$

where the critical current is

$$I_c = \frac{1}{2eR_{\text{Sh}}} \frac{8\hbar v_F}{d} e^{-d/\xi_N} \quad (3.41)$$

where $2R_{\text{Sh}}$ is the resistance of two SN contacts in the normal state.

We see that for $I < I_c$ the supercurrent can flow through the normal region that is in contact with superconductors. This is called the proximity effect: the superconductor induces Cooper-pair-like correlations between electrons in the normal state. These correlations decay exponentially into the normal metal over distances ξ_N inversely proportional to temperature. The exponential decay of correlations ensures a small value of the current which is required for the validity of our calculations.

There is not only the supercurrent in the normal metal but also an energy gap. Indeed, the energy spectrum is given by Eq. (3.27). The lowest energy of excitation is

$$\epsilon_0 = \hbar|\omega_x| \left(\frac{\phi}{2} - \frac{\pi}{2} \right)$$

It depends on the phase difference between the superconductors. The gap vanishes for $\phi = \pi$.

Problems

Problem 3.1.

Find the deflection angle of the trajectory during the Andreev reflection.

Problem 3.2.

Calculate the velocity of a slow drift of an Andreev state in a SNS structure with $d \gg \xi_0$ along the SN plane. Explain the origin of the drift.

Problem 3.3.

Find the wave functions for an SNS structure for $\epsilon > |\Delta|$.

Problem 3.4.

Find the energy spectrum and wave functions of the superconducting point contact for $\epsilon < |\Delta|$.

Chapter 4

Superconductor–Insulator– Normal-metal Interface

4.1 Transmission through the barrier

4.1.1 Transmission and reflection probabilities

Consider a junction such that the superconductor and the normal-metal half-spaces are separated by an insulating barrier in the (y, z) plane described by the potential $U(x)$. We assume that Δ depends only on the x coordinate. The momentum projections along the y, z plane are conserved. We start from the BdG equations

$$-\frac{\hbar^2}{2m} \left(\nabla - \frac{ie}{\hbar c} \mathbf{A} \right)^2 u - E_F u + \Delta v = \epsilon u \quad (4.1)$$

$$\frac{\hbar^2}{2m} \left(\nabla + \frac{ie}{\hbar c} \mathbf{A} \right)^2 v + E_F v + \Delta^* u = \epsilon v \quad (4.2)$$

Consider the wave function in the form

$$e^{ik_y y + ik_z z} \begin{pmatrix} u(x) \\ v(x) \end{pmatrix}$$

where $k_y = k_F \sin \theta \cos \phi$, $k_z = k_F \sin \theta \sin \phi$, and θ and ϕ are the incidence and azimuthal angle. The BdG equations are

$$\left[-\frac{\hbar^2}{2m} \frac{d^2}{dx^2} - E_x + U(x) \right] u + \Delta v = \epsilon u \quad (4.3)$$

$$-\left[-\frac{\hbar^2}{2m} \frac{d^2}{dx^2} - E_x + U(x) \right] v + \Delta^* u = \epsilon v \quad (4.4)$$

where

$$E_x = E_F - \frac{\hbar^2(k_y^2 + k_z^2)}{2m} = \frac{\hbar^2 k_x^2}{2m}$$

and $k_x = k_F \cos \theta$.

Assume that a particle is incident from the normal region on the left. It will be reflected back by both normal and Andreev reflection processes.

We model the insulating barrier by a δ function potential $U(x) = I\delta(x)$. The BdG equations take the form

$$\left[-\frac{\hbar^2}{2m} \frac{d^2}{dx^2} - E_x + I\delta(x) \right] u + \Delta v = \epsilon u \quad (4.5)$$

$$-\left[-\frac{\hbar^2}{2m} \frac{d^2}{dx^2} - E_x + I\delta(x) \right] v + \Delta^* u = \epsilon v \quad (4.6)$$

The boundary conditions at the barrier $x = 0$ are

$$\begin{pmatrix} u(0) \\ v(0) \end{pmatrix}_L = \begin{pmatrix} u(0) \\ v(0) \end{pmatrix}_R \quad (4.7)$$

and

$$\frac{d}{dx} \begin{pmatrix} u(0) \\ v(0) \end{pmatrix}_R - \frac{d}{dx} \begin{pmatrix} u(0) \\ v(0) \end{pmatrix}_L = 2|k_x|Z \begin{pmatrix} u(0) \\ v(0) \end{pmatrix} \quad (4.8)$$

We introduce here the barrier strength

$$Z = \frac{mI}{\hbar^2 |k_x|}$$

and assume that $Z \sim 1$. The barrier strength Z is generally a function of the incident angle θ , where $k_x = k_F \cos \theta$.

Scattering states

Consider first the case $\epsilon > |\Delta|$.

There are four independent solutions: (1) The wave function that has an incident particle on the left of the barrier, (2) the wave function with an incident

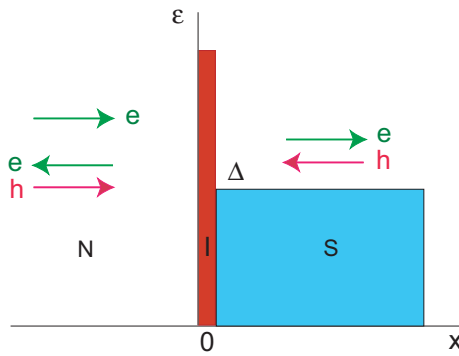


Figure 4.1: The NIS structure.

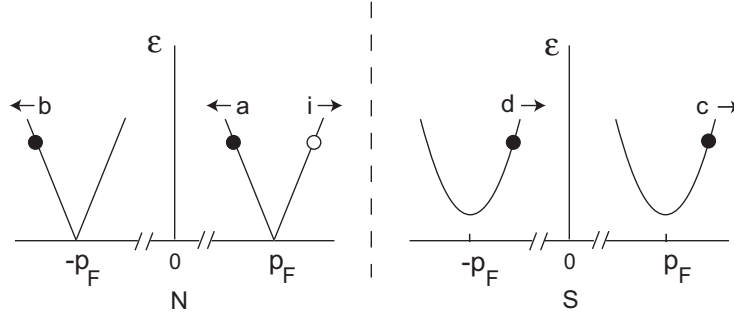


Figure 4.2: Left: The state in N region with an incoming particle (i) that is Andreev reflected as a hole (a) and normally reflected as a particle (b). Right: Transmitted particle (c) and hole (d) in S region.

hole on the left, (3) an incident particle on the right, and (4) an incident hole on the right.

(1) The wave function with an incident particle from the normal region (from the left) has the form (see Fig. 4.2)

$$\begin{pmatrix} u(x) \\ v(x) \end{pmatrix}_L = e^{iq_+(N)x} \begin{pmatrix} 1 \\ 0 \end{pmatrix} + ae^{iq_-(N)x} \begin{pmatrix} 0 \\ 1 \end{pmatrix} + be^{-iq_+(N)x} \begin{pmatrix} 1 \\ 0 \end{pmatrix} \quad (4.9)$$

Here

$$q_{\pm}(N) = k_x \pm \frac{\epsilon}{\hbar v_x}$$

The wave contains normally reflected particle with the amplitude b , and Andreev reflected hole with the amplitude a . On the right of the barrier it has transmitted particle c and a hole d

$$\begin{pmatrix} u(x) \\ v(x) \end{pmatrix}_R = ce^{iq_+(S)x} \begin{pmatrix} U \\ V \end{pmatrix} + de^{-iq_-(S)x} \begin{pmatrix} V \\ U \end{pmatrix} \quad (4.10)$$

Here

$$q_{\pm}(S) = k_x \pm \frac{\sqrt{\epsilon^2 - |\Delta|^2}}{\hbar v_x}$$

and

$$U = \frac{1}{\sqrt{2}} \left(1 + \frac{\sqrt{\epsilon^2 - |\Delta|^2}}{\epsilon} \right)^{1/2}, \quad V = \frac{1}{\sqrt{2}} \left(1 - \frac{\sqrt{\epsilon^2 - |\Delta|^2}}{\epsilon} \right)^{1/2}$$

The boundary conditions yield

$$\begin{aligned} 1 + b &= cU + dV \\ a &= cV + dU \end{aligned}$$

and

$$\begin{aligned} q_-(S)Vd - q_+(S)Uc - q_+(N)b + q_+(N) &= 2i|k_x|Z(1+b) \\ q_-(S)Ud - q_+(S)Vc + q_-(N)a &= 2i|k_x|Za \end{aligned}$$

We notice that $q_+ + q_- \approx 2k_x$ while $q_+ - q_- \sim \Delta/\hbar v_F$ so that $q_+ - q_- \ll q_+ + q_-$ and also $q_+ - q_- \ll k_F Z$. As a result, in the semiclassical approximation,

$$a = \frac{UV}{U^2 + (U^2 - V^2)Z^2} \quad (4.11)$$

$$b = -\frac{(U^2 - V^2)(Z^2 + iZ)}{U^2 + (U^2 - V^2)Z^2} = -\frac{(U^2 - V^2)|Z|\sqrt{Z^2 + 1}e^{i\delta}}{U^2 + (U^2 - V^2)Z^2} \quad (4.12)$$

$$c = \frac{(1 - iZ)U}{U^2 + (U^2 - V^2)Z^2} = -\frac{i\sqrt{Z^2 + 1}Ue^{i\delta}}{U^2 + (U^2 - V^2)Z^2} \quad (4.13)$$

$$d = \frac{iZV}{U^2 + (U^2 - V^2)Z^2} \quad (4.14)$$

where the scattering phase δ is defined as

$$\tan \delta = 1/Z$$

In the limit of the normal state $V = 0$, $U = 1$, and $a = d = 0$ while

$$b = -\frac{iZ}{1 + iZ}, \quad c = \frac{1}{1 + iZ}$$

so that

$$|b|^2 = \frac{Z^2}{1 + Z^2}, \quad |c|^2 = \frac{1}{1 + Z^2}$$

Without a barrier $Z = 0$ and $b = d = 0$ while

$$a = \frac{V}{U}, \quad c = \frac{1}{U}$$

as it should be for purely Andreev reflection, Eq. (3.12).

(2) The state with an incident hole in the normal region is

$$\begin{pmatrix} u(x) \\ v(x) \end{pmatrix}_L = e^{-iq_-(N)x} \begin{pmatrix} 0 \\ 1 \end{pmatrix} + a_2 e^{-iq_+(N)x} \begin{pmatrix} 1 \\ 0 \end{pmatrix} + b_2 e^{iq_-(N)x} \begin{pmatrix} 0 \\ 1 \end{pmatrix} \quad (4.15)$$

It contains normally reflected hole with the amplitude b_2 , and Andreev reflected particle with the amplitude a_2 . On the right of the barrier it has transmitted hole c_2 and a particle d_2

$$\begin{pmatrix} u(x) \\ v(x) \end{pmatrix}_R = c_2 e^{-iq_-(S)x} \begin{pmatrix} V \\ U \end{pmatrix} + d_2 e^{iq_+(S)x} \begin{pmatrix} U \\ V \end{pmatrix}$$

The coefficients a_2 , b_2 , c_2 , and d_2 are given by Eqs. (4.11)–(4.14) where Z is replaced with $-Z$:

$$a_2 = a(-Z), \quad b_2 = b(-Z), \quad c_2 = c(-Z), \quad d_2 = d(-Z)$$

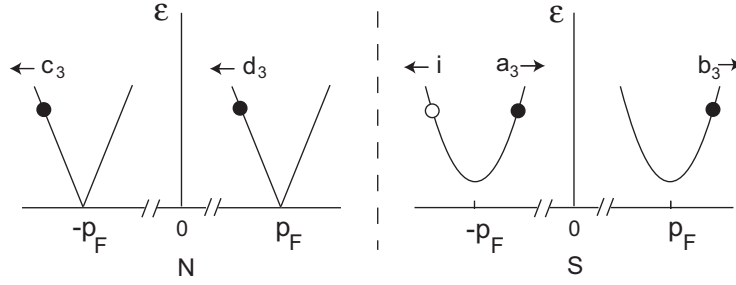


Figure 4.3: The states of incoming, reflected and transmitted particles and holes at a NIS interface when a incident particle approaches barrier from the superconducting side.

(3) Consider now the process when a particle is incident on a barrier from the superconducting side, i.e., from the right (see Fig. 4.3).

On the right of the barrier (in the S region) we have

$$\begin{pmatrix} u(x) \\ v(x) \end{pmatrix}_R = e^{-iq_+(S)x} \begin{pmatrix} U \\ V \end{pmatrix} + a_3 e^{-iq_-(S)x} \begin{pmatrix} V \\ U \end{pmatrix} + b_3 e^{iq_+(S)x} \begin{pmatrix} U \\ V \end{pmatrix}$$

On the left of the barrier (in the N region)

$$\begin{pmatrix} u(x) \\ v(x) \end{pmatrix}_L = c_3 e^{-iq_+(N)x} \begin{pmatrix} 1 \\ 0 \end{pmatrix} + d_3 e^{iq_-(N)x} \begin{pmatrix} 0 \\ 1 \end{pmatrix}$$

The boundary condition require

$$\begin{aligned} U + a_3 V + b_3 U &= c_3 \\ V + a_3 U + b_3 V &= d_3 \end{aligned}$$

and

$$\begin{aligned} q_+(N)c_3 - q_+(S)U - q_-(S)Va_3 + q_+(S)Ub_3 &= 2i|k_x|Zc_3 \\ -q_-(N)d_3 - q_+(S)V - q_-(S)Ua_3 + q_+(S)Vb_3 &= 2i|k_x|Zd_3 \end{aligned}$$

As a result, we find

$$a_3 = -a(-Z), \quad b_3 = b(-Z) \quad (4.16)$$

while

$$c_3 = \frac{v_g(S)}{v_g(N)} c(-Z) \quad (4.17)$$

$$d_3 = -\frac{v_g(S)}{v_g(N)} d(-Z) \quad (4.18)$$

Here

$$v_g(S) = \frac{\hbar k_x}{m} \frac{\sqrt{\epsilon^2 - |\Delta|^2}}{\epsilon}$$

is the group velocity of particles (holes) in the superconductor. Similarly,

$$v_g(N) = \frac{\hbar k_x}{m}$$

is the group velocity of particles (holes) in the normal metal.

The state (4) has an incident hole on the right

$$\begin{pmatrix} u(x) \\ v(x) \end{pmatrix}_R = e^{iq_-(S)x} \begin{pmatrix} V \\ U \end{pmatrix} + a_4 e^{iq_+(S)x} \begin{pmatrix} U \\ V \end{pmatrix} + b_4 e^{-iq_-(S)x} \begin{pmatrix} V \\ U \end{pmatrix}$$

On the left of the barrier (in the N region)

$$\begin{pmatrix} u(x) \\ v(x) \end{pmatrix}_L = c_4 e^{iq_-(N)x} \begin{pmatrix} 0 \\ 1 \end{pmatrix} + d_4 e^{-iq_+(N)x} \begin{pmatrix} 1 \\ 0 \end{pmatrix}$$

The coefficients a_4 , b_4 , c_4 , and d_4 are given by Eqs. (4.16)–(4.18) where Z is replaced with $-Z$.

The states (2) and (4) can be obtained from (1) and (3), respectively, by changing signs of ϵ and k_x in q_{\pm} and in U , V with simultaneous change of 1 to 0 and vice versa (which also corresponds to the change of U into V and vice versa) in the normal region coherence factors. The reflection and transmission coefficients $|a|^2$ to $|d|^2$ are determined Eqs. (4.11)–(4.14) and (4.16)–(4.18). Thus, to comply with the $\epsilon \rightarrow -\epsilon$ transformation the factors U and V in the coefficients $|a|^2$, $|b|^2$, $|c|^2$ and $|d|^2$ should be considered as even functions of ϵ :

$$U^2 = \frac{1}{2} \left(1 + \sqrt{\frac{\epsilon^2 - |\Delta|^2}{\epsilon^2}} \right), \quad V^2 = \frac{1}{2} \left(1 - \sqrt{\frac{\epsilon^2 - |\Delta|^2}{\epsilon^2}} \right)$$

With this definition, the reflection and transmission coefficients $|a|^2$ to $|d|^2$ are even functions of ϵ .

Subgap states

Consider now the case $\epsilon < |\Delta|$. For the state (1) with $k_x > 0$ we have on the right of the barrier in the superconducting region only the decaying waves

$$\begin{pmatrix} u(x) \\ v(x) \end{pmatrix}_R = c e^{i\tilde{q}_+(S)x} \begin{pmatrix} \tilde{U} \\ \tilde{V} \end{pmatrix} + d e^{-i\tilde{q}_-(S)x} \begin{pmatrix} \tilde{V} \\ \tilde{U} \end{pmatrix}$$

where

$$\tilde{q}_{\pm}(S) = k_x \pm \frac{im}{\hbar^2 k_x} \sqrt{|\Delta|^2 - \epsilon^2}$$

and

$$\tilde{U} = \frac{1}{\sqrt{2}} \left(1 + i \frac{\sqrt{|\Delta|^2 - \epsilon^2}}{\epsilon} \right)^{1/2}, \quad \tilde{V} = \frac{1}{\sqrt{2}} \left(1 - i \frac{\sqrt{|\Delta|^2 - \epsilon^2}}{\epsilon} \right)^{1/2} \quad (4.19)$$

The expressions Eqs. (4.11)–(4.14) for the coefficients hold with the replacement $U \rightarrow \tilde{U}$ and $V \rightarrow \tilde{V}$. However, since \tilde{U} and \tilde{V} are complex, we find

$$|a|^2 = \frac{|\Delta|^2}{\epsilon^2 + (|\Delta|^2 - \epsilon^2)(1 + 2Z^2)^2} \quad (4.20)$$

and

$$|a|^2 + |b|^2 = 1 \quad (4.21)$$

in accordance with the fact that the quasiparticle flow on the right vanishes $P_R = 0$. In other words, the incident particle is reflected backwards as a combination of a particle and a hole. Without a barrier, $|a|^2 = 1$, i.e., the particle is fully reflected as a hole as it should be, Eq. (3.16).

4.1.2 Probability conservation

As we know, the BdG equations (4.1), (4.2) conserve the quasiparticle flow Eq. (2.90) $\text{div } \mathbf{P} = 0$ where the quasiparticle flux is defined by Eq. (2.89). Consider the quasiparticle flow in the contact. The flow Eq. (2.89) on the left is according to Eq. (4.9)

$$P_L = 2q_+(N)(1 - |b|^2) - 2q_-(N)|a|^2$$

Flow on the right is, see Eq. (4.10)

$$\begin{aligned} P_R &= q_+(S)|c|^2(U^2 - V^2) + q_-(S)|d|^2(U^2 - V^2) \\ &\quad + c^*d[q_-(S)(VU - UV) + q_+(S)(VU - UV)]e^{-iq_-(S)x - iq_+(S)x} + c.c \\ &= 2(q_+(S)|c|^2 + q_-(S)|d|^2)(U^2 - V^2) \end{aligned}$$

The conservation of flow yields

$$q_+(N)(1 - |b|^2) - q_-(N)|a|^2 = [q_+(S)|c|^2 + q_-(S)|d|^2] \frac{\sqrt{\epsilon^2 - |\Delta|^2}}{\epsilon}$$

or

$$q_+(N)|b|^2 + q_-(N)|a|^2 + [q_+(S)|c|^2 + q_-(S)|d|^2] \frac{\sqrt{\epsilon^2 - |\Delta|^2}}{\epsilon} = q_+(N) \quad (4.22)$$

Note that

$$\hbar q_{\pm}(S) \frac{\sqrt{\epsilon^2 - |\Delta|^2}}{\epsilon} = m v_{g,\pm}(S)$$

where $v_{g,\pm}(S)$ is the group velocity of particles (holes) in the superconductor, which coincide in the quasiclassical approximation. Similarly,

$$\hbar q_{\pm}(N) = m v_{g,\pm}(N)$$

where $v_{g,\pm}(N)$ is the group velocity of particles (holes) in the normal metal. Therefore, the flow conservation implies the conservation of quasiparticle current probabilities: The sum of current probability of normally reflected particle

$v_{g+}(N)|b|^2$, Andreev reflected hole $v_{g-}(N)|a|^2$, transmitted particle $v_{g+}(S)|c|^2$, and transmitted hole $v_{g-}(S)|d|^2$ is equal to the incident flow $v_{g+}(N)$:

$$v_{g+}(N)|b|^2 + v_{g-}(N)|a|^2 + v_{g+}(S)|c|^2 + v_{g-}(S)|d|^2 = v_{g+}(N) \quad (4.23)$$

The coefficients in Eqs. (4.11) – (4.14) satisfy Eq. (4.23).

Similarly, equations (4.16)–(4.18) and the flow conservation Eq. (4.23) for the direct process of Fig. 4.2 comply with the conservation of flow in the reverse process of Fig. 4.3:

$$v_g(S)|a_3|^2 + v_g(S)|b_3|^2 + v_g(N)|c_3|^2 + v_g(N)|d_3|^2 = v_g(S) \quad (4.24)$$

Since the group velocities and the DOS are coupled through

$$\frac{N_S}{N_N} = \frac{v_F}{v_g(S)} \quad (4.25)$$

we find from Eqs.(4.17), (4.18)

$$(v_F|c_3|^2)N_S = (v_g|c|^2)N_N, \quad (v_F|d_3|^2)N_S = (v_g|d|^2)N_N \quad (4.26)$$

and also

$$(v_g(S)|a_3|^2)N_S = (v_F|a|^2)N_N, \quad (v_g(S)|b_3|^2)N_S = (v_F|b|^2)N_N \quad (4.27)$$

which express the detailed balance of particle flow within an energy interval dE .

4.2 Current through the NIS junction

Consider the case when a voltage V is applied across the interface. We assume that the potential of the superconductor is zero while the potential of the normal metal is V .

The current is

$$\mathbf{j} = -\frac{i\hbar e}{m} \sum_{n=1,\dots,4;\epsilon,\mathbf{p}} [f_{n,\epsilon,\mathbf{p}} (u_{n,\epsilon,\mathbf{p}}^* \nabla u_{n,\epsilon,\mathbf{p}}) + (1 - f_{n,\epsilon,\mathbf{p}}) (v_{n,\epsilon,\mathbf{p}} \nabla v_{n,\epsilon,\mathbf{p}}^*) - c.c] \quad (4.28)$$

It is more convenient to calculate it in the normal region. We have

$$\begin{aligned} \mathbf{j} &= -\frac{i\hbar e}{m} \sum_{n=1,3;\epsilon} [f_{n,\epsilon} (u_{n,\epsilon,\mathbf{p}}^* \nabla u_{n,\epsilon,\mathbf{p}}) + (1 - f_{n,\epsilon}) (v_{n,\epsilon,\mathbf{p}} \nabla v_{n,\epsilon,\mathbf{p}}^*) - c.c] \\ &\quad -\frac{i\hbar e}{m} \sum_{n=2,4;\epsilon} [f_{n,\epsilon} (u_{n,\epsilon,\mathbf{p}}^* \nabla u_{n,\epsilon,\mathbf{p}}) + (1 - f_{n,\epsilon}) (v_{n,\epsilon,\mathbf{p}} \nabla v_{n,\epsilon,\mathbf{p}}^*) - c.c] \end{aligned}$$

The state (1) has particles incident from the normal region [see Fig. 4.4(a)]. Therefore, their distribution corresponds to that in the normal region, $f_1 = f_\epsilon(N)$. The sum over the states is

$$\sum_{n=1} = \int_{\epsilon>0} N_N d\epsilon \int_{k_x>0} \frac{d\Omega_{\mathbf{k}}}{4\pi}$$

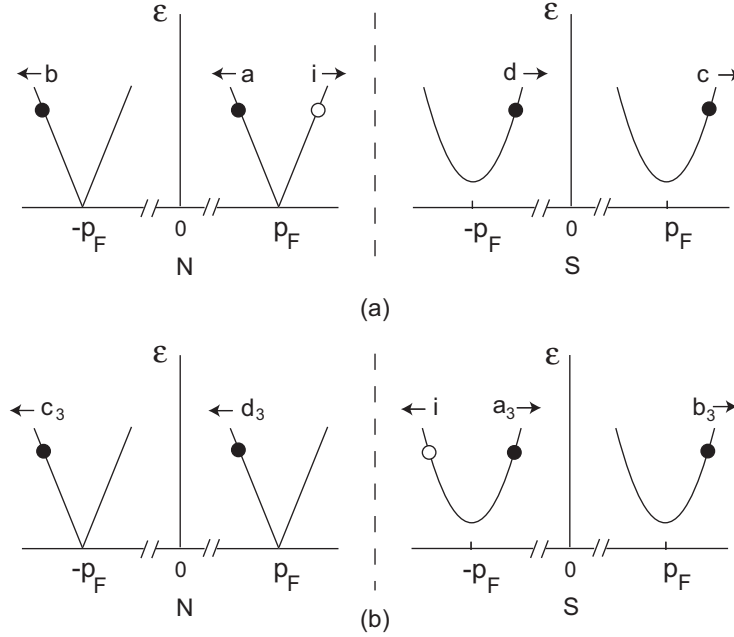


Figure 4.4: The states of incoming, reflected and transmitted particles and holes at a NIS interface that contribute to the current.

We have

$$-iu_{1,\epsilon,\mathbf{p}}^* \nabla_x u_{1,\epsilon,\mathbf{p}} + c.c. = 2k_x (1 - |b|^2), \quad -iv_{1,\epsilon,\mathbf{p}} \nabla_x v_{1,\epsilon,\mathbf{p}}^* + c.c. = -2k_x |a|^2$$

The state (2) has holes incident from the normal region [see Fig. 4.4(a)]. Therefore, their distribution corresponds to the distribution of holes in the normal region, $f_2 = 1 - f_{-\epsilon}(N)$. To get this distribution we note that the hole excitation with an energy $\epsilon > 0$ is the absence of particle in a state below the Fermi surface, i.e., with an energy $-\epsilon$. We have

$$-iu_{2,\epsilon,\mathbf{p}}^* \nabla_x u_{2,\epsilon,\mathbf{p}} + c.c. = -2k_x |a_2|^2, \quad -iv_{2,\epsilon,\mathbf{p}} \nabla_x v_{2,\epsilon,\mathbf{p}}^* + c.c. = 2k_x (1 - |b_2|^2)$$

At the same time, the state (3) has particles incident from the superconducting region [see Fig. 4.4(b)]. Therefore, their distribution corresponds to that in the superconductor $f_3 = f_{\epsilon}(S)$. The sum over the states is

$$\sum_{n=3} = \int_{\epsilon>0} N_S d\epsilon \int_{k_x>0} \frac{d\Omega_{\mathbf{k}}}{4\pi}$$

We have

$$-iu_{3,\epsilon,\mathbf{p}}^* \nabla_x u_{3,\epsilon,\mathbf{p}} + c.c. = -2k_x |c_3|^2, \quad -iv_{3,\epsilon,\mathbf{p}} \nabla_x v_{3,\epsilon,\mathbf{p}}^* + c.c. = -2k_x |d_3|^2$$

Similarly, the state (4) has holes incident from the superconducting region [see Fig. 4.4(b)]. Therefore, their distribution is $f_4 = 1 - f_{-\epsilon}(S)$, while

$$-iv_{4,\epsilon,\mathbf{p}}^* \nabla_x u_{4,\epsilon,\mathbf{p}} + c.c. = -2k_x |d_4|^2, \quad -iv_{4,\epsilon,\mathbf{p}} \nabla_x v_{4,\epsilon,\mathbf{p}}^* + c.c. = -2k_x |c_4|^2$$

Therefore, the total current through the junction area S is

$$\begin{aligned} I_{NIS} &= \frac{2\hbar e S}{m} \int N_N d\epsilon \frac{d\Omega}{4\pi} k_x [(1 - |b|^2)(f_\epsilon(N) + f_{-\epsilon}(N)) - |a|^2(2 - f_\epsilon(N) - f_{-\epsilon}(N))] \\ &\quad - \frac{2\hbar e S}{m} \int N_S d\epsilon \frac{d\Omega}{4\pi} k_x \left[(|c|^2(f_\epsilon(S) + f_{-\epsilon}(S)) + |d|^2(2 - f_\epsilon(S) - f_{-\epsilon}(S))) \frac{v_g^2(S)}{v_g^2(N)} \right] \\ &= \frac{2\hbar e S}{m} \int N_N d\epsilon \frac{d\Omega}{4\pi} k_x [(1 - |b|^2 + |a|^2)(f_\epsilon(N) + f_{-\epsilon}(N) - 1) \\ &\quad - (|c|^2 - |d|^2)(f_\epsilon(S) + f_{-\epsilon}(S) - 1) \frac{v_g(S)}{v_g(N)}] \\ &\quad + \frac{2\hbar e S}{m} \int N_N d\epsilon \frac{d\Omega}{4\pi} k_x \left[1 - |b|^2 - |a|^2 - (|d|^2 + |c|^2) \frac{v_g(S)}{v_g(N)} \right] \end{aligned}$$

We use here

$$\frac{v_g(S)}{v_g(N)} N_S = N_N$$

The last line vanishes due to the conservation of quasiparticle flow. As a result

$$\begin{aligned} I_{NIS} &= \frac{2\hbar e S}{m} \int_{\epsilon>0} N_N d\epsilon \int_{k_x>0} \frac{d\Omega_{\mathbf{k}}}{4\pi} k_x ([1 - |b|^2 + |a|^2] [f_\epsilon(N) + f_{-\epsilon}(N) - 1] \\ &\quad - [|c|^2 - |d|^2] [f_\epsilon(S) + f_{-\epsilon}(S) - 1] \frac{v_g(S)}{v_g(N)}) \end{aligned}$$

In the normal region, $f_\epsilon(N) = f_0(\epsilon - eV)$ where

$$f_0(\epsilon) = \frac{1}{e^{\epsilon/T} + 1}$$

is the equilibrium Fermi function. We thus have

$$f_\epsilon(N) + f_{-\epsilon}(N) - 1 = f_0(\epsilon - eV) + f_0(-\epsilon - eV) - 1 = f_0(\epsilon - eV) - f_0(\epsilon + eV)$$

which is an even function of ϵ . In the superconductor, $f_\epsilon(S) = f_0(\epsilon)$. Therefore,

$$f_\epsilon(S) + f_{-\epsilon}(S) - 1 = 0$$

The current becomes

$$\begin{aligned} I_{NIS} &= \frac{2\hbar e S}{m} \int_{\epsilon>0} d\epsilon \int_{k_x>0} \frac{d\Omega_{\mathbf{k}}}{4\pi} k_x [1 - |b|^2 + |a|^2] [f_\epsilon(N) + f_{-\epsilon}(N) - 1] N_N \\ &= \frac{\hbar e S}{m} \int_{-\infty}^{\infty} d\epsilon \int_{k_x>0} \frac{d\Omega_{\mathbf{k}}}{4\pi} k_x [1 - |b|^2 + |a|^2] [f_\epsilon(N) + f_{-\epsilon}(N) - 1] N_N. \end{aligned}$$

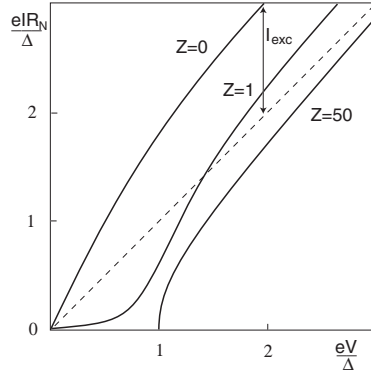


Figure 4.5: The current–voltage curves for a NIS interface at low temperatures [11]. The dashed line is the Ohm’s law.

We note that

$$\int_{-\infty}^{\infty} B(\epsilon) [f_0(\epsilon - eV) - f_0(\epsilon + eV)] d\epsilon = 2 \int_{-\infty}^{\infty} B(\epsilon) [f_0(\epsilon - eV) - f_0(\epsilon)] d\epsilon$$

where $B(\epsilon) = 1 - |b|^2 + |a|^2$ is an even function. Finally, if Z is independent of the incident angle,

$$I_{NIS} = AeN(0)v_FS \int_{-\infty}^{\infty} d\epsilon [1 - |b|^2 + |a|^2] [f_0(\epsilon - eV) - f_0(\epsilon)] \quad (4.29)$$

where $A \sim 1$ is a constant that depends on the geometry.

The factor

$$1 - |b|^2 + |a|^2$$

plays the role of the transmission coefficient for particle-hole reflection at the NIS interface. It is by the Andreev reflection coefficient $|a|^2$ *larger* than that in the normal state. The coefficients $|a|^2$ and $|b|^2$ are given by Eqs. (4.11), (4.12), (4.20), and (4.21).

The current–voltage curves for various barrier strengths at low temperatures, $T \ll T_c$ are shown in Fig. 4.5.

4.2.1 Normal tunnel resistance

Consider several limiting cases. First assume that the superconductor is in the normal state $|\Delta| = 0$. We have $|a|^2 = 0$ and

$$|b|^2 = \frac{Z^2}{1 + Z^2}$$

The current becomes

$$I_{NIN} = \frac{AeN(0)v_FS}{1 + Z^2} \int_{-\infty}^{\infty} [f_0(\epsilon - eV) - f_0(\epsilon)] d\epsilon = \frac{Ae^2N(0)v_FS V}{1 + Z^2} = \frac{V}{R_N}$$

where

$$\frac{1}{R_N} = \frac{Ae^2 N(0)v_F S}{1 + Z^2} \quad (4.30)$$

We use here

$$\int_{-\infty}^{\infty} [f_0(\epsilon - eV) - f_0(\epsilon)] d\epsilon = eV . \quad (4.31)$$

To prove this we write

$$\begin{aligned} & \int_{-\infty}^{\infty} [f_0(\epsilon - eV) - f_0(\epsilon)] d\epsilon \\ &= \int_{-\infty}^{\infty} [f_0(\epsilon - eV) - \Theta(eV - \epsilon)] d\epsilon - \int_{-\infty}^{\infty} [f_0(\epsilon) - \Theta(-\epsilon)] d\epsilon \\ &+ \int_{-\infty}^{\infty} [\Theta(eV - \epsilon) - \Theta(-\epsilon)] d\epsilon \end{aligned}$$

Since the first integral in the r.h.s. converges, we can now make the shift $\epsilon - eV \rightarrow \epsilon$ in it, after which it cancels the second integral. The third term gives

$$\int_0^{eV} d\epsilon = eV$$

The current through the NIS junction can be written as

$$I_{NIS} = \frac{1 + Z^2}{eR_N} \int_{-\infty}^{\infty} d\epsilon [1 - |b|^2 + |a|^2] [f_0(\epsilon - eV) - f_0(\epsilon)] \quad (4.32)$$

4.2.2 Landauer formula

For $Z = 0$ we have from Eq. (4.30)

$$\frac{1}{R_N} = Ae^2 N(0)v_F S \equiv \frac{1}{R_{Sh}} \quad (4.33)$$

It is the inverse Sharvin resistance which exists without a barrier.

To explain this result we should recall our assumption that the two conducting electrodes separated by a contact have different voltages. For $Z = 0$ this may happen only if the contact has an area much smaller than the cross sections of the two electrodes. This is exactly similar to the point contacts considered in the previous chapter.

Consider a point contact between two normal metals in more detail. We assume that the barrier is absent so that the electrons fly freely (ballistically) through the constriction from one electrode to another. The current through the constriction is

$$\begin{aligned} I &= e \sum_{p_x > 0; p_y, p_z} [|v_x| f_0(\epsilon - eV) - |v_x| f_0(\epsilon)] \\ &= 2e \sum_{p_y, p_z} \int_0^{\infty} \frac{dp_x}{2\pi\hbar} \frac{\partial \epsilon_{p_y, p_z}(p_x)}{\partial p_x} [f_0(\epsilon - eV) - f_0(\epsilon)] \end{aligned}$$

The factor 2 comes due to the spin. The summation runs over such p_y, p_z whose states penetrate through the constriction. We further have

$$\begin{aligned} I &= \frac{2e}{h} \sum_{p_y, p_z} \int_{-E_F}^{\infty} d\epsilon [f_0(\epsilon - eV) - f_0(\epsilon)] = \frac{2e^2}{h} V \sum_{p_y, p_z} \int_{-\infty}^{\infty} \frac{df_0(\epsilon)}{d\epsilon} d\epsilon \\ &= \frac{2e^2 N_{>}}{h} V \end{aligned} \quad (4.34)$$

Here $N_{>}$ is the number of states with $p_x > 0$ that go through the constriction.

Equation (4.34) is the well-known Landauer formula for a ballistic constriction [12]. It shows that the conductance of the ballistic constriction $G = (2e^2/h)N$ is an integer multiple of the *quantum of conductance* $G_0 = 2e^2/h$ where

$$R_0 = \frac{1}{G_0} = \frac{h}{2e^2} \approx 12.9 \text{ k}\Omega \quad (4.35)$$

is the *quantum of resistance*. The dissipation of energy is concentrated in the electrodes where the incoming particles relax to the local chemical potential.

The Sharvin conductance in Eq. (4.33) can be written as

$$\frac{1}{R_{\text{Sh}}} = \frac{2e^2 N_{>}}{h} = \frac{N_{>}}{R_0}$$

where

$$N_{>} = \pi \hbar A N(0) v_F S = A \frac{2\pi p_F^2 S}{(2\pi \hbar)^2}$$

is the number of penetrating modes.

In general, for a contact between two normal metals separated by a constriction with a barrier, the conductance in E. (4.30) can be written as

$$G_{NIN} = \frac{2e^2}{h} \sum_{n=1}^{N_{>}} \mathcal{T}_n \quad (4.36)$$

where

$$\mathcal{T}_n = 1 - |b_n|^2 = \frac{1}{1 + Z_n^2} \quad (4.37)$$

is the transmission coefficient for the mode n . Equation (4.36) is known as the Landauer-Büttiker formula.

4.2.3 Tunnel current

Consider a junction with a strong barrier $Z^2 \gg 1$. For $|\epsilon| > |\Delta|$ we find from Eqs. (4.11) and (4.12)

$$|b|^2 = 1 - \frac{1}{Z^2(U^2 - V^2)} = 1 - \frac{\epsilon}{Z^2 \sqrt{\epsilon^2 - |\Delta|^2}} = 1 - \frac{N_S(\epsilon)}{Z^2 N(0)}$$

while $|a|^2 \sim Z^{-4}$. For $|\epsilon| < |\Delta|$ Eqs. (4.20) and (4.21) yield $|a|^2 \sim Z^{-4}$ thus $|b|^2 = 1$ and $1 - |b|^2 + |a|^2 = 0$.

Therefore,

$$I_{NIS} = \frac{1}{eR_N} \int_{-\infty}^{\infty} \frac{N_S(\epsilon)}{N(0)} [f_0(\epsilon - eV) - f_0(\epsilon)] d\epsilon \quad (4.38)$$

where we put

$$\frac{N_S(\epsilon)}{N(0)} = \frac{\epsilon}{\sqrt{\epsilon^2 - |\Delta|^2}} \Theta(\epsilon^2 - |\Delta|^2)$$

with $\Theta(x)$ being the Heaviside step function. This is the well known expression for the tunnel current. Thus the contact with large barrier strength Z is equivalent to the tunnel junction.

For low temperatures $T \ll T_c$ we find

$$I_{NIS} = \frac{\sqrt{(eV)^2 - |\Delta|^2}}{eR_N} \Theta(eV - |\Delta|) \quad (4.39)$$

4.2.4 Excess current

For large voltages, $eV \gg |\Delta|$ the integral in Eq. (4.32) for the current through the junction is determined by energies of the order of eV . Indeed, for $\epsilon \gg |\Delta|$

$$|a|^2 = \frac{|\Delta|^2}{\epsilon^2(1 + Z^2)^2}, \quad |b|^2 = \frac{Z^2}{1 + Z^2} - \frac{|\Delta|^2 Z^2}{4\epsilon^2(1 + Z^2)^2}$$

Therefore $I \approx V/R_N$. The curve $I(V)$ for large V goes parallel to the Ohm's law, but it is shifted by a constant current which is called the excess current (see Fig. 4.5). We define the excess current as

$$\begin{aligned} I_{exc}(V) &= I_{NIS}(V) - I_N(V) \\ &= \frac{1}{eR_N} \int_{-\infty}^{\infty} d\epsilon \left([1 + Z^2] [1 - |b|^2 + |a|^2] - 1 \right) [f_0(\epsilon - eV) - f_0(\epsilon)] \end{aligned}$$

The term in the brackets under the integral decays as ϵ^{-2} , therefore the integral converges at $\epsilon \sim |\Delta|$ for large voltages and becomes independent of V for $eV \gg |\Delta|, T$. The current I_{exc} thus saturates for high voltages $V \rightarrow \infty$:

$$\begin{aligned} I_{exc}(\infty) &= \frac{1}{eR_N} \int_{-\infty}^{\infty} d\epsilon \left([1 + Z^2] [1 - |b|^2 + |a|^2] - 1 \right) [1 - f_0(\epsilon)] \\ &= \frac{1}{2eR_N} \int_{-\infty}^{\infty} d\epsilon \left([1 + Z^2] [1 - |b|^2 + |a|^2] - 1 \right) \quad (4.40) \end{aligned}$$

since $1 - 2f_0(\epsilon)$ is an odd function. Here we put $f_0(\epsilon - eV) = 1$ for $\epsilon \sim |\Delta|$ and $eV \gg |\Delta|, T$. The current $I_{exc}(\infty)$ vanishes for $Z \rightarrow \infty$.

4.2.5 NS Andreev current. Current conversion

One more important limit is for the Andreev-reflection mediated current at low temperatures for a zero barrier strength. For $T \ll T_c$ and low voltages $eV \ll |\Delta|$ we need only $\epsilon \ll |\Delta|$. We have $|a|^2 = 1$ while $|b|^2 = 0$. Therefore, the current becomes

$$I_x = \frac{2}{eR_{\text{Sh}}} \int_{-\infty}^{\infty} [f_0(\epsilon - eV) - f_0(\epsilon)] d\epsilon = \frac{2V}{R_{\text{Sh}}}$$

The conductance is twice the normal-state conductance (see Fig. 4.5). This is due to the fact that both particles and holes contribute to the current. The current in the normal region is carried by the normal excitations. However, the wave function of the normal excitations decays into the superconducting region. The normal current is then converted into the supercurrent. This follows from Eq. (2.91)

$$\text{div } \mathbf{J}_n = -\frac{2ie}{\hbar} (\Delta u_n^* v_n - \Delta^* u_n v_n^*) ,$$

according to which the current carried by the subgap states alone is not conserved in the superconducting region, while the total current is conserved, of course.

4.3 SIS contact

4.3.1 Wave functions and the energy of bound states

Consider now one more example of a barrier structure which consists of two superconducting half-spaces separated by a barrier of strength Z in the plane (y, z) . The gap has the form $\Delta = |\Delta|e^{\pm i\phi/2}$ in the right (left) superconductor, respectively. Consider the states with energies $\epsilon < |\Delta|$.

On the right of the barrier, the decaying wave function has the form

$$\begin{pmatrix} u \\ v \end{pmatrix} = c_2 e^{i\tilde{q}_+ x} \begin{pmatrix} \tilde{U} e^{i\phi/4} \\ \tilde{V} e^{-i\phi/4} \end{pmatrix} + d_2 e^{-i\tilde{q}_- x} \begin{pmatrix} \tilde{V} e^{i\phi/4} \\ \tilde{U} e^{-i\phi/4} \end{pmatrix} \quad (4.41)$$

where

$$q_{\pm} = k_x \pm i \frac{\sqrt{|\Delta|^2 - \epsilon^2}}{\hbar^2 k_x}$$

and

$$\tilde{U} = \frac{1}{\sqrt{2}} \left(1 + i \frac{\sqrt{|\Delta|^2 - \epsilon^2}}{\epsilon} \right)^{1/2}, \quad \tilde{V} = \frac{1}{\sqrt{2}} \left(1 - i \frac{\sqrt{|\Delta|^2 - \epsilon^2}}{\epsilon} \right)^{1/2}$$

In the left superconductor,

$$\begin{pmatrix} u \\ v \end{pmatrix} = c_1 e^{-i\tilde{q}_+ x} \begin{pmatrix} \tilde{U} e^{-i\phi/4} \\ \tilde{V} e^{i\phi/4} \end{pmatrix} + d_1 e^{i\tilde{q}_- x} \begin{pmatrix} \tilde{V} e^{-i\phi/4} \\ \tilde{U} e^{i\phi/4} \end{pmatrix}$$

The boundary conditions Eqs. (4.7), (4.8) yield

$$\begin{aligned} c_1 \tilde{U} e^{-i\phi/4} + d_1 \tilde{V} e^{-i\phi/4} &= c_2 \tilde{U} e^{i\phi/4} + d_2 \tilde{V} e^{i\phi/4} \\ c_1 \tilde{V} e^{i\phi/4} + d_1 \tilde{U} e^{i\phi/4} &= c_2 \tilde{V} e^{-i\phi/4} + d_2 \tilde{U} e^{-i\phi/4} \end{aligned}$$

and

$$\begin{aligned} (c_2 \tilde{U} e^{i\phi/4} - d_2 \tilde{V} e^{i\phi/4}) - (-c_1 \tilde{U} e^{-i\phi/4} + d_1 \tilde{V} e^{-i\phi/4}) &= -2iZ (c_2 \tilde{U} e^{i\phi/4} + d_2 \tilde{V} e^{i\phi/4}) \\ (c_2 \tilde{V} e^{-i\phi/4} - d_2 \tilde{U} e^{-i\phi/4}) - (-c_1 \tilde{V} e^{i\phi/4} + d_1 \tilde{U} e^{i\phi/4}) &= -2iZ (c_2 \tilde{V} e^{-i\phi/4} + d_2 \tilde{U} e^{-i\phi/4}) \end{aligned}$$

Solving the first pair of equations for c_1 and d_1 we find two equations for c_2 and d_2

$$\begin{aligned} c_2 \tilde{U} \left[(\tilde{U}^2 + iZ(\tilde{U}^2 - \tilde{V}^2)) e^{i\phi/2} - \tilde{V}^2 e^{-i\phi/2} \right] \\ + d_2 \tilde{V} \left[(\tilde{V}^2 + iZ(\tilde{U}^2 - \tilde{V}^2)) e^{i\phi/2} - \tilde{U}^2 e^{-i\phi/2} \right] &= 0 \end{aligned} \quad (4.42)$$

and

$$\begin{aligned} c_2 \tilde{V} \left[(\tilde{V}^2 - iZ(\tilde{U}^2 - \tilde{V}^2)) e^{-i\phi/2} - \tilde{U}^2 e^{i\phi/2} \right] \\ + d_2 \tilde{U} \left[(\tilde{U}^2 - iZ(\tilde{U}^2 - \tilde{V}^2)) e^{-i\phi/2} - \tilde{V}^2 e^{i\phi/2} \right] &= 0 \end{aligned} \quad (4.43)$$

Requiring zero of the determinant we find the condition of existence of a nonzero solution

$$4\tilde{U}^2 \tilde{V}^2 \cos^2(\phi/2) = 1 + Z^2 (\tilde{U}^2 - \tilde{V}^2)^2 \quad (4.44)$$

This yields $\epsilon = \pm \epsilon_\phi$ where [13]

$$\epsilon_\phi = |\Delta| \sqrt{1 - \mathcal{T} \sin^2(\phi/2)} \quad (4.45)$$

where $\mathcal{T} = 1/(1 + Z^2)$ is the transmission coefficient in the normal state as defined by Eq. (4.37). The spectrum of Eq. (4.45) is shown in Fig. 4.6.

Without a barrier $Z = 0$ when $\mathcal{T} = 1$ we recover the spectrum of a ballistic point contact Eq. (3.26). For a finite \mathcal{T} the gap $|\Delta| \sqrt{1 - \mathcal{T}} = |\Delta| \sqrt{\mathcal{R}}$ appears for $\phi = \pi$. Here $\mathcal{R} = 1 - \mathcal{T}$ is the reflection coefficient. The bound state energy is shifted towards the gap $|\Delta|$ and merges with $|\Delta|$ for a tunnel junction with very low transmission $\mathcal{T} \rightarrow 0$.

4.3.2 Supercurrent

Using the wave functions Eqs. (4.41) and the spectrum Eq. (4.45) one can calculate the current through the SIS junction from Eq. (3.30) for an equilibrium

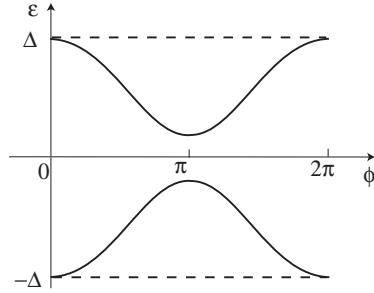


Figure 4.6: The energy spectrum of a SIS contact

distribution. Near the contact, $\lambda_s x \ll 1$ we have from Eq. (3.30)

$$\begin{aligned}
 I &= \frac{2\hbar e}{m} \sum_n k_x \text{Re} \left[f(\epsilon_n) \left(c_2^* \tilde{U}^* e^{-ik_x x} + d_2^* \tilde{V}^* e^{ik_x x} \right) \left(c_2 \tilde{U} e^{ik_x x} - d_2 \tilde{V} e^{-ik_x x} \right) \right. \\
 &\quad \left. - [1 - f(\epsilon_n)] \left(c_2 \tilde{V} e^{ik_x x} + d_2 \tilde{U} e^{-ik_x x} \right) \left(c_2^* \tilde{V}^* e^{-ik_x x} - d_2^* \tilde{U}^* e^{ik_x x} \right) \right] \\
 &= -\frac{2\hbar e}{m} \sum_n k_x [1 - 2f(\epsilon_n)] (|c_2|^2 - |d_2|^2) |\tilde{U}|^2
 \end{aligned}$$

Using Eqs. (4.42), (4.43) and the normalization of the wave function, we find similarly to Eq. (3.32), that the supercurrent is [13] (see Problem 4.4)

$$I = \frac{N_{>} \mathcal{T} e |\Delta|^2}{2\hbar} \frac{\sin \phi}{\epsilon_\phi} \tanh\left(\frac{\epsilon_\phi}{2T}\right) \quad (4.46)$$

Here $N_{>}$ is the number of channels,

$$N_{>} = R_0 / R_{\text{Sh}} = \frac{\pi \hbar}{e^2 R_{\text{Sh}}}$$

It is easy to see that the current can be written in the form of Eq. (3.33)

$$I = -\frac{2eN_{>}}{\hbar} \frac{\partial \epsilon_\phi}{\partial \phi} \tanh\left(\frac{\epsilon_\phi}{2T}\right)$$

where ϵ_ϕ is given now by Eq. (4.45).

This current is a supercurrent since it flows without voltage. The current can be written also as

$$I = \frac{\pi |\Delta|^2}{2eR_N} \frac{\sin \phi}{\epsilon_\phi} \tanh\left(\frac{\epsilon_\phi}{2T}\right)$$

where

$$\frac{1}{R_N} = \frac{\mathcal{T}}{R_{\text{Sh}}}$$

is the conductance of a contact with a transparency \mathcal{T} .

For a ballistic contact $\mathcal{T} = 1$ we recover Eq. (3.37). For a tunnel junction $\mathcal{T} \ll 1$ the current becomes

$$I = I_c \sin \phi$$

where the critical current is [14]

$$I_c = \frac{\pi|\Delta|}{2eR_N} \tanh\left(\frac{|\Delta|}{2T}\right) \quad (4.47)$$

4.4 Scattering matrix

Consider the energies $|\epsilon| < |\Delta|$. In general, the waves incident on the interface from the left contain the particle wave $\propto e^{iq+x}$ with an amplitude u^+ and the positive group velocity and momentum, and the hole wave $\propto e^{-iq-x}$ with an amplitude v^- and the negative momentum but positive group velocity. They are reflected at the interface and transformed into reflected particle $\propto e^{-iq+x}$ with an amplitude u^- (negative momentum and group velocity) and reflected hole $\propto e^{iq-x}$ with an amplitude v^+ (positive momentum but negative group velocity). Reflection couples these amplitudes such that

$$\begin{pmatrix} u^- \\ v^+ \end{pmatrix} = \hat{S} \begin{pmatrix} u^+ \\ v^- \end{pmatrix}$$

Here

$$\hat{S} = \begin{pmatrix} S_{11} & S_{12} \\ S_{21} & S_{22} \end{pmatrix}$$

is the scattering matrix. The method of scattering matrix for superconducting tunnel structures was first used by Beenakker in 1991 [13].

Since for $|\epsilon| < |\Delta|$ the flow of quasiparticles Eq. (2.89) to the right from the interface (in the superconducting region) is zero, it should also vanish in the normal region due to the conservation of the quasiparticle flow. This is equivalent to the requirement that \hat{S} is a unitary matrix : $\hat{S}^\dagger \hat{S} = 1$ where $\hat{S}^\dagger = (\hat{S}^*)^t$,

$$\hat{S}^\dagger = \begin{pmatrix} S_{11}^* & S_{21}^* \\ S_{12}^* & S_{22}^* \end{pmatrix}.$$

One has

$$\begin{aligned} |S_{11}|^2 + |S_{21}|^2 &= 1 \\ |S_{22}|^2 + |S_{12}|^2 &= 1 \\ S_{11}^* S_{12} + S_{21}^* S_{22} &= 0 \end{aligned}$$

One can express the components of this matrix through the coefficients a and b calculated previously [see Eqs. (4.11), (4.12)]. Consider the wave in the normal region determined by Eq. (4.9)

$$\begin{pmatrix} u(x) \\ v(x) \end{pmatrix}_L = e^{iq_+(N)x} \begin{pmatrix} 1 \\ 0 \end{pmatrix} + a e^{iq_-(N)x} \begin{pmatrix} 0 \\ 1 \end{pmatrix} + b e^{-iq_+(N)x} \begin{pmatrix} 1 \\ 0 \end{pmatrix} \quad (4.48)$$

The first term is the incident particle wave with an amplitude $u^+ = 1$, the second is the reflected hole wave with an amplitude $v^+ = a$ while the third term is the reflected particle wave with an amplitude $u^- = b$. In other words, the amplitudes of the waves here are related according to

$$\begin{aligned} v^+ &= au^+ \\ u^- &= bu^+ \\ v^- &= 0 \end{aligned}$$

The scattering matrix gives for $v^- = 0$ the relations $u^- = S_{11}u^+$ and $v^+ = S_{21}u^+$. Therefore, $S_{21} = a$ and $S_{11} = b$. Let us take now the incident hole wave Eq. (4.15) with the incident hole amplitude $v^- = 1$. It has

$$\begin{aligned} u^- &= a(-Z)v^- \\ v^+ &= b(-Z)v^- \\ u^+ &= 0 \end{aligned}$$

Therefore, $S_{12} = a(-Z)$ and $S_{22} = b(-Z)$.

Finally,

$$\hat{S} = \begin{pmatrix} b(Z) & a(-Z) \\ a(Z) & b(-Z) \end{pmatrix}$$

and

$$\hat{S}^\dagger = \begin{pmatrix} b^*(Z) & a^*(Z) \\ a^*(-Z) & b^*(-Z) \end{pmatrix}$$

If the superconducting gap has a phase $\Delta = |\Delta|e^{i\chi}$, the coefficients are

$$\hat{S} = \begin{pmatrix} b(Z) & a(-Z)e^{i\chi} \\ a(Z)e^{-i\chi} & b(-Z) \end{pmatrix} \equiv \begin{pmatrix} S_N e^{i\delta} & S_A e^{i\chi} \\ S_A e^{-i\chi} & S_N e^{-i\delta} \end{pmatrix} \quad (4.49)$$

where we introduce new amplitudes of Andreev S_A and normal S_N reflections

$$S_N = -\frac{(\tilde{U}^2 - \tilde{V}^2)|Z|\sqrt{Z^2 + 1}}{\tilde{U}^2 + (\tilde{U}^2 - \tilde{V}^2)Z^2}, \quad S_A = \frac{\tilde{U}\tilde{V}}{\tilde{U}^2 + (\tilde{U}^2 - \tilde{V}^2)Z^2}$$

The unitarity $|S_N|^2 + |S_A|^2 = 1$ follows from $|a|^2 + |b|^2 = 1$ and $(\tilde{U}^2)^* = \tilde{V}^2$.

4.4.1 SINIS structures

Consider a SINIS structure where the normal region occupies $-d/2 < x < d/2$. The superconductor 1 at $-d/2 < x$ has a phase χ_1 while the superconductor 2 at $x > d/2$ has a phase χ_2 . Particles (holes) in N region get Andreev reflected as holes (particles) and normally reflected as particles (holes) at each interface and form bound states in N region with a discrete energy spectrum. Using the scattering matrix approach it is quite simple to find the eigenstates and the energy spectrum.

Consider reflections at each interface. At the right end of the normal region $x = d/2$ we have

$$\begin{pmatrix} u^- \\ v^+ \end{pmatrix}_R = \hat{S}_R \begin{pmatrix} u^+ \\ v^- \end{pmatrix}_R \quad (4.50)$$

Similarly, at the left end of the normal region $x = -d/2$ we have

$$\begin{pmatrix} u^+ \\ v^- \end{pmatrix}_L = \hat{S}_L \begin{pmatrix} u^- \\ v^+ \end{pmatrix}_L \quad (4.51)$$

The scattering matrixes satisfy $\hat{S}_R = S(\chi_2)$ and $\hat{S}_L = S(\chi_1)$. The waves at different ends of the normal channel have different phase factors

$$\begin{pmatrix} u^\pm \\ v^\pm \end{pmatrix}_R = e^{\pm i(\alpha + \hat{\sigma}_z \beta)} \begin{pmatrix} u^\pm \\ v^\pm \end{pmatrix}_L$$

where

$$\alpha = k_x d, \quad \beta = \frac{\epsilon d}{\hbar v_x}$$

Therefore,

$$\begin{pmatrix} u^\pm \\ v^\mp \end{pmatrix}_R = e^{\pm i(\alpha \hat{\sigma}_z + \beta)} \begin{pmatrix} u^\pm \\ v^\mp \end{pmatrix}_L$$

We have at the right end

$$\begin{pmatrix} u^- \\ v^+ \end{pmatrix}_R = \hat{S}_R \begin{pmatrix} u^+ \\ v^- \end{pmatrix}_R = \hat{S}_R e^{i(\alpha \hat{\sigma}_z + \beta)} \begin{pmatrix} u^+ \\ v^- \end{pmatrix}_L = \hat{S}_R e^{i(\alpha \hat{\sigma}_z + \beta)} \hat{S}_L \begin{pmatrix} u^- \\ v^+ \end{pmatrix}_L$$

Therefore

$$\left[1 - e^{i(\alpha \hat{\sigma}_z + \beta)} \hat{S}_R e^{i(\alpha \hat{\sigma}_z + \beta)} \hat{S}_L \right] \begin{pmatrix} u^- \\ v^+ \end{pmatrix}_L = 0$$

The solvability condition requires

$$\det \left[1 - e^{i(\alpha \hat{\sigma}_z + \beta)} \hat{S}_R e^{i(\alpha \hat{\sigma}_z + \beta)} \hat{S}_L \right] = 0 \quad (4.52)$$

This equation determines the energy spectrum of the bound states.

Symmetric case

Assume $Z_R = Z_L$. Eq. (4.52) yields

$$\begin{aligned} 4\tilde{U}^2 \tilde{V}^2 \cos^2(\phi/2) &= 1 + \left(\tilde{U}^2 - \tilde{V}^2 \right)^2 A \\ &\quad - (1 - e^{2i\beta}) \left[\tilde{V}^2 - Z^2(\tilde{U}^2 - \tilde{V}^2) \right]^2 \\ &\quad - (1 - e^{-2i\beta}) \left[\tilde{U}^2 + Z^2(\tilde{U}^2 - \tilde{V}^2) \right]^2 \end{aligned} \quad (4.53)$$

This equation is an analogue to Eq. (4.44) obtained earlier for a SIS structure. Here the effective barrier strength is

$$A = 4Z^2(1 + Z^2) \sin^2 \alpha' \quad (4.54)$$

where

$$\alpha = \alpha' + \delta$$

The barrier strength disappears when $\sin \alpha' = 0$, i.e., when

$$\alpha = \pi n - \delta$$

which corresponds to a “resonant transmission” for $Z_R = Z_L$.

SIS contact

The limit of SIS contact is obtained if we assume $d = 0$ which implies both $\alpha = 0$ and $\beta = 0$. In this case the effective barrier strength

$$A = 4Z^2 = Z_2^2$$

corresponds to a barrier of a double thickness $Z_2 = 2Z$. Equation (4.53) becomes

$$4\tilde{U}^2\tilde{V}^2 \cos^2(\phi/2) = 1 + Z_2^2 (\tilde{U}^2 - \tilde{V}^2)^2$$

which coincides with Eq. (4.44).

4.4.2 Interference effects in short contacts

Consider now contacts of a finite length such that $\alpha \neq 0$. We consider first short contacts such that β can be neglected. This requires generally $d \ll \xi$. We have from Eq. (4.53)

$$4\tilde{U}^2\tilde{V}^2 \cos^2(\phi/2) = 1 + (\tilde{U}^2 - \tilde{V}^2)^2 A \quad (4.55)$$

where the effective barrier strength is given by Eq. (4.54). This gives the spectrum

$$\frac{\epsilon^2}{|\Delta|^2} = 1 - \mathcal{T} \sin^2(\phi/2) \quad (4.56)$$

of Eq. (4.45) with the transmission coefficient

$$\mathcal{T} = \frac{1}{1 + A}$$

The barrier strength Eq. (4.54) vanishes $A = 0$ in the resonance when $\sin \alpha' = 0$ and the transmission becomes unity.

Problem 4.1

Derive Eq. (4.39).

Problem 4.2

Calculate the differential conductance of a tunnel NIS junction at low temperatures and show that it is proportional to the density of states in the superconductor at an energy $\epsilon = eV$.

Problem 4.3

Calculate the saturated excess current for $Z = 0$.

Problem 4.4

Derive Eq. (4.46).

Chapter 5

Weak links

5.1 Josephson effect

We have seen that a supercurrent can flow through a junction of two superconductors separated by narrow constriction, by a normal region or by a high-resistance insulating barrier, or by combinations of these. The current is a function of the phase difference between the two superconductors. These junctions are called weak links.

There may be various dependencies of the current on the phase difference. The form of this dependence and the maximum supercurrent depend on the conductance of the junction: The smaller is the conductance the closer is the dependence to a simple sinusoidal shape. The examples considered in the previous Chapters are: ballistic contact Eq. (3.37) at temperatures close to T_c , long SNS structures, Eq. (3.41), and a tunnel junction, Eq. (4.47).

The presence of a supercurrent is a manifestation of the fundamental property of the phase coherence that exists between two superconductors separated by a weak link; it is called the *Josephson effect*.

5.1.1 D.C and A.C. Josephson effects

The general features of the Josephson effect can be understood using a very general example of transitions between two superconductors. Assume that two superconducting pieces are separated by a thin insulating layer. Electrons can tunnel through this barrier. Assume also that a voltage V is applied between the two superconductors.

The wave function of superconducting electrons is a sum

$$\Psi = \sum_{\alpha} C_{\alpha}(t)\psi_{\alpha}$$

of the states ψ_1 and ψ_2 in superconductor 1 or superconductor 2, respectively. Each wave function ψ_1 and ψ_2 of an uncoupled superconductor, taken separately,

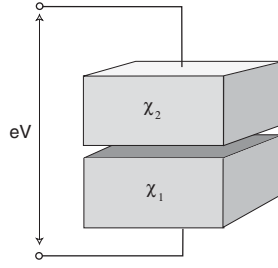


Figure 5.1: The Josephson junction of two superconductors separated by an insulating barrier.

obeys the Schrödinger equation

$$i\hbar \frac{\partial \psi_\alpha}{\partial t} = E_\alpha \psi_\alpha$$

Here E_α ($\alpha = 1, 2$) are the energies of the states in uncoupled superconductors 1 and 2.

When these superconductors are coupled, the wave function Ψ satisfies the Schrödinger equation

$$i\hbar \frac{\partial \Psi}{\partial t} = \hat{H} \Psi$$

where \hat{H} is the total Hamiltonian. This equation determines the variations of the coefficients. If the wave functions ψ_α are normalized such that

$$\int \psi_\beta^* \psi_\alpha dV = \delta_{\alpha\beta}$$

the coefficients obey

$$i\hbar \frac{\partial C_\beta}{\partial t} = \sum_\alpha [H_{\beta\alpha} - E_\alpha \delta_{\beta\alpha}] C_\alpha(t) .$$

Here

$$H_{\beta\alpha} = \int \psi_\beta^* \hat{H} \psi_\alpha dV$$

are the matrix elements. The diagonal elements

$$H_{11} = E_1 + e^* \varphi_1 = E_1 + e^* V/2 , \quad H_{22} = E_2 + e^* \varphi_2 = E_2 - e^* V/2$$

correspond to the energies of the state 1 and 2, respectively. The charge of the Cooper pair is $e^* = 2e$. The off-diagonal matrix elements describe transitions between the states 1 and 2

$$H_{12} = H_{21} = -K .$$

The equation becomes

$$i\hbar \frac{\partial C_1}{\partial t} = eVC_1(t) - KC_2(t) , \quad (5.1)$$

$$i\hbar \frac{\partial C_2}{\partial t} = -KC_1(t) - eVC_2(t) . \quad (5.2)$$

The coefficients are normalized such that $|C_1|^2 = N_1$, $|C_2|^2 = N_2$ where $N_{1,2}$ are the number of superconducting electrons in the respective electrodes. We put

$$C_1 = \sqrt{N_1}e^{i\chi_1} , C_2 = \sqrt{N_2}e^{i\chi_2} .$$

Inserting this into Eqs. (5.1), (5.2) we obtain, separating the real and imaginary parts

$$\begin{aligned} \hbar \frac{dN_1}{dt} &= -2K\sqrt{N_1N_2} \sin(\chi_2 - \chi_1) \\ \hbar \frac{dN_2}{dt} &= 2K\sqrt{N_1N_2} \sin(\chi_2 - \chi_1) \end{aligned}$$

and

$$\begin{aligned} \hbar N_2 \frac{d\chi_2}{dt} &= eVN_2 + K\sqrt{N_1N_2} \cos(\chi_2 - \chi_1) \\ \hbar N_1 \frac{d\chi_1}{dt} &= -eVN_1 + K\sqrt{N_1N_2} \cos(\chi_2 - \chi_1) \end{aligned}$$

From the first two equations we obtain the charge conservation $N_1 + N_2 = \text{const}$ together with the relation

$$I_s = I_c \sin \phi \quad (5.3)$$

where

$$I_s = 2e \frac{dN_2}{dt} = -2e \frac{dN_1}{dt}$$

is the current flowing from the first into the second electrode, $I_c = 4eK\sqrt{N_1N_2}/\hbar$ is the critical Josephson current, while $\phi = \chi_2 - \chi_1$ is the phase difference.

To interpret the second pair of equations we note that the overall phase of the device plays no role. Therefore we can put $\chi_2 = \phi/2$ while $\chi_1 = -\phi/2$. We find after subtracting the two equations

$$\hbar \frac{\partial \phi}{\partial t} = 2eV . \quad (5.4)$$

Equation (5.3) has a familiar form and describes the so called d.c. Josephson effect: The supercurrent can flow through the insulating layer provided there is an interaction between the superconducting regions. Equation (5.4) describes the a.c. Josephson effect: the phase difference grows with time if there is a voltage between two superconductors. The d.c. and a.c. Josephson effects are manifestations of the macroscopic quantum nature of superconductivity. Various devices which employ these effects can be used for observations and for practical implementations of the quantum properties of the superconducting state.

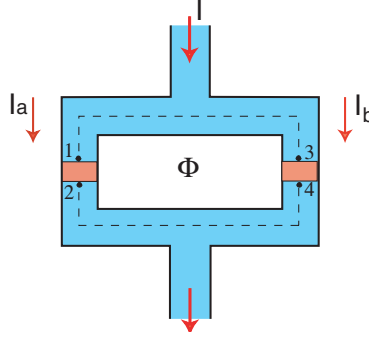


Figure 5.2: A SQUID of two Josephson junctions connected in parallel.

5.1.2 Superconducting Quantum Interference Devices

Equation (5.3) form a basis of SQUIDS. Consider a device consisting of two Josephson junctions in parallel connected by bulk superconductors, Fig. 5.2. Let us integrate \mathbf{v}_s defined by Eq. (1.8) along the contour that goes clockwise all the way inside the superconductors (dashed line in Fig. 5.2). We have

$$\chi_3 - \chi_1 + \chi_2 - \chi_4 - \frac{2e}{\hbar c} \left(\int_1^3 \mathbf{A} \cdot d\mathbf{l} + \int_4^2 \mathbf{A} \cdot d\mathbf{l} \right) = 0$$

since $\mathbf{v}_s = 0$ in the bulk. Neglecting the small sections of the contour between the points 1 and 2 and between 3 and 4, we find

$$\phi_a - \phi_b = \frac{2e}{\hbar c} \oint \mathbf{A} \cdot d\mathbf{l} = \frac{2\pi\Phi}{\Phi_0} \quad (5.5)$$

where $\phi_a = \chi_2 - \chi_1$ and $\phi_b = \chi_4 - \chi_3$.

The total current through the device is

$$I = I_c \sin \phi_a + I_c \sin \phi_b = 2I_c \cos \left(\frac{\pi\Phi}{\Phi_0} \right) \sin \left(\phi_a - \frac{\pi\Phi}{\Phi_0} \right).$$

The maximum current thus depends on the magnetic flux through the loop

$$I_{\max} = 2I_c \cos \left(\frac{\pi\Phi}{\Phi_0} \right). \quad (5.6)$$

Monitoring the current through the SQUID one can measure the magnetic flux.

5.2 Josephson vortices in extended junctions.

Consider two large superconductors 1 and 2 separated by a thin insulating layer with a thickness d and placed into the magnetic field. The (x, y) plane is in

the middle of the insulating layer. The superconductor 1 is at $z < -d/2$, the superconductor 2 occupies the region $z > d/2$. The magnetic field is applied parallel to the insulating layer along the x axis, Fig. 5.3. We choose $\mathbf{A} = (0, A_y, 0)$. Therefore,

$$h_x = -\frac{\partial A_y}{\partial z}$$

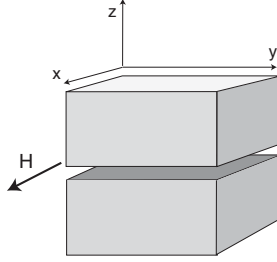


Figure 5.3: A long Josephson junction in a magnetic field.

Deep in the superconductors we have

$$\frac{\partial \chi}{\partial y} = \frac{2e}{\hbar c} A_y$$

since $\mathbf{v}_s = 0$ due to the Meissner screening. The field decays as

$$h_x(z) = \begin{cases} H e^{-(z-d/2)/\lambda_2} & z > d/2 \\ H e^{(z+d/2)/\lambda_1} & z < -d/2 \end{cases}$$

We denote H the field in between the two superconductors at $z = 0$; $\lambda_{1,2}$ is the London penetration length in the superconductor 1 or 2, respectively. The phase χ is essentially independent of z because the current through the junction is small. In the bulk it is thus the same as at the boundary of the contact.

The vector potential deep in the superconductor 2 is

$$A_y(2) = -\int_0^\infty h_x dz = -\int_0^{d/2} h_x dz - \int_{d/2}^\infty h_x dz = -H \frac{d}{2} - H \lambda_2$$

Here we put $A_y(0) = 0$ and assume that H is independent of z at $0 < z < d/2$. Similarly,

$$A_y(1) = -\int_0^{-\infty} h_x dz = \int_{-d/2}^0 h_x dz + \int_{-\infty}^{-d/2} h_x dz = H \left(\frac{d}{2} + \lambda_1 \right)$$

As a result

$$H = \frac{\hbar c}{2e(\lambda_1 + d/2)} \frac{\partial \chi_1}{\partial y} = -\frac{\hbar c}{2e(\lambda_2 + d/2)} \frac{\partial \chi_2}{\partial y}$$

so that

$$\frac{\partial \phi}{\partial y} = -\frac{2e(\lambda_1 + \lambda_2 + d)H}{\hbar c} \quad (5.7)$$

where

$$\phi = \chi_2 - \chi_1$$

The magnetic field H is generally a function of the coordinate y into the junction.

Using the Maxwell equation

$$\frac{c}{4\pi} \text{curl}_z \mathbf{h} = j_c \sin \phi \quad \text{or} \quad -\frac{c}{4\pi} \frac{\partial H}{\partial y} = j_c \sin \phi$$

we obtain

$$\frac{\hbar c^2}{8\pi e(\lambda_2 + \lambda_1 + d)} \frac{\partial^2 \phi}{\partial y^2} = j_c \sin \phi$$

or

$$\lambda_J^2 \frac{\partial^2 \phi}{\partial y^2} = \sin \phi \quad (5.8)$$

where

$$\lambda_J = \sqrt{\frac{\hbar c^2}{8\pi e j_c (\lambda_2 + \lambda_1 + d)}} \quad (5.9)$$

is called the Josephson length. Equation (5.8) is called Ferrell and Prange [1963] equation.

We can write Eq. (5.7) in the form

$$H = -\frac{4\pi j_c \lambda_J^2}{c} \frac{\partial \phi}{\partial y} \quad (5.10)$$

Equation (5.8) is similar to equation of motion for a pendulum. Indeed, the latter has the form

$$\frac{d\theta^2}{dt^2} = -\frac{g}{l} \sin \theta$$

where the angle θ is measured from the bottom. Equation (5.8) is obtained from it by replacing $\theta = \pi - \phi$ and putting $\lambda_J^{-2} = g/l$. This means that the pendulum angle ϕ is measured from the top, Fig. 5.4.

5.2.1 Low field limit

Consider first a low field H applied outside the junction at $y = 0$. In this case ϕ is also small. Expanding Eq. (5.8) we find

$$\lambda_J^2 \frac{\partial^2 \phi}{\partial y^2} = \phi$$

whence (see Fig. 5.5, curve 1)

$$\phi = \phi_0 e^{-y/\lambda_J}$$

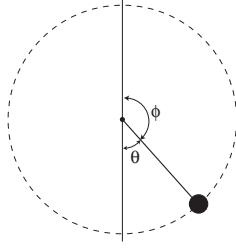


Figure 5.4: A pendulum moves in time similar to variations of ϕ along the y axis.

The magnetic field decays as

$$H(y) = H(0)e^{-y/\lambda_J}$$

where we find from Eq. (5.10)

$$H(0) = \frac{4\pi j_c \lambda_J \phi_0}{c} \quad (5.11)$$

Magnetic field decays into the junction in a way similar to the Meissner effect. The penetration length is λ_J . This length is larger than λ_L because the screening current cannot exceed the Josephson critical current j_c . Such behavior exists for fields smaller than $8\pi j_c \lambda_J / c$.

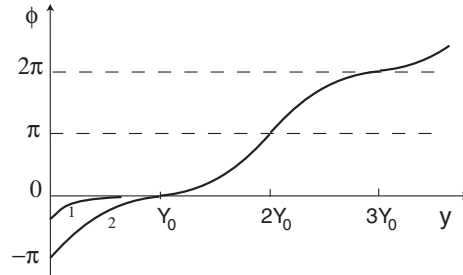


Figure 5.5: The phase difference ϕ as a function of the distance into the junction measured from the left edge. Curve 1: small magnetic fields. Curve 2: large fields, phase runs from $\phi = -\pi$ at the edge through $2\pi n$ values making Josephson vortices. The curves correspond to $H(0) < 0$.

5.2.2 Higher fields. Josephson vortices.

To find a solution of Eq. (5.8) for larger fields, we multiply it by $\partial\phi/\partial y$ and obtain

$$\frac{\lambda_J^2}{2} \left(\frac{\partial\phi}{\partial y} \right)^2 + \cos\phi = A \quad (5.12)$$

where A is a constant. Eq. (5.12) gives

$$\frac{\lambda_J}{\sqrt{2}} \int_{\phi_0}^{\phi} \frac{d\phi}{\sqrt{A - \cos \phi}} = y \quad (5.13)$$

As discussed above, the stable solution for $y \rightarrow \infty$ corresponds to $\phi = 0$ and $\partial\phi/\partial y = 0$. Eq. (5.12) results in $A = 1$. The applied field is then

$$H(0) = -\frac{4\pi j_c \lambda_J^2}{c} \frac{\partial\phi(0)}{\partial y} = \frac{8\pi j_c \lambda_J}{c} \sin \frac{\phi_0}{2}$$

The sign is chosen to agree with Eq. (5.11) for small fields. Increasing field leads to an increase in ϕ_0 until it reaches $\pm\pi$. This threshold corresponds to the field

$$H_1 = \frac{8\pi j_c \lambda_J}{c} = \frac{\Phi_0}{\pi \lambda_J (\lambda_1 + \lambda_2 + d)}$$

Above this field, the constant $A > 1$, and the phase ϕ can vary within unlimited range. Consider for example the case $H(0) < 0$. The phase runs indefinitely from $-\pi$ at the edge through the values $2\pi n$ producing the so called solitons (Fig. 5.5, curve 2). The phase solitons are also called the Josephson vortices: the phase difference across the junction varies by 2π each time as we go past one Josephson vortex. The distance between vortices is $L = 2Y_0 \sim \lambda_J$.

Consider the case $H \gg H_1$. In this case $A \gg 1$ and the slope coincides with the magnetic field

$$\frac{\partial\phi}{\partial y} = \frac{Hc}{4\pi j_c \lambda_J^2}$$

whence

$$\phi = \frac{Hcy}{4\pi j_c \lambda_J^2} + \phi_0$$

The supercurrent becomes

$$j_s = j_c \sin \left(\frac{2\pi y}{L} + \phi_0 \right)$$

where

$$L = \frac{8\pi^2 j_c \lambda_J^2}{cH} = \frac{\Phi_0}{(\lambda_1 + \lambda_2 + d)H}$$

is the distance between the Josephson vortices.

The total current through the junction of the width W is

$$I = j_c \int_{-W/2}^{W/2} \sin \left(\frac{2\pi y}{L} + \phi_0 \right) dy = W j_c \frac{\sin(\pi W/L)}{\pi W/L} \sin \phi_0$$

Its maximum is

$$I_{max} = I_c \left| \frac{\sin(\pi\Phi/\Phi_0)}{\pi\Phi/\Phi_0} \right|$$

where $I_c = j_c W$ and

$$\Phi = HW(\lambda_1 + \lambda_2 + d)$$

is the total flux through the junction.

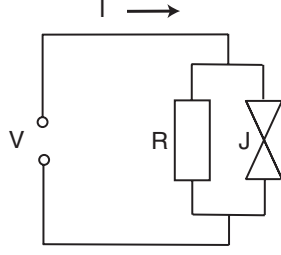


Figure 5.6: The resistively shunted Josephson junction.

5.3 Dynamics of Josephson junctions

5.3.1 Resistively shunted Josephson junction

Here we consider the a.c. Josephson effects in systems which carry both Josephson and normal currents in presence of a voltage. As we know, the normal current has a complicated dependence on the applied voltage which is determined by particular properties of the junction. In this Section, we consider a simple model that treats the normal current as being produced by usual Ohmic resistance subject to a voltage V . This current should be added to the supercurrent. Therefore, the total current has the form

$$I = \frac{V}{R} + I_c \sin \phi \quad (5.14)$$

where the phase difference is $\phi = \chi_2 - \chi_1$. Since the Josephson current through the junction is small, the current density in the bulk electrodes is also small. Thus, the phases χ_1 and χ_2 do not vary in the bulk, $\chi_{1,2} = \text{const}$. The difference of the phases at the both sides from the hole obeys the Josephson relation

$$\hbar \frac{\partial \phi}{\partial t} = 2eV \quad (5.15)$$

This equation describes the so called resistively shunted Josephson junction (RSJ) model (see Fig. 5.6).

The full equation for the current is

$$I = \frac{\hbar}{2eR} \frac{\partial \phi}{\partial t} + I_c \sin \phi \quad (5.16)$$

If $I < I_c$, the phase is stationary:

$$\phi = \arcsin(I/I_c)$$

and voltage is zero. The phase difference reaches $\pi/2$ for $I = I_c$.

If $I > I_c$, the phase starts to grow with time, and a voltage appears. Let t_0 be the time needed for the phase to grow from $\pi/2$ to $\pi/2 + 2\pi$. The average voltage is then

$$(2e/\hbar)\bar{V} = 2\pi/t_0 \equiv \omega_J \quad (5.17)$$

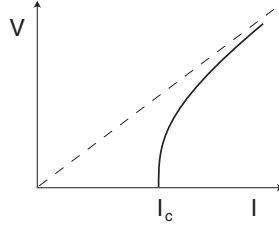


Figure 5.7: The current–voltage curve for resistively shunted Josephson junction.

Calculating t_0 (see Problem 5.1) we find the current–voltage curve dependence

$$\bar{V} = R\sqrt{I^2 - I_c^2} \quad (5.18)$$

It is shown in Fig. 5.7.

5.3.2 The role of capacitance

The Josephson junction has also a finite capacitance. Let us discuss its effect on the dynamic properties of the junction.

The current through the capacitor (see Fig. 5.8) is

$$I = C \frac{\partial V}{\partial t}$$

The total current becomes

$$I = \frac{\hbar C}{2e} \frac{\partial^2 \phi}{\partial t^2} + \frac{\hbar}{2eR} \frac{\partial \phi}{\partial t} + I_c \sin \phi \quad (5.19)$$

Let us discuss this equation. Consider first the work

$$\delta A = \int_0^{\delta t} IV dt = \frac{\hbar}{2e} I \delta \phi$$

produced by an external current source. We find

$$\delta A = \int_0^{\delta t} \frac{\partial}{\partial t} \left[\frac{\hbar^2 C}{8e^2} \left(\frac{\partial \phi}{\partial t} \right)^2 - \frac{\hbar I_c}{2e} \cos \phi \right] dt + \frac{\hbar^2}{4e^2 R} \int_0^{\delta t} \left(\frac{\partial \phi}{\partial t} \right)^2 dt$$

This equation has the form of a balance of energy

$$\delta [E_{\text{capacitor}} + E_{\text{junction}}] = \delta A - \frac{\hbar^2}{4e^2 R} \int_0^{\delta t} \left(\frac{\partial \phi}{\partial t} \right)^2 dt$$

where the energy of the capacitor is

$$E_{\text{capacitor}} = \frac{\hbar^2 C}{8e^2} \left(\frac{\partial \phi}{\partial t} \right)^2 = \frac{CV^2}{2} \quad (5.20)$$

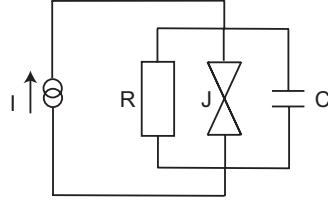


Figure 5.8: The capacitively and resistively shunted Josephson junction.

The energy of the Josephson junction is

$$E_{\text{junction}} = E_J[1 - \cos \phi], \quad \text{where } E_J = \frac{\hbar I_c}{2e} \quad (5.21)$$

The last term in the energy balance is the dissipative function.

Eq. (5.19) can also be written as a mechanical analogue equation

$$J \frac{\partial^2 \phi}{\partial t^2} + \eta \frac{\partial \phi}{\partial t} + E_J \sin \phi = F \quad (5.22)$$

of a pendulum with the moment of inertia (or “mass”)

$$J = \frac{\hbar^2 C}{4e^2} = \frac{\hbar^2}{8E_C}$$

and the maximum gravity force torque $mgl = E_J$ in a viscous medium with a viscosity

$$\eta = \frac{\hbar^2}{4e^2 R} = \frac{\hbar^2}{8E_C R C}$$

under action of a constant torque

$$F = \frac{\hbar I}{2e}$$

Here we introduce the energy

$$E_C = \frac{e^2}{2C}$$

associated with charging the capacitor C with one electron charge. We will meet this quantity later when we discuss the Coulomb blockade effects in small junctions.

The resonance frequency of the pendulum is

$$\omega_p = \sqrt{\frac{E_J}{J}} = \sqrt{\frac{2eI_c}{\hbar C}} = \sqrt{\frac{2\pi c I_c}{\Phi_0 C}} = \frac{\sqrt{8E_J E_C}}{\hbar} \quad (5.23)$$

It is called the plasma frequency.

Equation (5.22) can be considered as an equation of motion of a particle with a coordinate ϕ , a mass J in a potential

$$U(\phi) = E_J[1 - \cos \phi] - (\hbar I/2e)\phi = E_J [1 - \cos \phi - \phi I/I_c] \quad (5.24)$$

in presence of viscosity. The potential Eq. (5.24) is called a tilted washboard potential, Fig. 5.9.

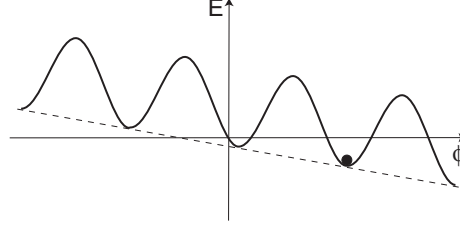


Figure 5.9: The tilted washboard potential. The tilting angle is determined by the ratio I/I_c . The dot shows a particle with a coordinate ϕ in a potential minimum.

Sometimes it is convenient to introduce an effective inductance equivalent to the Josephson junction if the phase variations are small. For example, for small ϕ the Josephson current becomes $I_J = I_c \phi$. On the other hand, due to the Josephson relation,

$$\phi = \frac{2e}{\hbar} \int V dt$$

Therefore, the Josephson current is

$$I_J = \frac{2eI_c}{\hbar} \int V dt$$

It looks like a current through an inductance where the voltage across the inductance is

$$V = \frac{1}{c} \frac{\partial \Phi}{\partial t} = \frac{L}{c^2} \frac{\partial I}{\partial t}$$

(in Gaussian units) whence

$$I = \frac{c^2}{L} \int V dt$$

Therefore, the effective inductance is

$$L_J = \frac{\hbar c^2}{2eI_c} \quad (5.25)$$

In terms of the effective inductance, the plasma frequency is

$$\omega_p = \sqrt{\frac{2eI_c}{\hbar C}} = \frac{c}{\sqrt{L_J C}}$$

which coincides with the resonance frequency of an LC circuit.

Equation (5.19) can be written also as

$$\omega_p^{-2} \frac{\partial^2 \phi}{\partial t^2} + Q^{-1} \omega_p^{-1} \frac{\partial \phi}{\partial t} + \sin \phi = \frac{I}{I_c} \quad (5.26)$$

where we introduce the quality factor

$$Q = \omega_p RC = \sqrt{\frac{2eI_c R^2 C}{\hbar}} \quad (5.27)$$

that characterizes the relative dissipation in the system. This parameter is large when resistance is large so that the normal current and dissipation are small.

Consider the dynamics of the Josephson junction in an increasing current. As long as the current is below I_c , the phase ϕ is stationary: it is determined by $I = I_c \sin \phi$. The junction is superconducting. In the representation of a mechanical particle with a coordinate ϕ in a tilted washboard potential this means that the particle is localized in one of the minima of the potential (state ϕ_0 in Fig. 5.10). As I increases and approaches I_c , the tilt increases, and the minima gradually disappear as shown in Fig. 5.10. For $I > I_c$ the particle begins to roll down the potential relief. A nonzero velocity $\partial \phi / \partial t$ determines the voltage across the junction.

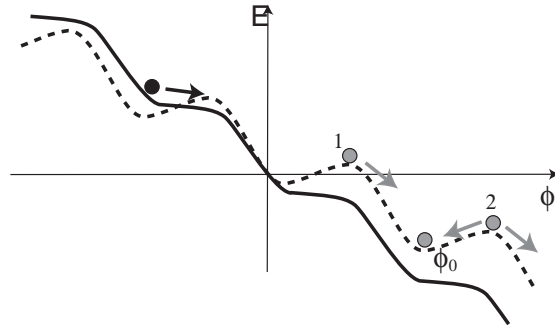


Figure 5.10: The tilted washboard potential for I/I_c close to unity. Dashed line: $I < I_c$, the potential has minima. Solid line: $I > I_c$, the minima disappear.

The current–voltage dependence is most simple for an overdamped junction which corresponds to small Q i.e., to small capacitance and large dissipation. In this case we can neglect the term with the second derivative in Eq. (5.22). We thus return to the case considered in the previous section where the current–voltage dependence is determined by Eq. (5.18).

For a finite Q the current–voltage dependence becomes hysteretic (see Fig. 5.11). With increasing current voltage is zero and the phase ϕ is localized (state ϕ_0 in Fig. 5.10) until I reaches I_c . For $I > I_c$ the particle rolls down the potential (solid line in Fig. 5.10), and a finite voltage appears which corresponds to a voltage jump shown by a solid line in Fig. 5.11. However, when the current

is decreased, a dissipative regime with a finite voltage extends down to currents smaller than I_c . The current at which the voltage disappears is called retrapping current. It corresponds to trapping of the particle back into one of the potential minima ϕ_0 in Fig. 5.10.

This behavior has a simple explanation. A particle with a small dissipation will roll down the potential overcoming the potential maxima by inertia even if $I < I_c$ provided the loss of energy during its motion from one maximum (state 1 in Fig. 5.10) to the next (state 2) is smaller than the energy gain $(\hbar/2e)I\delta\phi = \pi\hbar I/e$. If the dissipation is larger (i.e., Q is smaller), the energy loss exceeds the energy gain and the particle has no energy to continue its motion, thus it falls down into the potential minimum and remains trapped there (state ϕ_0 in Fig. 5.10). In a sense, this describes a transition from “insulating” to superconducting state with *increasing dissipation*.

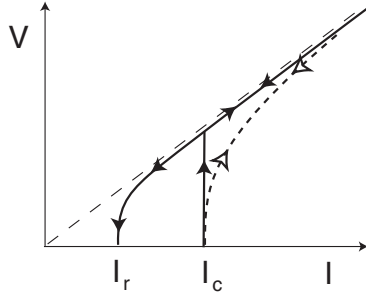


Figure 5.11: The current–voltage curve for resistively and capacitively shunted Josephson junction. The dotted line (coinciding with Fig. 5.7) is for resistively shunted junction, small Q . The solid lines show the hysteretic behavior of a contact with a large Q .

It can be shown that, for a highly underdamped junction, i.e., for large $Q \rightarrow \infty$, the retrapping current goes to zero while the I–V curve has the linear Ohmic dependence. For large Q , the voltage is almost constant $V \approx \bar{V}$, even at $I \sim I_c$ and the phase has the form

$$\phi = 2e\bar{V}t/\hbar + \delta\phi$$

where $\delta\phi \ll 1$. Indeed, Eq. (5.26) yields for the time-independent component

$$\frac{2e\bar{V}}{\hbar} = \frac{Q\omega_p I}{I_c} = \frac{2eIR}{\hbar}$$

where we use Eqs. (5.23) and (5.27) so that the I–V curve is linear

$$\bar{V} = IR$$

For the oscillating component we have

$$\omega_p^{-2} \frac{\partial^2 \delta\phi}{\partial t^2} + Q^{-1} \omega_p^{-1} \frac{\partial \delta\phi}{\partial t} + \sin(\omega_J t) = 0$$

where we put

$$\omega_J = \frac{2e\bar{V}}{\hbar}$$

For a large Q we neglect the first derivative and find

$$\delta\phi = \frac{\omega_p^2}{\omega_J^2} \sin(\omega_J t)$$

The variation $\delta\phi$ is small if $\omega_p/\omega_J \ll 1$. This condition reads

$$\frac{\omega_p^2}{\omega_p\omega_J} = \frac{I_c}{I\omega_p RC} = \frac{I_c}{IQ} \ll 1$$

Therefore it should be $I_c/IQ \ll 1$. If the current does not satisfy this condition, $\delta\phi$ becomes large, and the finite voltage regime breaks down. Therefore, the retrapping current is

$$I_r \sim I_c/Q \quad (5.28)$$

It goes to zero as $Q \rightarrow \infty$.

5.3.3 Thermal fluctuations

Consider first overdamped junction. A particle with a coordinate ϕ is mostly sitting in one of the minima of the washboard potential in Fig. 5.9. It can go into the state in a neighboring minimum if it receives the energy enough to overcome the barrier. This energy can come from the heat bath, for example, from phonons. The probability of such a process is proportional to $\exp(-U/T)$ where U is the height of the barrier as seen from the current state of the particle. The probability P_+ to jump over the barrier from the state ϕ_0 to the state $\phi_0 + 2\pi$ and the probability P_- to jump over the barrier from the state $\phi_0 + 2\pi$ back to the state ϕ_0 are

$$P_{\pm} = \omega_a \exp \left[-\frac{U_0 \mp (\pi\hbar I/2e)}{T} \right]$$

where ω_a is a constant attempt frequency, and U_0 is the average barrier height. Therefore, the probability that the particle will go from the state ϕ_0 to the state $\phi_0 + 2\pi$ is

$$P = P_+ - P_- = 2\omega_a \exp \left[-\frac{U_0}{T} \right] \sinh \left(\frac{\pi\hbar I}{2eT} \right)$$

This will produce a finite voltage

$$\bar{V} = \left(\frac{\hbar}{2e} \right) 2\pi P = \frac{2\pi\hbar\omega_a}{e} \exp \left[-\frac{U_0}{T} \right] \sinh \left(\frac{\pi\hbar I}{2eT} \right)$$

For low currents, $I \ll I_c$, the barrier height is independent of the current $U_0 = 2E_J$. For $I \rightarrow 0$ we find

$$\bar{V} = \frac{\pi^2\hbar^2\omega_a I}{e^2 T} \exp \left(-\frac{2E_J}{T} \right)$$

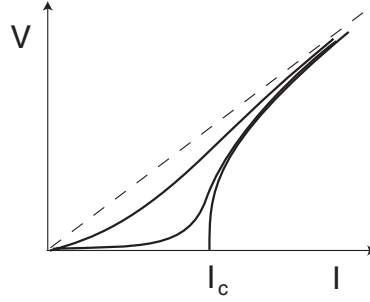


Figure 5.12: The current–voltage curves of a RSJ junction in presence of thermal fluctuations. The curves from bottom to top correspond to decreasing E_J/T ; the curve starting at $I = I_c$ refers to $E_J = \infty$.

This is a linear dependence characterized by certain resistance that depends on the attempt frequency. One can express the attempt frequency in terms of the resistance in the normal state R . Indeed, for $T^* \sim E_J$ the Josephson barrier is ineffective thus the exponent can be replaced by unity, and the current voltage dependence defines the normal resistance

$$\frac{\pi^2 \hbar^2 \omega_a}{e^2 T^*} = R$$

whence $\omega_a = e^2 E_J R / \pi^2 \hbar^2$. Using this we find for the voltage

$$\bar{V} = \frac{E_J R I}{T} \exp\left(-\frac{2E_J}{T}\right)$$

This determines the effective resistance of the junction [15]

$$R_J = \frac{E_J R}{T} \exp\left(-\frac{2E_J}{T}\right) \quad (5.29)$$

It is exponentially small for low temperatures.

We see that the junction has a finite (though small) resistance even for low currents. The current–voltage curve for an overdamped RSJ junction in presence of thermal fluctuations is shown in Fig. 5.12.

In the case of underdamped junctions, the particle will roll down the potential relief as soon as it gets above the potential barrier. The probability of this process is just $P = \omega_a \exp(-U/T)$. The attempt frequency ω_a is now the oscillation frequency in the potential minimum determined by $\sin \phi = I/I_c$ such that

$$\omega_a^2 = \omega_p^2 \frac{\partial^2}{\partial \phi^2} \cos \phi = \omega_p^2 \left(1 - \frac{I^2}{I_c^2}\right)^{1/2}$$

The barrier height is $U = U_{max} - U_{min}$ where U_{min} is the value of the energy Eq. (5.24) at $\phi = \arcsin(I/I_c)$ while U_{max} is its value at $\phi = \pi - \arcsin(I/I_c)$.

Therefore

$$\begin{aligned} U &= 2E_J \left[\cos \arcsin \frac{I}{I_c} - \frac{I}{I_c} \arccos \frac{I}{I_c} \right] \\ &= 2E_J \sqrt{1 - \frac{I^2}{I_c^2}} - \frac{2IE_J}{I_c} \arccos \left(\frac{I}{I_c} \right) \end{aligned} \quad (5.30)$$

The probability is more important for large currents $I \rightarrow I_c$ when the barrier is small,

$$U \approx \frac{4\sqrt{2}}{3} E_J (1 - I/I_c)^{3/2} \quad (5.31)$$

This can be approximated in the whole range as

$$U \approx 2E_J (1 - I/I_c)^{3/2}$$

As the current increases from zero to I_c the probability $P = \omega_a \exp(-U/T)$ of an escape from the potential minimum increases from exponentially small up to $P \sim \omega_p \sim 10^{10} \text{ sec}^{-1}$. The voltage generated by escape processes is $V \sim (\pi\hbar/e)P$. The measuring device will detect a voltage at a current I_{cf} when it is above the sensitivity limit V_0 . Thus

$$V_0 = \frac{\pi\hbar\omega_p}{e} \exp \left[-\frac{U(I_{cf})}{T} \right]$$

The threshold current in Fig. 5.11 is thus

$$I_{cf} = I_c \left(1 - [(T/2E_J) \ln(\pi\hbar\omega_p/eV_0)]^{2/3} \right)$$

which is smaller than I_c .

The rising part of the I-V curve in Fig. 5.12 for an overdamped junction near I_c is also determined by an exponential dependence $V = (\pi\hbar/e)P_+$ where the probability P_+ contains the barrier from Eq. (5.31). Indeed, the probability of the reverse process P_- is now strongly suppressed by a considerably higher barrier seen from the next potential minimum.

5.3.4 Shapiro steps

When a Josephson junction is driven by an a.c. voltage (or is subject to a microwave irradiation) with a frequency ω , the d.c. component of supercurrent through the junction exhibits the so called Shapiro steps: jumps of the current at constant voltages satisfying $V_n = n\hbar\omega/2e$.

Let the voltage across the junction be

$$V = V_0 + V_1 \cos(\omega t)$$

The phase difference across the junction is then

$$\phi = \phi_0 + \omega_J t + (2eV_1/\hbar\omega) \sin(\omega t)$$

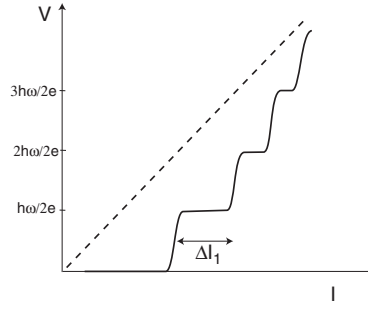


Figure 5.13: The current–voltage curves of a RSJ junction irradiated by a microwave with frequency ω .

where $\omega_J = 2eV_0/\hbar$. The supercurrent becomes

$$I = I_c \sin \phi = I_c \sum_{k=-\infty}^{\infty} (-1)^k J_k(2eV_1/\hbar\omega) \sin(\phi_0 + \omega_J t - k\omega t)$$

where k runs over integer numbers. We use here the expansion

$$\begin{aligned} e^{iz \sin \alpha} &= J_0(z) + 2 \sum_{k=1}^{\infty} J_{2k}(z) \cos(2k\alpha) + 2i \sum_{k=0}^{\infty} J_{2k+1}(z) \sin[(2k+1)\alpha] \\ &= \sum_{k=-\infty}^{\infty} J_k(z) \cos(k\alpha) + i \sum_{k=-\infty}^{\infty} J_k(z) \sin(k\alpha) \end{aligned}$$

with $z = 2eV_1/\hbar\omega$ and $\alpha = \omega t$. We note that due the parity $J_k(z) = (-1)^k J_{-k}(z)$ of the Bessel functions, the components with odd k drop out from the first sum in the second line, while the components with even k drop out from the second sum. Using this we arrive at the above expression for the current.

We see that for $\omega_J = k\omega$, i.e., for

$$V_k = k\hbar\omega/2e$$

the supercurrent has a d.c. component $I_k = I_c J_k(2eV_1/\hbar\omega) \sin(\phi_0 + \pi k)$. This d.c. component adds to the total d.c. current and produces the step parallel to the current axis with the width $\Delta I_k = 2I_c J_k(2eV_1/\hbar\omega)$.

Problems**Problem 5.1.**

Find the distance between Josephson vortices for H close to H_1 .

Problem 5.2.

Derive Eq. (5.18).

Problem 5.3

Two Josephson junctions have the critical currents $I_{c1} = 500 \mu\text{A}$ and $I_{c2} = 700 \mu\text{A}$ are connected in parallel by superconductors. The total current through both of them is $I = 1 \text{ mA}$. Find the currents through each junction.

Problem 5.4.

The junction has a critical current $I_c = 1 \text{ mA}$ and the normal resistance $R = 2 \Omega$. Find the d.c. voltage and the Josephson frequency ω_J if the current through the junction is $I = 1.2 \text{ mA}$.

Problem 5.5.

The critical current of the junction is I_c . The current through the junction has d.c. and a.c. components such that

$$I = I_0 + I_1 \sin(\omega t)$$

where $I_0 < I_c$ and $I_1 \ll I_0$. Find the voltage across the junction.

Chapter 6

Coulomb blockade in normal double junctions

6.1 Orthodox description of the Coulomb blockade

For more detailed description including the effects of environment see, for example, review [18].

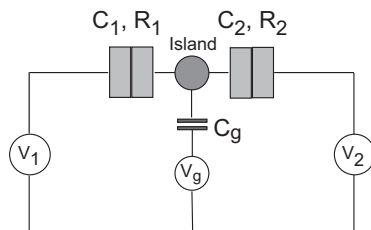


Figure 6.1: The equivalent circuit of a SET. The island is coupled to the voltage source via two contacts with resistances R_1 , R_2 and capacitances C_1 , C_2 , and to the gate through the capacitor C_g . The bias voltage is $V = V_1 - V_2$.

Consider the device called the single electron transistor (SET) with the equivalent circuit shown in Fig. 6.1. For simplicity we assume a symmetric situation $C_1 = C_2$, $R_1 = R_2 \equiv R_T$ such that $V_1 = V/2$, $V_2 = -V/2$, and that the capacitance of the gate C_g is small. Let the charge on the island provided by the gate voltage be $Q_0 = V_g C_g$.

For zero bias voltage $V = 0$, the electrostatic energy of the island having a charge Q consisting of the continuous offset charge Q_0 provided by the gate electrode and a discrete charge of k electrons that have tunneled into the island,

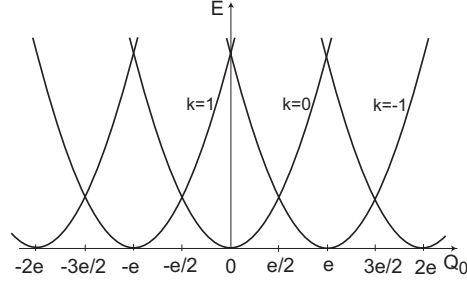


Figure 6.2:

$Q = ke + Q_0$, is

$$\frac{Q^2}{2C_\Sigma} = \frac{(Q_0 + ke)^2}{2C_\Sigma} = \frac{Q_0^2}{2C_\Sigma} + \frac{ke(Q_0 + ke/2)}{C_\Sigma}$$

Here $C_\Sigma = C_1 + C_2$ is the total capacitance. The spectrum is shown in Fig. 6.2. The parabolas intersect at $Q_0 = -ke/2$.

If the temperature is low, $T \ll E_C$, the tunneling into the island at small bias voltage becomes possible and the current can flow through the junction only for those gate charges for which the parabolas intersect. For other gate charges, the low-voltage current is zero. Let us consider the conditions for the current as functions of the bias voltage and the gate charge.

The energy difference between the state of the island after k electrons have tunneled from the source which has the bias potential V_b is

$$\delta E = \frac{(Q_0 + ke)^2}{2C_\Sigma} - \frac{Q_0^2}{2C_\Sigma} - keV_b = \frac{ke(Q_0 + ke/2)}{C_\Sigma} - keV_b$$

The difference vanishes when $V_b = V_{b,k}$, where

$$V_{b,k} = \frac{Q_0 + ke/2}{C_\Sigma}$$

For tunneling of one electron the voltage when the tunneling starts is

$$V_{b,1} = \frac{Q_0 + e/2}{C_\Sigma}$$

[see Fig. 6.3 (a)]. It vanishes if the offset charge on the island provided by the gate is $Q_0 = -e/2$. For this charge, the I-V curve starts from zero voltage, Fig. 6.3 (b).

If the bias voltage is increased, the two-electron tunneling becomes possible when

$$V_{b,2} = \frac{Q_0 + e}{C_\Sigma}$$

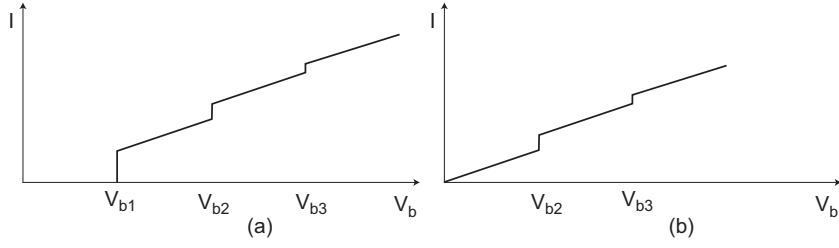


Figure 6.3: The Coulomb staircase: The current exhibits steps at $V = V_{b,k}$. (a) Zero offset charge $Q - 0 = 0$, when $V_{b,k} = (ke/2C)$; (b) Offset charge $Q_0 = -e$. The steps with $k \neq 1$ have smaller amplitudes due to smaller probabilities of tunneling.

and so on. The appearance of the two-electron process is seen on the I-V curve as another step. The steps associated with multiple-charge tunneling are called the Coulomb staircase.

Let us consider now the one-electron processes and calculate the tunneling rates.

In the presence of the bias voltage, the electrostatic energy change in a state with a charge Q on the island for adding an electron to the normal island through the left junction is

$$\Delta E_L^+ = \frac{(Q+e)^2}{2C_\Sigma} - \left(\frac{Q^2}{2C_\Sigma} + \frac{eV}{2} \right) = \frac{e(Q+e/2)}{C_\Sigma} - \frac{eV}{2} = 2E_C \left(\tilde{n} + \frac{1}{2} \right) - \frac{eV}{2} \quad (6.1)$$

Here $E_C = e^2/2C_\Sigma$ is the characteristic charging energy of the island, and $\tilde{n} = Q/e = n + Q_0/e$ where n is an integer number of extra electrons.

In general, the electrostatic energy change in a state with a charge $\tilde{n} = n + Q_0/e$ on the island for adding (+) or removing (-) an electron to the normal island through the left junction is

$$\Delta E_L^\pm(n) = \pm 2E_C(\tilde{n} \pm 1/2) \mp eV/2$$

The electrostatic energy change in a state with a charge \tilde{n} on the island for adding (+) or removing (-) an electron to the normal island through the right junction is

$$\Delta E_R^\pm(n) = \pm 2E_C(\tilde{n} \pm 1/2) \pm eV/2$$

The tunnelling rates are

$$\Gamma_{L(R)}^\pm(n) = \frac{1}{e^2 R_T} \int_{-\infty}^{\infty} dE f_1(E) [1 - f_2(E - \Delta E_{L(R)}^\pm(n))]. \quad (6.2)$$

Here R_T is the resistance of one contact, $f_1(E)$ is the distributions on the source electrode, while $f_2(E - \Delta E)$ is the distribution on the target electrode before the tunneling event; therefore $1 - f_2(E - \Delta E)$ is the probability to find that the

state is empty where the tunneling should occur. The probability of tunneling is proportional to the transparency of the contact $\mathcal{T} \propto 1/R_T$. The other factors in the coefficient in front of the integral in Γ are chosen in such a way as to provide the correct expression for the resistance of the contact in the Ohmic regime, see Eq. (6.7) below.

For equilibrium distribution $f_i(E) = (1 + e^{E/T_i})^{-1}$ with $T_1 = T_2$, we have

$$f(E)[1 - f(E - \Delta E^\pm(n))] = \frac{f(E) - f(E - \Delta E^\pm)}{1 - \exp(\Delta E^\pm/T)}$$

and

$$\int_{-\infty}^{\infty} dE [f(E) - f(E + x)] = x$$

which is nothing but Eq. (4.31) proven earlier.

Therefore, Eq. (6.2) yields

$$\Gamma^\pm(n) = \frac{1}{e^2 R_T} \frac{\Delta E^\pm}{\exp(\Delta E^\pm/T) - 1} \quad (6.3)$$

The current *into* the island through the left (right) junction is

$$I_{L(R)} = e \sum_{n=-\infty}^{\infty} \sigma(n) [\Gamma_{L(R)}^+(n) - \Gamma_{L(R)}^-(n)] \quad (6.4)$$

where $\sigma(n)$ is the probability of having n extra electrons on the island. We have

$$\sum_{n=-\infty}^{\infty} n\sigma(n) = 0 \quad (6.5)$$

by symmetry, and

$$\sum_{n=-\infty}^{\infty} \sigma(n) = 1, \quad \sum_{n=-\infty}^{\infty} \tilde{n}\sigma(n) = Q_0/e \quad (6.6)$$

6.1.1 Low temperature limit

For $T \rightarrow 0$ the tunneling rates Eq. (6.3) are

$$\Gamma_{L(R)}^\pm(n) = \frac{1}{e^2 R_T} |\Delta E_{L(R)}^\pm| \Theta(-\Delta E_{L(R)}^\pm)$$

The rates vanish when all $\Delta E_{L(R)}^\pm$ are positive. This takes place when

$$\Delta E_L^{(+)} > 0 : eV/2 - 2E_C(\tilde{n} + 1/2) < 0 \quad (a)$$

$$\Delta E_L^{(-)} > 0 : eV/2 - 2E_C(\tilde{n} - 1/2) > 0 \quad (b)$$

$$\Delta E_R^{(+)} > 0 : eV/2 + 2E_C(\tilde{n} + 1/2) > 0 \quad (c)$$

$$\Delta E_R^{(-)} > 0 : eV/2 + 2E_C(\tilde{n} - 1/2) < 0 \quad (d)$$

In Fig. 6.4 the diamond-shaped region in the plane $(V, Q = e\tilde{n})$ is shaded where all the rates are zero. This is the region where the current to and out of the island is zero, and the charge on the island does not change due to the Coulomb blockade. If the offset charge Q_0 is in the range $-e/2 < Q_0 < e/2$, the state with $n = 0$ is stable.

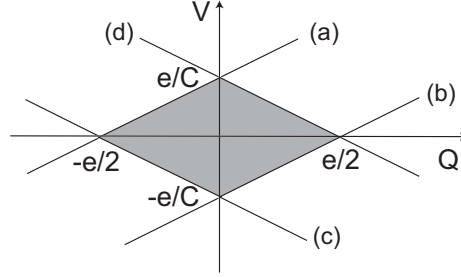


Figure 6.4: The region of stable charge is shaded. The lines (a)–(d) correspond to equalities in Eqs. (a) to (d).

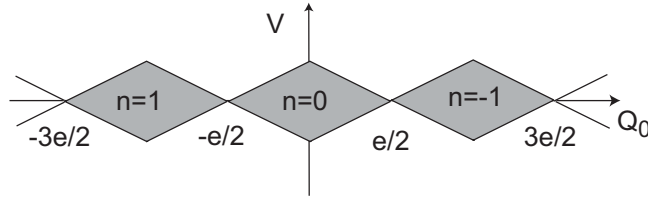


Figure 6.5: The regions of stable charge $n = 0, \pm 1, \dots$ as functions of the gate charge.

With change in the gate voltage, the stable charge on the island will vary by integer number of electrons due to tunneling to or from the respective electrode. The regions of stable states with $n = 0, \pm e, \dots$ as functions of the gate charge are shown in Fig. 6.5.

6.1.2 Conductance in the high temperature limit

We have for the left junction

$$\Gamma_L^+(n) - \Gamma_L^-(n) = \frac{1}{e^2 R_T} \left[\frac{\Delta E_L^+}{\exp(\Delta E_L^+/T) - 1} - \frac{\Delta E_L^-}{\exp(\Delta E_L^-/T) - 1} \right]$$

Up to the first order in $E_C/k_B T_e$ we have

$$\Gamma_L^+(n) - \Gamma_L^-(n) = \frac{T}{e^2 R_T} \left[v \left(\frac{1}{1 - e^v} + \frac{1}{1 - e^{-v}} \right) \right]$$

$$\begin{aligned}
& -\frac{2\tilde{n}E_C}{T}[f(v) + f(-v)] + \frac{E_C}{T}[f(v) - f(-v)] \\
= & \frac{T}{e^2 R_T} \left[v - \frac{2\tilde{n}E_C}{T} + \frac{E_C}{T}[f(v) - f(-v)] \right]
\end{aligned}$$

Here we introduce the reduced voltage $v \equiv eV/2T$ and denote

$$f(v) = \frac{1}{1 - e^v} + \frac{ve^v}{(1 - e^v)^2}$$

We also use

$$f(v) + f(-v) = \frac{1}{1 - e^v} + \frac{1}{1 - e^{-v}} = 1$$

Using Eqs. (6.5) and (6.6) we find

$$\begin{aligned}
I_L &= \frac{T}{eR_T} \left[v - \frac{2Q_0 E_C}{eT} + \frac{E_C}{T}[f(v) - f(-v)] \right] \\
&= \frac{T}{eR_T} \left[v - \frac{2Q_0 E_C}{eT} - \frac{E_C}{T} \frac{\sinh v - v}{2 \sinh^2 v} \right]
\end{aligned}$$

We find for the differential conductance [19]

$$\frac{G}{G_T} = 2R_T \frac{dI}{dV} = 1 - \frac{E_C}{T} \frac{v \sinh v - 4 \sinh^2(v/2)}{4 \sinh^4(v/2)} \quad (6.7)$$

where $G_T^{-1} = 2R_T$ is the total resistance of the contacts. This equation shows in particular that the resistance of the junction in the absence of charging effects is $2R_T$, i.e., the resistance of each tunnel contact is R_T . This confirms the choice of the coefficient in Eq. (6.2). The depth of the conductance minimum at $V = 0$ in Eq. (6.7) is

$$\Delta G/G_T = -\frac{E_C}{3T}$$

The behavior of the conductance is shown in Fig. 6.6.

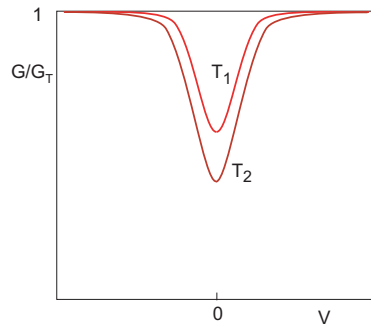


Figure 6.6: The minimum in conductance as a function of the bias voltage due to Coulomb effects at high temperatures. The two temperatures satisfy $T_2 < T_1$.

Problem 6.1.

Derive the Ohm's law from Eq. (6.4) for $E_C = 0$.

Problem 6.2.

Find the differential conductance of overheated double junction when the lead temperature is zero while the island temperature is T .

Chapter 7

Quantum phenomena in Josephson junctions

7.1 Quantization

7.1.1 Quantum conditions

Quantum effects can be observed in Josephson structures consisting, for example, of a very small superconducting grain connected to superconducting charge reservoirs through small tunnel junctions having very low capacitance and high tunnel resistance, as shown in Fig. 7.1. The equivalent circuit is shown in Fig. 6.1. The necessary constraints can be easily estimated from general arguments. First, the Coulomb charging energy for one electron $e^2/2C$ should be larger than temperature T to avoid thermal smearing of the charge states on the superconducting island. For $T \sim 1$ K this gives $C < 10^{-15}$ F which strongly restricts the size of the junction by an area $\sim 10^{-8}$ cm². Second, the tunnel resistance should be large enough to avoid averaging out by quantum fluctuations in the particle number. To be observable, the charging energy $e^2/2C$ must exceed the quantum uncertainty in energy $\hbar/\Delta t \sim \hbar/RC$ associated with the finite lifetime of the charge on the capacitor. Equating $e^2/2C$ to \hbar/RC we find that the capacitance drops out and the condition becomes $R > R_0$ where R_0 is the resistance quantum $R_0 = h/2e^2 \approx 12$ k Ω , the quantity already familiar from Eq. (4.35).

Another realization may be a small Josephson junction with a capacitance C and tunnel resistance R satisfying the above conditions, which is connected through small-capacitance, $C_{ext} \ll C$, high-resistance contacts such that $R_0 \ll R_{ext} \ll R$ to the external current source, Fig. 7.2.

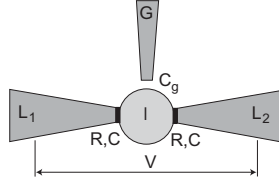


Figure 7.1: Realization of the quantum Josephson junction device: A small island I is connected to the external leads L_1 and L_2 by tunnel contacts. The tunnel resistance R should be larger than R_0 . An additional gate electrode G is connected to the island through a capacitor C_g to control the voltage on the island.

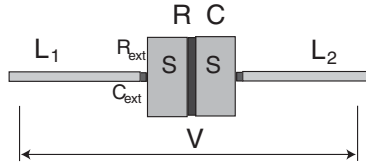


Figure 7.2: Another realization of the quantum Josephson junction device: A small Josephson junction is connected to the external leads L_1 and L_2 by high-resistance R_{ext} and low capacity $C_{ext} \ll C$ contacts. Both R_{ext} and the tunnel resistance R should be larger than R_0 .

7.1.2 Charge operator

Consider an isolated Josephson junction. The charging energy of the capacitor is

$$\frac{Q^2}{2C} = \frac{CV^2}{2} = \frac{C}{2} \left(\frac{\hbar}{2e} \frac{\partial \phi}{\partial t} \right)^2$$

If the phase difference ϕ is treated as a particle coordinate, the time derivative $\partial \phi / \partial t$ should be considered as a velocity, while the charging energy is equivalent to the kinetic energy.

In quantum mechanical description, the kinetic energy is written in terms of the momentum operator. If the coordinate is ϕ then the momentum operator is defined as

$$\hat{p}_\phi = -i\hbar \frac{\partial}{\partial \phi} \quad (7.1)$$

This definition complies with the usual commutation rule

$$[\hat{p}_\phi, \phi]_- = -i\hbar \quad (7.2)$$

To find out the physical meaning of the momentum operator let us consider the continuity equation for the supercurrent

$$\frac{d(eN_s)}{dt} = - \int \frac{\partial j_{sx}}{\partial x} d^3r$$

The current density j has the form of the charge flow density $en_s v_s$ which is

$$e \frac{\partial E_s}{\partial p_s}$$

where p_s is the momentum of a superconducting particle and E_s is the superconducting energy density. The momentum of the Cooper pair is $2p_s = \hbar \partial \chi / \partial x$ so that the continuity equation takes the form

$$\frac{d(eN_s)}{dt} = -e \int \frac{\partial}{\partial x} \frac{\partial E_s}{\partial p_s} d^3r = -\frac{2e}{\hbar} \int \frac{\partial}{\partial x} \frac{\partial E_s}{\partial(\phi/x)} d^3r = -\frac{2e}{\hbar} \frac{\partial \mathcal{E}_s}{\partial \phi}$$

since the phase gradient over the length x is $\partial \chi / \partial x = \phi/x$ where ϕ is the (given) phase difference. The quantity

$$\mathcal{E}_s = \int E_s d^3r$$

is the superconducting energy. Therefore,

$$\frac{\hbar}{2} \frac{dN_s}{dt} = -\frac{\partial \mathcal{E}_s}{\partial \phi} \quad (7.3)$$

This equation can be considered as one of the Hamiltonian equations $\partial p / \partial t = -\partial \mathcal{H} / \partial x$. Since ϕ is the coordinate and \mathcal{E} is the energy, the quantity $\hbar N_s / 2$ is the momentum of the particle. However, according to Eq. (7.2) the canonically conjugated momentum operator is \hat{p}_ϕ . Therefore, $\hat{p}_\phi = \hbar N_s / 2$ and

$$-i \frac{\partial}{\partial \phi} = \frac{N_s}{2} = N_p \quad (7.4)$$

is the operator of the number of Cooper pairs $N_p = N_s / 2$. The second Hamiltonian equation has the form

$$\frac{\partial x}{\partial t} = \frac{\partial \mathcal{H}}{\partial p} \Rightarrow \frac{\partial \phi}{\partial t} = \frac{\mathcal{E}}{\partial(\hbar N_s / 2)} \quad \text{or} \quad \frac{1}{2} \frac{\partial \phi}{\partial t} = \frac{\partial \mathcal{E}_s}{\partial(\hbar N_s)} = \frac{\mu_s}{\hbar}$$

where μ_s is the chemical potential of Cooper pairs. This equation coincides with the Josephson relation since $\mu_s = eV$.

Equation (7.4) defines the operator of "superconducting charge" transferred through the junction

$$\hat{Q} = e\hat{N}_s = 2e\hat{N}_p = -2ie \frac{\partial}{\partial \phi} \quad (7.5)$$

The commutation relation takes the form

$$[\hat{Q}, \phi]_- = -2ie$$

Therefore, the quantum uncertainty in phase $\Delta\phi$ and in charge ΔQ are restricted by the charge of a Cooper pair $\Delta\phi \Delta Q \sim 2e$.

The eigenfunction of a state with the charge Q obeys the equation

$$\hat{Q}\Psi_Q = Q\Psi_Q \quad \text{or} \quad -2ie\frac{\partial\Psi_Q}{\partial\phi} = Q\Psi_Q$$

It is

$$\Psi_Q(\phi) = Ce^{iQ\phi/2e} \quad (7.6)$$

Assuming a single-valued wave function

$$\Psi_Q(\phi + 2\pi) = \Psi_Q(\phi)$$

we obtain *quantization of charge* of a Cooper pair $\pi Q/e = 2\pi n$, i.e.,

$$Q = 2en$$

where n is a integer.

Note that ϕ is the phase of the wave function of a Cooper *pair* of electrons. The single electron phase would be $\phi_1 = \phi/2$. If we now require a single-valued *one-electron* wave function,

$$\Psi_Q(\phi_1) = Ce^{iQ\phi_1/e}$$

so that $\Psi(\phi_1 + 2\pi) = \Psi(\phi_1)$, we obtain $2\pi Q/e = 2\pi n$ such that the single-electron charge is integer: $Q = en$.

7.1.3 The Hamiltonian

The charging energy of a capacitor can be written as

$$\frac{Q^2}{2C} = -\frac{4e^2}{2C} \frac{\partial^2}{\partial\phi^2} = -4E_C \frac{\partial^2}{\partial\phi^2}$$

where

$$E_C = \frac{e^2}{2C}$$

is the the charging energy for the charge of one electron.

The total energy of the Josephson junction becomes

$$\mathcal{H} = -4E_C \frac{\partial^2}{\partial\phi^2} + E_J[1 - \cos\phi] \quad (7.7)$$

This is the Hamiltonian of the junction in the quantum mechanical description.

If the junction is connected to a current source, the charge operator changes

$$\hat{Q} = -2ie\frac{\partial}{\partial\phi} + q(t)$$

where $q(t)$ is a continuous charge supplied by the current source. The Hamiltonian becomes

$$\mathcal{H} = 4E_C \left(-i\frac{\partial}{\partial\phi} + \frac{q(t)}{2e} \right)^2 + E_J[1 - \cos\phi] \quad (7.8)$$

In the classical limit this Hamiltonian is equivalent to the washboard potential. Indeed, the classical analogue of Eq. (7.8) is

$$\mathcal{E} = \frac{[Q + q(t)]^2}{2C} + E_J[1 - \cos \phi]$$

where Q is the charge that is transferred through the junction. Using the Josephson relation $V = (\hbar/2e)(d\phi/dt)$ the charging energy can be transformed as

$$\begin{aligned} \frac{[Q + q(t)]^2}{2C} &= \frac{Q^2}{2C} + \frac{[Q + q(t)]q(t)}{C} - \frac{q^2(t)}{2C} \\ &= \frac{Q^2}{2C} + Vq(t) - \frac{q^2(t)}{2C} = \frac{Q^2}{2C} - \frac{\hbar\phi}{2e} \frac{dq}{dt} + \frac{d}{dt} \left[\frac{\hbar\phi}{2e} q(t) \right] - \frac{q^2(t)}{2C} \\ &= \frac{Q^2}{2C} - \frac{\hbar\phi}{2e} I + \frac{dF(t)}{dt} \end{aligned}$$

Here $I = dq/dt$. The last term $dF(t)/dt$ is a full derivative of certain function. It can be omitted. With Eq. (7.5) for the operator Q , the total Hamiltonian assumes the usual form of a Hamiltonian of a particle in the tilted washboard potential

$$\mathcal{H} = -4E_C \frac{\partial^2}{\partial \phi^2} + E_J[1 - \cos \phi] - \frac{\hbar I}{2e} \phi \quad (7.9)$$

The quantum-mechanical description goes over into the classical picture described in Chapter 5 when the charge Q in the charge eigen-function Eq. (7.6) is large as compared to the electron charge and can be considered as a continuous variable.

7.2 Macroscopic quantum tunnelling

With the account of quantum effects, the behavior of the junction in presence of a high bias current is different from that considered in the previous chapter. Consider the Hamiltonian Eq. (7.9) for a representative particle in a washboard potential. The representative particle with the coordinate ϕ can now escape from the potential minimum at ϕ_0 by tunnelling through the potential barrier, see Fig. 7.3, maximum 1. If the maximum 2 in Fig. 7.3 is lower than the minimum ϕ_0 , the particle needs one tunnelling through the barrier shown by a gray region in the figure.

Tunnelling of the representative particle means a tunnelling of the entire system from one macroscopic state that contains many particles to another macroscopic state. This process involves a macroscopic number of particles and thus its probability should be inherently small. However, the Josephson junction provides a tool that can help us to observe these *macroscopic quantum tunnelling* (MQT) events.

The easiest way to solve the Schrödinger equation

$$\left[-4E_C \frac{\partial^2}{\partial \phi^2} + U(\phi) \right] \Psi(\phi) = E\Psi(\phi)$$

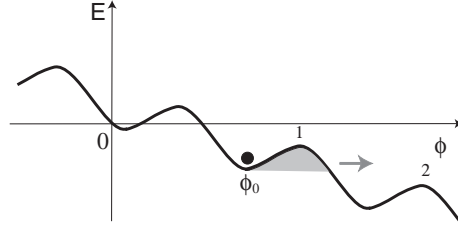


Figure 7.3: The tilted washboard potential in the quantum case. A quantum particle can escape from the potential minimum by tunnelling through the barrier (grey region).

with the washboard potential

$$U(\phi) = E_J \left[1 - \cos \phi - \frac{I}{I_c} \phi \right]$$

is to use the WKB approximation

$$\Psi = \exp \left(i \int \lambda(\phi) d\phi \right)$$

assuming $d\lambda/d\phi \ll \lambda^2$. We find

$$\lambda^2 = \frac{E - U_J(\phi)}{4E_C}$$

The WKB approximation holds if $dU/d\phi \ll \lambda^3 E_C$ or when $E_J \gg E_C$.

For the energy below the potential maximum we have

$$\lambda = i\tilde{\lambda} = \frac{i\sqrt{U_J(\phi) - E}}{2E_C^{1/2}}$$

which ensures the decay of the wave function for positive ϕ . The transmission probability through the barrier is proportional to the square of the transmission amplitude

$$\exp \left(- \int_{\phi_0}^{\phi'} \tilde{\lambda} d\phi \right)$$

where ϕ_0 and ϕ' are the turning points satisfying $E = U(\phi)$. The probability of tunnelling becomes

$$P \sim \omega_a \exp \left(-E_C^{-1/2} \int_{\phi_0}^{\phi'} \sqrt{U_J(\phi) - E} d\phi \right) \quad (7.10)$$

The exponent is generally of the order of

$$(E_J/E_C)^{1/2} \Delta\phi \gg 1$$

where $\Delta\phi = \phi' - \phi_0$. This results in a very small probability. For zero current, $\delta\phi \sim \pi$. Writing $\hbar\omega_p = (8E_J E_C)^{1/2}$ we can present the probability as

$$P \sim \omega_p \exp(-2\pi E_B / \hbar\omega_p)$$

where $E_B \sim 2E_J$ is the barrier height. This will transform into the Boltzmann factor $\exp(-E_B/T)$ for the crossover temperature

$$T_{cr} \sim \hbar\omega_p / 2\pi$$

For typical value of $\omega_p \approx 10^{11} \text{ sec}^{-1}$ this corresponds to $T_{cr} \approx 100 \text{ mK}$.

The tunnelling probability increases for $I \rightarrow I_c$, when the barrier height is getting small, see Eq. (5.31). We have

$$U \approx \frac{4\sqrt{2}}{3} E_J (1 - I/I_c)^{3/2}$$

while

$$\Delta\phi = \arccos(I/I_c) = \sqrt{1 - (I^2/I_c^2)}$$

so that the factor in the exponent for the probability becomes

$$\sim -(E_J/E_C)^{1/2} [1 - (I/I_c)]^{5/4}$$

7.2.1 Effects of dissipation on MQT

For low temperatures, the system occupies the low energy states in the potential minimum with the oscillator frequency ω_p . Consider the limit of low currents. The characteristic “time” it takes for the system to tunnel through the barrier is $t_t \sim 2\pi/\omega_p$. The energy dissipated during this time is

$$E_D \sim \frac{\hbar^2}{4e^2 R} \left(\frac{d\phi}{dt} \right)^2 t_t \sim \frac{2\pi\hbar^2\omega_p}{4e^2 R}$$

It should be smaller than the energy itself, $E_D \ll \hbar\omega_p/2$, otherwise the system cannot tunnel into a state in another potential minimum. This gives the condition

$$R \gg R_0 = \frac{h}{2e^2}$$

R_0 being the quantum of resistance. If this condition is fulfilled, the MQT is possible. The phase can escape from the potential minimum, and the current driven junction will exhibit a finite voltage. It will not be superconducting in a strict sense. However, if the dissipation is larger, i.e., $R < R_0$, the phase cannot tunnel. There will be no voltage: the junction is superconducting. Therefore, the dissipation helps the superconductivity, which is a counterintuitive result.

We can look at this estimate also in a different way. When the phase is fixed to one of the potential minima, the charge Q on the superconducting island is not defined due to the quantum uncertainty relation. Thus, the quantum fluctuations of charge are large. On the contrary, when the phase can tunnel, its uncertainty increases and the charge becomes more localized. This agrees with the estimates on the barrier resistance made in the beginning of the present Chapter.

7.3 Band structure

7.3.1 Bloch's theorem

The Band structure of the energy states in a periodic potential is a consequence of the Bloch's theorem known in solid state physics [16]: Any solution of the Schrödinger equation for a particle in a potential $U(x)$ periodic with a period a has the form

$$\Psi_k(x) = u_k(x)e^{ikx}$$

where $u_k(x)$ is a periodic function

$$u_k(x+a) = u_k(x)$$

An equivalent formulation of the Bloch's theorem is that for a particle in a potential $U(x)$ periodic with a period a there exists a quantity k such that the wave function obeys

$$\Psi_k(x+a) = e^{ika}\Psi_k(x) \quad (7.11)$$

The quantity k is called quasimomentum. The energy, i.e., the eigenvalue of the Schrödinger equation

$$\left[-\frac{\hbar^2}{2m} \frac{d^2}{dx^2} + U(x) \right] \Psi_k(x) = E_k \Psi_k(x)$$

depends on the quasimomentum. The energy spectrum is split into intervals continuously filled by the values E_k as functions of k (energy bands) separated by intervals where there are no values of E_k (forbidden bands). These energy bands are labelled by the band numbers n such that $E = E_{kn}$.

The quasimomentum is defined within an interval

$$-\frac{\pi}{a} \leq k \leq \frac{\pi}{a}$$

which is called the first Brillouin zone. All the quasimomenta that differ by an integer multiple of $2\pi/a$ are equivalent, i.e., the quasimomenta

$$k' = k + (2\pi/a)n$$

refer to the same quasimomentum. Indeed, Eq. (7.11) shows that $\Psi_{k'}(x+a) = e^{ika}\Psi_{k'}(x)$, i.e., belongs to the same quasimomentum as Ψ_k . However, there may be *many* states belonging to the same quasimomentum, so that k and $k + (2\pi/a)n$ do not necessarily belong to the same state. An example can be constructed for a free particle with a spectrum $E = p^2/2m$ if one introduces a very small (zero) potential with an (arbitrary) period a . This spectrum is shown in Fig. 7.4.

Since the quasimomenta π/a and $-\pi/a$ differ by $2\pi/a$, the points at the right and left boundary of the Brillouin zone are equivalent. One can thus consider the so called extended zone scheme where the energy is periodic as a function of quasimomentum with a period $2\pi/a$. This is shown in Fig. 7.4 by dashed curves.

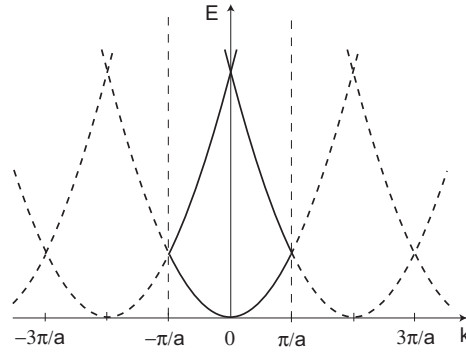


Figure 7.4: The energy spectrum for a free particle in the presence of a small periodic potential. The spectrum shown by solid lines is reduced to the first Brillouin zone $-\pi/a < k < \pi/a$. The dashed lines refer to the extended zone scheme.

7.3.2 Bloch's theorem in Josephson devices

In the case of Josephson junctions, the coordinate is ϕ . If the junction is not connected to the current source, the period of the Josephson potential is 2π . Therefore, solutions of the Schrödinger equation with the Hamiltonian Eq. (7.7)

$$-4E_C \frac{\partial^2}{\partial \phi^2} \Psi_k + E_J [1 - \cos \phi] \Psi_k = E \Psi_k \quad (7.12)$$

should obey

$$\Psi_k(\phi + 2\pi) = e^{i2\pi k} \Psi_k(\phi) \quad (7.13)$$

where k is defined within the first Brillouin zone $-1/2 < k < 1/2$. Equation (7.12) is known in mathematics as the Mathieu equation.

Without the potential we would have

$$\Psi_k = e^{ik\phi}$$

Comparing this with Eq. (7.6) we recognize that k plays the role of charge $Q/2e$. Therefore, the quasimomentum k in the presence of potential is the *quasicharge*

$$Q = 2ek$$

defined within the first Brillouin zone

$$-e < Q < e \quad (7.14)$$

If we require a single-valued wave function $\Psi_k(\phi + 2\pi) = \Psi_k(\phi)$ we find that $k = n$ so that the quasicharge defined within the first Brillouin zone is zero, i.e., $Q = 0$. The energies of a free charge (see Fig. 7.4) are

$$E_Q = 4E_C n^2 = \frac{(2en)^2}{2C}$$

which corresponds to an integer number of electron pairs on the junction.

The situation changes if we have an external current source. The Hamiltonian has the form of Eq. (7.8). The Schrödinger equation becomes

$$4E_C \left(-i \frac{\partial}{\partial \phi} + \frac{q(t)}{2e} \right)^2 \Psi + E_J [1 - \cos \phi] \Psi = E \Psi \quad (7.15)$$

We make a gauge transformation

$$\Psi = \tilde{\Psi} e^{-iq(t)\phi/2e}$$

where the function $\tilde{\Psi}$ satisfies Eq. (7.12) and obeys the Bloch's theorem, Eq. (7.13), i.e.,

$$\tilde{\Psi}_Q(\phi + 2\pi) = e^{i\pi Q/\epsilon} \tilde{\Psi}_Q(\phi) \quad (7.16)$$

As a result the function Ψ satisfies

$$\Psi_Q(\phi + 2\pi) = e^{i\pi[Q-q(t)]/\epsilon} \Psi_Q(\phi) \quad (7.17)$$

Requiring it to be single valued we find

$$Q = q(t) + 2en \quad (7.18)$$

whence

$$\frac{dQ}{dt} = \frac{dq}{dt} = I \quad (7.19)$$

We see that the quantum mechanics of the Josephson junction connected to the current source can be described by the Hamiltonian Eq. (7.7) where the quasimomentum depends on time according to Eq. (7.19).

7.3.3 Large Coulomb energy: Free-phase limit

This limit is realized when the Josephson energy E_J is much smaller than the charging energy E_C , i.e., $E_J \ll E_C$. The Schrödinger equation (7.12)

$$-4E_C \frac{\partial^2}{\partial \phi^2} \Psi_Q + E_J [1 - \cos \phi] \Psi_Q = E_Q \Psi_Q \quad (7.20)$$

It has the solutions which are close to the eigenstates for fixed charge Eq. (7.6). The spectrum has the form of parabolas

$$E - E_J = E_C \frac{Q^2}{e^2} = \frac{(q + 2en)^2}{2C}$$

shown in Fig. 7.5. The parabolas are shifted by integer multiple of the Cooper pair charge $2e$.

The quantum-mechanical description implies that the charge q in Fig. 7.5 is replaced by a quasicharge Q reduced to the first Brillouin zone, $-e < Q < e$.

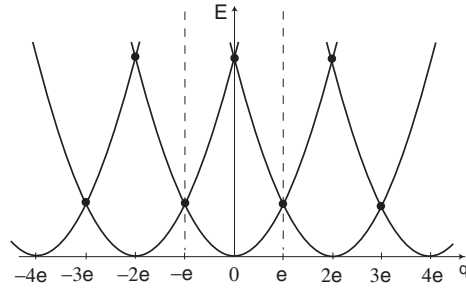


Figure 7.5: The energy spectrum of a free charge (in a zero Josephson potential) as a function of the bias charge q .

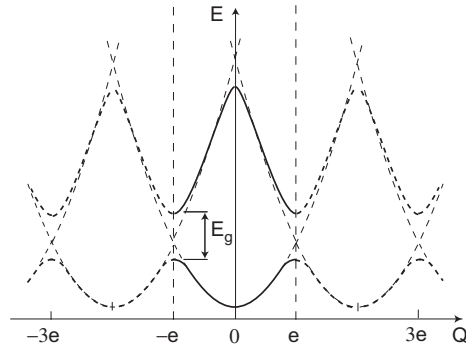


Figure 7.6: The energy spectrum for a Josephson junction in the limit of nearly free phase. The spectrum in the first Brillouin zone $-e < Q < e$ is shown by solid lines.

A small Josephson potential introduces small energy gaps at the boundary of the Brillouin zone where the free-charge parabolas cross (black point in Fig. 7.5). To calculate the first energy gap we note that the potential

$$-E_J \cos \phi = -\frac{E_J}{2} [e^{i\phi} + e^{-i\phi}]$$

couple the states at the $Q = e$ boundary of the Brillouin zone

$$\Psi_{Q=e} = e^{i\phi/2}$$

and the states at the $Q = -e$ boundary

$$\Psi_{Q=-e} = e^{-i\phi/2}$$

which differ by $\delta Q = 2e$ and thus belong to the same quasicharge Q . The wave function at $Q = e$ will thus be a linear combination

$$\Psi_e = c_1 e^{i\phi/2} + c_2 e^{-i\phi/2}$$

Inserting this into the Schrödinger equation (7.20) we find

$$\begin{aligned} E_C \left[c_1 e^{i\phi/2} + c_2 e^{-i\phi/2} \right] - \frac{E_J}{2} \left[c_1 e^{3i\phi/2} + c_2 e^{i\phi/2} + c_1 e^{-i\phi/2} + c_2 e^{-3i\phi/2} \right] \\ = (E - E_J) \left[c_1 e^{i\phi/2} + c_2 e^{-i\phi/2} \right] \end{aligned}$$

The harmonics with $\pm 3i\phi/2$ couple to the $Q = 3e$ quasicharge. Comparing the coefficients at the $\pm i\phi/2$ harmonics we find

$$\begin{aligned} (E_C - E + E_J)c_1 - \frac{E_J}{2}c_2 &= 0 \\ (E_C - E + E_J)c_2 - \frac{E_J}{2}c_1 &= 0 \end{aligned}$$

whence

$$E = (E_C + E_J) \pm \frac{E_J}{2}$$

This means that the energy gap has the width $E_g = E_J$ with the middle at $E_C + E_J$, see Fig. 7.6. The middle point is shifted with respect to its free-phase-limit ($E_J = 0$) location at E_C due to the constant component of the potential. The lowest energy is also shifted above zero, see Problem 7.1.

Since the boundaries $Q = -e$ and $Q = e$ of the Brillouin zone are equivalent, as well as they are, in general, for any $Q = 2em$ (m is an integer), one can use the so called extended zone scheme where the energy in each band $E_{Q,n} \equiv E_n(Q)$ is a periodic function of Q :

$$E_n(Q + 2em) = E_n(Q)$$

This is shown by dashed lines in Figs. 7.4, 7.6.

7.3.4 Low Coulomb energy: Tight binding limit

In this limit the Josephson energy is larger than the charging energy $E_J \gg E_C$ which implies large capacitance. The system behavior is close to that for a particle in a series of deep potential wells. One can expand the potential near each minimum

$$U(\phi) = \frac{E_J \phi^2}{2}$$

to get the oscillator potential. The Schrödinger equation (7.20) transforms into the oscillator equation

$$-4E_C \frac{d^2 \psi}{d\phi^2} + \frac{E_J \phi^2}{2} \psi = E \psi$$

The energy spectrum is

$$E_n = \sqrt{8E_C E_J} \left(n + \frac{1}{2} \right) = \hbar \omega_p \left(n + \frac{1}{2} \right)$$

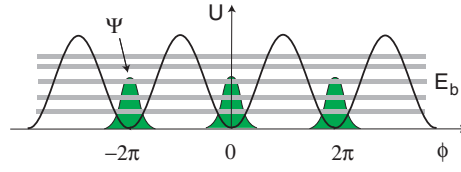


Figure 7.7: The energy band spectrum for a Josephson junction in the limit of large Josephson energy (tight binding). The energy bands are widened oscillator levels for a localized particle with the wave function ψ .

The energy spacing $\hbar\omega_p \sim E_J \sqrt{E_C/E_J} \ll E_J$. The lowest energy wave function is

$$\psi_0(\phi) = C \exp\left(-\frac{\phi^2}{4} \sqrt{\frac{E_J}{2E_C}}\right)$$

Due to the periodic nature of the potential one can construct the true wave function

$$\Psi_{Q,n}(\phi) = \sum_m e^{i2\pi m(Q/2e)} \Psi_n(\phi - 2\pi m)$$

where $\Psi_n(\phi - 2\pi m)$ is a function centered at $\phi = 2\pi m$. The function $\Psi_n(\phi)$ is called the Wannier function [16]. It is close to the wave function $\psi_n(\phi)$ obtained by solving the equation near each minimum. This wave function $\Psi_{Q,n}(\phi)$ satisfies the Bloch condition Eq. (7.16). Each level is broadened into an energy band (see Problem 7.3)

$$E_Q = E_n - \frac{1}{2} E_{b,n} \cos \frac{\pi Q}{e} \quad (7.21)$$

The band width is determined by overlaps of the wave functions $\Psi_n(\phi)$ centered at $\phi_m = 2\pi m$. It is exponentially small. For example, the lowest band width is

$$E_{b,0} = 32 \left(\frac{E_J E_C}{\pi}\right)^{1/2} \left(\frac{E_J}{2E_C}\right)^{1/2} \exp\left(-\sqrt{\frac{8E_J}{E_C}}\right)$$

The quantum properties of Josephson junctions are discussed in review [17].

7.4 Coulomb blockade

Let us consider Fig. 7.5. If we increase, by a bias current from the external source, the charge starting from $q = 0$ for $n = 0$ the energy will increase until it reaches the crossing point (black dot) at $q = e$ corresponding to the charge e on the capacitor and to the voltage e/C across the capacitor. With a further increase in q the system will go over to a state with $n = -1$ corresponding to the parabola shifted by $2e$ to the right that has a lower energy. The transition from $n = 0$ to $n = -1$ corresponds to the $2e$ charge transfer through the

tunnel Josephson junction. We see that the charge transfer (current) through the capacitor occurs only when the voltage reaches a threshold value $V_C = e/C$. This is the *Coulomb blockade*: preventing of the charge transfer by the charging energy. To describe the Coulomb blockade quantum-mechanically, we need first to consider the semi-classical equation of motion in a periodic potential.

7.4.1 Equation of motion

In the semi-classical theory than neglects transition between energy bands, the equation of motion for the quasimomentum of a particle is [16]

$$\hbar \frac{\partial k}{\partial t} = F$$

For a constant force F this gives $\hbar k = Ft$. The velocity is

$$\frac{\partial x}{\partial t} = \frac{\partial E_n}{\hbar \partial k}$$

where $E_n(k)$ is the band energy. This yields

$$\frac{\partial x}{\hbar \partial k} = \frac{1}{F} \frac{\partial E_n}{\hbar \partial k}$$

or

$$x = F^{-1} E_n(k), \quad \hbar k = Ft$$

For a free particle in zero potential $E(k) = \hbar^2 k^2 / 2m$, so that the particle is continuously accelerated. However, in a periodic potential, $E(k)$ is a periodic function. Therefore, instead of being accelerated, the coordinate of particle performs *Bloch oscillations* with the amplitude $\Delta x = 2E_b/F$ and a period

$$t = \frac{2\pi\hbar}{aF}$$

In a first Brillouin zone picture, the particle is moving until it is reflected at the zone boundary such that its quasimomentum changes from $k_B = \pi/a$ at one boundary to $k_B - 2\pi/a = -k_B$ at another boundary.

7.4.2 Bloch oscillations and the Coulomb blockade in Josephson junctions

Consider low currents such that the (Zener) transitions from one band to another have low probability. In a Josephson junction, the force equation has the form

$$\frac{\partial Q}{\partial t} = I \tag{7.22}$$

while

$$\frac{\partial \phi}{\partial t} = \frac{\partial E_{Q,n}}{\hbar \partial k} = \frac{2e}{\hbar} \frac{\partial E_{Q,n}}{\partial Q} \tag{7.23}$$

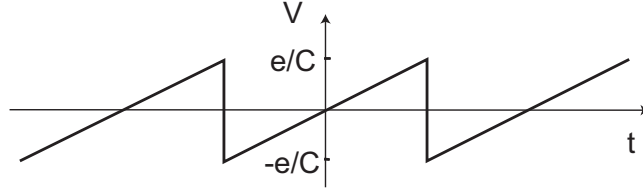


Figure 7.8: The voltage across the junction as a function of time for a constant current bias.

Therefore, for a constant current,

$$\frac{\partial \phi}{\partial Q} = \frac{2e}{I\hbar} \frac{\partial E_{Q,n}}{\partial Q}$$

so that

$$\phi = \frac{2e}{I\hbar} E_n(Q)$$

The period of Bloch oscillations is from Eq. (7.22)

$$t_B = \frac{2e}{I}$$

The amplitude of Bloch oscillations is

$$\Delta\phi = \frac{2e}{I\hbar} E_b$$

In the limit of large Coulomb energy (free phase), $E_C \gg E_J$

$$E_b \approx E_C$$

and

$$\Delta\phi \approx E_C/E_J \sim t_B/R_0C \gg 1$$

The phase is not fixed: it oscillates rapidly with a large amplitude. The voltage is

$$V = \frac{\hbar}{2e} \frac{\partial \phi}{\partial t} = \frac{\partial E_{Q,n}}{\partial Q} \approx \frac{Q}{C}$$

Each time when the quasicharge Q approaches the boundary of the Brillouin zone $Q_B = +e$ (or $Q_B = -e$), the quasicharge changes $Q_B \rightarrow Q_B \pm 2e$ such that the voltage jumps from $+e/C$ to $-e/C$ (or vice versa). The average voltage is zero.

The change in the quasicharge Q by $2e$ means the $2e$ charge transfer through the Josephson junction. We see that the charge transfer through the junction occurs only when the voltage across the junction reaches a threshold value e/C . This is the quantum-mechanical picture of the *Coulomb blockade*. The charging energy of the junction prevents the charge transfer through it unless the voltage

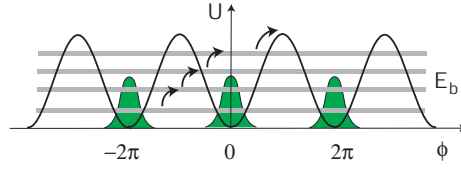


Figure 7.9: MQT is equivalent to Landau–Zener transitions between the energy bands up to the continuum. The energy bands are widened oscillator levels for a localized particle with the wave function ψ .

exceeds the threshold. At the threshold $V_C = e/C$, the charging energy $Q^2/2C$ of a charge $Q = e$ becomes equal to the charging energy $(Q - 2e)^2/2C$ of the charge $Q = e - 2e = -e$ on the capacitor after the Cooper pair has tunneled through the junction. To see the Coulomb blockade one needs a junction with a rather low capacity.

On the contrary, if the capacity is high such that $E_J \gg E_C$, the band width is very narrow, and the amplitude of phase oscillations is exponentially small. The phase is essentially fixed such that the current $I_c \cos \phi$ flows without voltage: the junction is superconducting. A finite voltage can then appear as a result of *macroscopic quantum tunnelling* considered in the previous Section within the semiclassical approach. In the semiclassical picture of Eqs. (7.22) and (7.23), the macroscopic quantum tunnelling is equivalent to Zener transitions from a lower band up to higher bands in Fig. 7.7 and finally to the continuum for $E > E_J$ (see Fig. 7.9). Neglecting the Zener transitions implies absence of MQT and assumes that the bias current is small.

7.4.3 Effect of dissipation

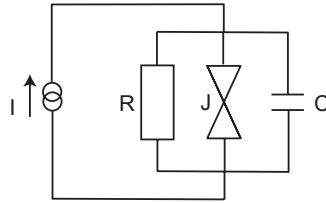


Figure 7.10: The resistively shunted Josephson junction.

Consider the resistively shunted junction, Fig. 7.10, described by [17]

$$I = \frac{\partial Q_n}{\partial t} + \frac{V}{R} \quad (7.24)$$

where, as before, the voltage across the junction

$$V = \frac{\partial E_{Q,n}}{\partial Q}$$

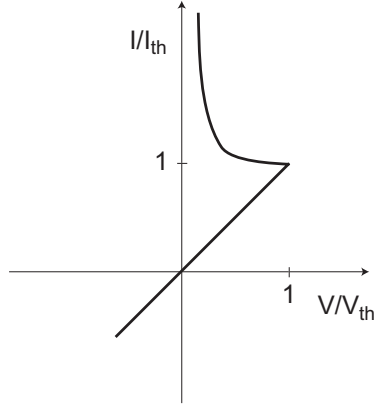


Figure 7.11: The d.c. I-V curve for resistively shunted quantum junction for the limit of high Coulomb energy. $V_{th} = I_{th}R = e/C$.

We again neglect the inter-band transitions assuming that the current is smaller than what is required for Zener transitions.

For high Coulomb energy,

$$\frac{\partial E_{Q,n}}{\partial Q} = \frac{Q}{C}$$

Eq. (7.24) becomes

$$\frac{\partial Q_n}{\partial t} = I - \frac{Q}{RC} \quad (7.25)$$

Assume that the charge is within the first Brillouin zone $-e \leq Q \leq +e$.

If the current is below the threshold value $I < I_{th}$ where

$$I_{th} = \frac{e}{RC}$$

the current flows entirely through the shunt resistance, such that the charge and voltage are constant, $V = Q/C = const$ and

$$I = V/R$$

If $I > I_{th}$, the Bloch oscillations begin. Eq. (7.25) has the solution

$$Q = Ae^{-t/RC} + IRC$$

For $t = 0$ we have $Q = 0$ and $\partial Q/\partial t = I$. This gives

$$A = -IRC$$

Assume that at $t = -t_1$ the charge was at the end $Q = -e$ of the Brillouin zone, while at $t = t_2$ the charge was at the end $Q = +e$ of the Brillouin zone. We find

$$A \exp(-t_2/RC) = e - IRC, \quad A \exp(t_1/RC) = -e - IRC$$

Therefore

$$\exp\left(\frac{t_1 + t_2}{RC}\right) = \frac{IRC + e}{IRC - e}$$

The average voltage is found from

$$\begin{aligned} (t_1 + t_2) \frac{\bar{V}}{R} &= \int_{-t_1}^{t_2} \left[\frac{A}{RC} \exp\left(-\frac{t}{RC}\right) + I \right] dt \\ &= (t_1 + t_2) \left(I + \frac{A}{t_1 + t_2} [\exp(t_1/RC) - \exp(-t_2/RC)] \right) \end{aligned}$$

Finally,

$$\frac{\bar{V}}{R} = I - 2I_{th} \left[\ln \frac{I + I_{th}}{I - I_{th}} \right]^{-1}$$

The second term is zero for $I = I_{th}$ and diverges for $I \rightarrow \infty$. The I-V curve is shown in Fig. 7.11. The maximum d.c. voltage \bar{V} is $V_{th} = I_{th}R = e/C$. For $R \rightarrow \infty$ the I-V curve is vertical which means zero d.c. voltage.

7.5 Parity effects

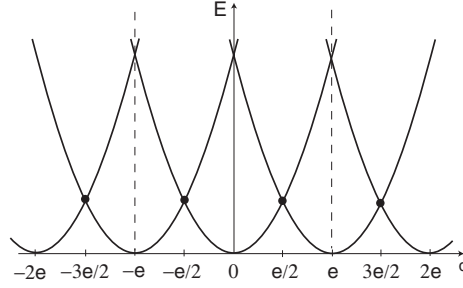


Figure 7.12: The e -periodic energy dependence of a normal junction as a function of the continuous charge q supplied by the external source.

Let us consider a junction in Fig. 7.1 made of normal conductors and study how its properties change when a superconducting gap is introduced.

In the case of a normal junction, the wave function depends on a single-electron phase $\phi_1 = \phi/2$ such that the charge operator in Eq. (7.5) becomes

$$\hat{Q} = -2ie \frac{\partial}{\partial \phi} = -ie \frac{\partial}{\partial \phi_1} \quad (7.26)$$

The eigenfunction has the form

$$\Psi_Q = e^{iQ\phi_1/e}$$

which is 2π -periodic for $Q = ne$. The Josephson current disappears, and the Hamiltonian becomes

$$\mathcal{H} = -E_C \frac{\partial^2}{\partial \phi_1^2}$$

If the junction is connected to the external leads, the Hamiltonian takes the form

$$\mathcal{H} = E_C \left(-i \frac{\partial}{\partial \phi_1} + \frac{q(t)}{e} \right)^2$$

The solution of the corresponding Schrödinger equation has the form

$$\Psi = e^{i(Q-q)\phi_1/e}$$

The condition of 2π -periodicity gives $Q = q + me$ where m is an integer.

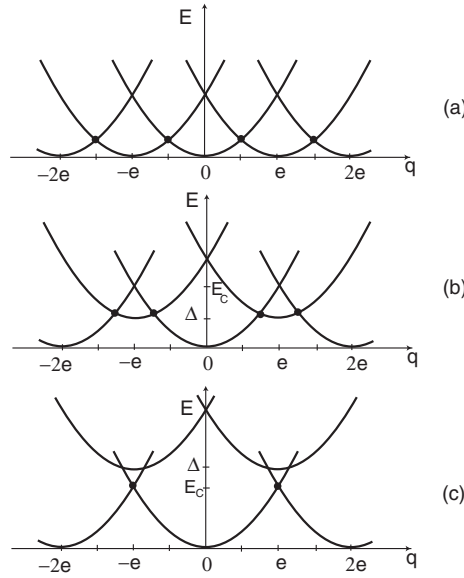


Figure 7.13: The energy of junctions. (a) e -periodic dependence in the normal state. (b) Energy of odd-number states is shifted by $\Delta < E_C$. The charge transfer occurs at the crossing points (black dots). (c) $\Delta > E_C$, the charge transfer occurs with a $2e$ periodicity.

The energy is

$$E_Q = E_C \frac{Q^2}{e^2} = E_C \frac{(q + me)^2}{e^2}$$

It is shown in Fig. 7.12. The different parabolas correspond to different values of m .

Assume we start with $m = 0$. As we increase the charge q supplied by the external source, the energy grows until q reaches $e/2$ which corresponds to the

voltage $V_C = e/2C$. At this moment, the energy of the capacitor becomes equal to the energy for the state with $m = -1$, i.e., to $(q - e)^2/2C$. At this point the charge at the capacitor decreases by e , one electron being transferred through the junction via tunnelling. We see again that the charge transfer (current) does not occur unless voltage reaches the threshold value V_C (Coulomb blockade).

Consider again the device shown in Fig. 7.1 and apply a gate voltage V_G between the island and the gate electrode. If $V_G = V_C$, the energy of the junction corresponds to the level where the parabolas cross (black dots in Fig. 7.12). This means that an infinitely small voltage V can lead to a continuous transfer of charge from lead L_1 to lead L_2 .

Let us now assume that the island I is superconducting with an energy gap Δ . For simplicity we restrict ourselves to zero temperatures. If the number of electrons on it is even, they all are included into Cooper pairs and form the ground state with zero energy plus the charging energy. If now we add an extra (odd) particle, it can only occupy a state above the gap thus the energy will be Δ plus the charging energy. One more particle will make a pair with the previous one thus decreasing the total energy down to simply the charging energy. Therefore, the states with odd number of particles will have energy which is the charging energy for the given number of particles shifted by $+\Delta$ with respect to the energy for the even number of particles. This is shown in Fig. 7.13.

Shift of the parabolas for odd particle numbers destroys the e -periodicity of the energy spectrum. When Δ becomes larger than the charging energy $\Delta > E_C$, the charge transfer occurs only within the states with even number of particles, and the $2e$ -periodicity characteristic for a superconducting system is restored (Fig. 7.13(c)).

When also the leads become superconducting, the Josephson energy appears, and the gaps open at the crossing points shown by black dots. The energy dependence returns to Fig. 7.6 for a superconducting Josephson junction considered before.

Problem 7.1

Find the quasiclassical probability of MQT from the minimum of the washboard potential for I close to I_c .

Problem 7.2

Find the lowest energy in the nearly free-phase limit, $E_J \ll E_C$.

Problem 7.3

Derive Eq. (7.21).

Bibliography

- [1] P.G. de Gennes *Superconductivity of Metals and Alloys* (W.A. Benjamin, Inc, 1965).
- [2] M. Tinkham, *Introduction to superconductivity* (McGraw-Hill, New York, 1996).
- [3] J. Bardeen, L.N. Cooper, and J.R. Schrieffer, *Phys. Rev.* **108**, 1175 (1957).
- [4] L.D. Landau and E.M. Lifshitz, *Statistical Physics Part 2: Theory of the condensed state*, by E.M. Lifshitz and L.P. Pitaevskii (Pergamon, Oxford 1980), Chapter III.
- [5] Abrikosov, A. A. *Fundamentals of The Theory of Metals*. (North Holland, Amsterdam, 1998).
- [6] D. Saint-James, G. Sarma, and E.J. Thomas *Type II superconductivity* (Pergamon Press, 1969).
- [7] R. Feynman, in: *Progress in Low Temperature Physics* vol. 1, edited by C. J. Gorter (North Holland, Amsterdam, 1955) p. 36.
- [8] A.A. Abrikosov, *Zh. Eksp. Teor. Fiz.* **32**, 1442 (1957) [*Sov. Phys. JETP* **5**, 1174 (1957)].
- [9] P.W. Anderson, *Journ. Phys. Chem. Solids* **11**, 26 (1959).
- [10] A. F. Andreev, *Zh. Eksp. Teor. Fiz.* **49**, 655 (1965) [*Sov. Phys. JETP* **22**, 455 (1966)].
- [11] G.E. Blonder, M. Tinkham, and T.M. Klapwijk, *Phys. Rev. B*, **25**, 4515 (1982).
- [12] S. Datta, *Electronic Transport in Mesoscopic Systems*, Cambridge University Press (Cambridge, 1995).
- [13] C.W.J. Beenakker, *Phys. Rev Lett.* **67**, 3836, (1991).
- [14] V. Ambegaokar and A. Baratoff, *Phys. Rev. Lett.* **10**, 486, (1963); **11**, 104(E) (1963).

- [15] V. Ambegaokar and B. I. Halperin, Phys. Rev. Lett. **22**, 1364, (1969).
- [16] J.M. Ziman, *Principles of the theory of solids*, (Cambridge University Press, 1965).
- [17] G. Schön and A.D. Zaikin, Phys Reports **198**, 237 (1990).
- [18] G.-L. Ingold and Yu. V. Nazarov, “Charge tunneling rates in ultrasmall junctions”, in: *Single Charge Tunneling*”, H. Grabert and M.H. Devoret, eds., NATO ASI Series, Vol. 294, pp. 21–107 (Plenum Press, New York, 1992); arXiv:cond-mat/0508728v1
- [19] J.P. Pekola, K.P. Hirvi, J.P. Kauppinen, and M.A. Paalanen, Phys. Rev. Lett. **94**, 2903 (1994).